

# Pareto Active Learning with Gaussian Processes and Adaptive Discretization

**Andi Nika**

*Department of Electrical and Electronics Engineering  
Bilkent University  
Turkey*

ANDI.NIKA@BILKENT.EDU.TR

**Kerem Bozgan**

*Department of Electrical and Electronics Engineering  
Bilkent University  
Turkey*

KEREM.BOZGAN@BILKENT.EDU.TR

**Sephehr Elahi**

*Department of Electrical and Electronics Engineering  
Bilkent University  
Turkey*

SEPEHR.ELAHI@UG.BILKENT.EDU.TR

**Çağın Ararat**

*Department of Industrial Engineering  
Bilkent University  
Turkey*

CARARAT@BILKENT.EDU.TR

**Cem Tekin**

*Department of Electrical and Electronics Engineering  
Bilkent University  
Turkey*

CEMTEKIN@EE.BILKENT.EDU.TR

## Abstract

We consider the problem of optimizing a vector-valued objective function  $\mathbf{f}$  sampled from a Gaussian Process (GP) whose index set is a well-behaved, compact metric space  $(\mathcal{X}, d)$  of designs. We assume that  $\mathbf{f}$  is not known beforehand and that evaluating  $\mathbf{f}$  at design  $x$  results in a noisy observation of  $\mathbf{f}(x)$ . Since identifying the Pareto optimal designs via exhaustive search is infeasible when the cardinality of  $\mathcal{X}$  is large, we propose an algorithm, called Adaptive  $\epsilon$ -PAL, that exploits the smoothness of the GP-sampled function and the structure of  $(\mathcal{X}, d)$  to learn fast. In essence, Adaptive  $\epsilon$ -PAL employs a tree-based adaptive discretization technique to identify an  $\epsilon$ -accurate Pareto set of designs in as few evaluations as possible. We provide both information-type and metric dimension-type bounds on the sample complexity of  $\epsilon$ -accurate Pareto set identification. We also experimentally show that our algorithm outperforms other Pareto set identification methods on several benchmark datasets.

**Keywords:** Active learning, multi-objective optimization, Gaussian processes, Pareto optimal, adaptive discretization.

## 1. Introduction

Many complex scientific problems require optimization of multi-dimensional ( $m$ -variate) performance metrics (objectives) under uncertainty. When developing a new drug, scientists

need to identify the optimal therapeutic doses that maximize benefit and tolerability (Schmidt, 1988). When designing a new hardware, engineers need to identify the optimal designs that minimize energy consumption and runtime (Almer et al., 2011). In general, there is no design that can simultaneously optimize all objectives, and hence, one seeks to identify the set of Pareto optimal designs. Moreover, design evaluations are costly, and thus, the optimal designs should be identified with as few evaluations as possible. In practice, this is a formidable task for at least two reasons: design evaluations only provide noisy feedback about ground truth objective values, and the set of designs to explore is usually very large (even infinite). Luckily, in practice, one only needs to identify the set of Pareto optimal designs up to a desired level of accuracy. Within this context, a practically achievable goal is to identify an  $\epsilon$ -accurate Pareto set of designs whose objective values form an  $\epsilon$ -approximation of the true Pareto front for a given  $\epsilon = [\epsilon^1, \dots, \epsilon^m]^\top \in \mathbb{R}_+^m$  (Zuluaga et al., 2016).

We model identification of an  $\epsilon$ -accurate Pareto set of designs as an active learning problem. Specifically, we assume that the designs lie in a well-behaved, compact metric space  $(\mathcal{X}, d)$ , where the set of designs  $\mathcal{X}$  might be very large. The vector-valued objective function  $\mathbf{f} = [f^1, \dots, f^m]^\top$  defined over  $(\mathcal{X}, d)$  is unknown at the beginning of the experiment. The learner is given prior information about  $\mathbf{f}$ , which states that it is a sample from a multi-output GP with known mean and covariance functions. Then, the learner sequentially chooses designs to evaluate, where evaluating  $\mathbf{f}$  at design  $x$  immediately yields a noisy observation of  $\mathbf{f}(x)$ . The learner uses data from its past evaluations in order to decide which design to evaluate next, until it can confidently identify an  $\epsilon$ -accurate Pareto set of designs.

## 1.1 Our contribution

We propose a new learning algorithm, called Adaptive  $\epsilon$ -PAL, that solves the Pareto active learning (PAL) problem described above, by performing as few design evaluations as possible. Our algorithm employs a tree-based adaptive discretization strategy to dynamically partition  $\mathcal{X}$ . It uses the GP posterior on  $\mathbf{f}$  to decide which regions of designs in the partition of  $\mathcal{X}$  to discard or to declare as a member of the  $\epsilon$ -accurate Pareto set of designs. On termination, Adaptive  $\epsilon$ -PAL guarantees that the returned set of designs forms an  $\epsilon$ -accurate Pareto set with a high probability. To the best of our knowledge, Adaptive  $\epsilon$ -PAL is the first algorithm that employs an adaptive discretization strategy in the context of PAL, which turns out to be very effective when dealing with a large  $\mathcal{X}$ .

We prove information-type and metric dimension-type upper bounds on the sample complexity of Adaptive  $\epsilon$ -PAL. Our information-type bound yields a sample complexity upper bound of  $\tilde{O}(g(\epsilon))$  where  $\epsilon = \min_j \epsilon^j$ ,  $g(\epsilon) = \min\{\tau \geq 1 : \sqrt{\gamma_\tau/\tau} \leq \epsilon\}$ , and  $\gamma_\tau$  is the maximum information gain after  $\tau$  evaluations. To the best of our knowledge, this is the first information-type bound for dependent objectives in the context of PAL. In addition, our metric dimension-type bound yields a sample complexity of  $\tilde{O}(\epsilon^{-\frac{\bar{D}}{\alpha}+2})$  for all  $\bar{D} > D_1$ , where  $D_1$  represents the metric dimension of  $(\mathcal{X}, d)$  and  $\alpha \in (0, 1]$  represents the Hölder exponent of the metric induced by the GP on  $\mathcal{X}$ . As far as we know, this is the first metric dimension-type bound in the context of PAL. Our bounds complement each other: as we show in the appendix, neither of them dominates the other for all possible GP kernels. Specifically, we provide an example under which the information-type bound can be very loose compared to the metric dimension-type bound. Besides theory, we also show

via extensive simulations on several benchmark datasets that Adaptive  $\epsilon$ -PAL significantly improves over  $\epsilon$ -PAL (Zuluaga et al., 2016) in terms of accuracy and sample complexity.

## 1.2 Related work

Learning the Pareto optimal set of designs and the Pareto front has received considerable attention in recent years (Auer et al., 2016; Zuluaga et al., 2013, 2016; Hernández-Lobato et al., 2016; Shah and Ghahramani, 2016; Paria et al., 2020; Belakaria and Deshwal, 2019; Belakaria et al., 2020; Daulton et al., 2020).

Auer et al. (2016) consider a finite set of designs and formulate the identification of the Pareto front as a pure exploration multi-armed bandit (MAB) problem in the fixed confidence setting. Under the assumption that the centered outcomes are 1-subgaussian and independent, they provide gap-dependent bounds on its sample complexity, which, in the single objective case, yield the well-known gap-dependent sample-complexity bounds for pure exploration in the multi-armed bandit setting (Mannor and Tsitsiklis, 2004). Two cases are analyzed: in the first case, their algorithm takes as input the precision parameter  $\epsilon_0$  and returns a set  $P$  of designs which, with high probability, is guaranteed to contain the true Pareto set (see Section 2.1).  $P^*$  and other suboptimal designs which are no farther than  $\epsilon_0$  away from  $P^*$ , in the sense that there is no point  $x$  in  $P$  such that the gap between any objectives corresponding to  $x$  and any point in  $P^*$  is greater than  $\epsilon_0$ ; in the second case, the algorithm takes two input parameters and returns a sparse cover of  $P^*$ , that is, again all designs in  $P$  are close to  $P^*$  in the above sense, but in this case  $P$  covers  $P^*$ , instead of containing all of it.

Knowles (2006a) and Ponweiser et al. (2008) consider multi-objective adaptations of the Efficient Global Optimization (EGO) algorithm (Jones et al., 1998). The latter is one of the prominent examples of Design and Analysis of Computer Experiments (DACE, Sacks et al. (1989)), a GP-based supervised learning approach used to tackle optimization problems with expensive evaluations. The practicality of DACE-based algorithms is in their utilization of the similarity information between close designs by assuming correlated measurement noise. Given a set of  $D$ -dimensional designs  $x_1, \dots, x_n$ , where  $x_k = [x_k^1, \dots, x_k^D]^\top$ , corresponding to the respective observations  $y_1, \dots, y_n$ , we want to estimate  $f$ , where  $y_k = f(x_k) + \kappa_k$  and  $\kappa_k$  is  $\mathcal{N}(0, \sigma^2)$  noise. For any  $i, j \leq n$ , we have

$$\text{Corr}(\kappa_i, \kappa_j) = \exp\left(-\sum_{k=1}^D \theta_k |x_i^k - x_j^k|^{p_k}\right),$$

where  $\theta_k > 0$ , and  $p_k \in [1, 2]$ , for all  $1 \leq k \leq D$ ; the parameters  $\theta_k$  and  $p_k$  capture the activity in dimension  $k$  and the smoothness of the estimated function, respectively. Given the values of these parameters, EGO then computes estimates  $\hat{\mu}$  and  $\hat{\sigma}^2$  of  $\mu$  and  $\sigma^2$  by maximizing the likelihood function. This approach inherently captures an exploration-exploitation balance, since it takes into consideration the measurement error as well as the estimated values. Finally, EGO determines the next design for evaluation by maximizing the expected value of improvement compared to the best observation so far (Jones et al., 1998).

Knowles (2006a) proposes ParEGO, which is an adaptation of EGO in the  $m$ -objective case. Using an augmented Tchebycheff aggregation, the problem is reduced to a single-objective case and then solved by using EGO. After choosing uniformly at random an  $m$ -

dimensional vector  $\mathbf{\Lambda}$ , ParEGO computes the scalar cost of a design  $x$  using the augmented Tchebycheff function

$$f_{\mathbf{\Lambda}}(x) = \max_{1 \leq j \leq m} \{\lambda_j f_j(x)\} + \rho \sum_{j=1}^m \lambda_j f_j(x) ,$$

where  $\rho = 0.05$  in their paper. The max part of the function allows for minimizers in non-convex regions of the image space (which may be the case in a multi-objective optimization scenario), while the linear part is responsible for giving smaller rewards to weakly dominated solutions (see Definition 1). Using the computed values  $(f_{\mathbf{\Lambda}}(x_i))_{i=1}^n$  as observations, EGO is then used to return the design to be evaluated next, by maximizing the expected improvement.

On the other hand, SMS-EGO (Ponweiser et al., 2008) does not reduce the problem to a single-objective one, but instead maximizes the gain in hypervolume from optimistic estimates based on a GP model. SMS-EGO first estimates a set  $P$  of Pareto designs. Then, given design  $x \in \mathcal{X}$ , its optimistic estimate is defined as  $\hat{\mu}(x) + c \cdot \hat{\sigma}(x)$ , where  $c$  is a granularity parameter, while  $\hat{\mu}(x)$  and  $\hat{\sigma}(x)$  are the GP posterior vectors evaluated at design  $x$ . Then, the gain is defined as the hypervolume difference (Emmerich, 2005) yielded between the lower confidence bound of  $x$  and the estimated Pareto front (see Section 2.1). Note that maximizing the hypervolume gain is a valid approach for the multi-objective optimization problem, since no sub-optimal set would yield a maximum gain.

The hypervolume approach to Pareto learning is further exploited by Shah and Ghahramani (2016), and Daulton et al. (2020). Given a set  $\mathcal{Y} = \{\mathbf{y}_1, \dots, \mathbf{y}_n\}$  of evaluations, the subset of  $\mathcal{Y}$  containing all non-dominated evaluations is denoted by  $\mathcal{P}(\mathcal{Y})$ . Then, the Pareto hypervolume of  $\mathcal{P}(\mathcal{Y})$  with respect to a reference point  $\mathbf{y}_{\text{ref}} \in \mathbb{R}^m$  is given as

$$\text{Vol}_{\mathbf{y}_{\text{ref}}}(\mathcal{P}(\mathcal{Y})) = \int_{\mathbb{R}^m} \mathbb{I}(\mathbf{y}_{\text{ref}} \preceq \mathbf{y}) \left( 1 - \prod_{\mathbf{u} \in \mathcal{P}(\mathcal{Y})} \mathbb{I}(\mathbf{y} \not\leq \mathbf{u}) \right) d\mathbf{y} .$$

Informally, the Pareto hypervolume represents the volume of the space between the reference point and  $\mathcal{P}(\mathcal{Y})$ . The most important point of Shah and Ghahramani (2016) is to capture the potential correlation between the objectives by using multi-output GP priors. In the multi-output GP case, the problem of computing the expected improvement in the Pareto hypervolume becomes computationally intractable. Using a scaled probability density function as an approximation strategy, they provide a closed form analytical expression of an approximation of the hypervolume. Although they empirically show that capturing correlations between objectives grants substantial advantage to their method, it comes without theoretical guarantees. The computational complexity of computing the expected hypervolume gain is improved by extending the problem to the parallel constrained evaluation setting in Daulton et al. (2020). Apart from the computational efficiency and empirical superiority, their algorithm comes with theoretical convergence guarantees.

Furthermore, Hernández-Lobato et al. (2016) consider a (possibly infinite) bounded design space  $\mathcal{X}$  and assume that the individual objectives are samples from independent GPs. Their algorithm, PESMO, sequentially queries designs that maximize the acquisition function defined as the expected reduction in the entropy of the posterior distribution over the predicted Pareto set  $\mathcal{X}^*$ , given the previously sampled data  $\mathcal{D}$ . The acquisition function

at a data point  $(x, \mathbf{y})$  is thus formally defined as

$$\alpha(x) = H(\mathcal{X}^*|\mathcal{D}) - \mathbb{E}_{\mathbf{y}} [H(\mathcal{X}^*|\mathcal{D} \cup (x, \mathbf{y}))] .$$

Due to the practical difficulties in the exact evaluation of such a function, they equivalently formulate it as a predictive entropy search (Hernández-Lobato et al., 2014). Moreover, using properties of the Gaussian distribution, they use closed form approximations for this acquisition function. Although there are no theoretical guarantees provided, they give comprehensive experimental comparisons between PESMO and other multi-objective optimization methods over various objectives and dimensions, in both noisy and noiseless cases. The comparison is done with respect to the relative difference between the hypervolume of the predicted set and the maximum such hypervolume for the given number of evaluations. They also provide experimental comparison with respect to the prediction error over time.

Finally, the work on which our method is based is that of Zuluaga et al. (2013, 2016). Zuluaga et al. (2013) consider a finite design space and assume that each objective  $f_i$  in  $\mathbf{f}$ , for  $1 \leq i \leq m$ , is a sample from an independent GP. Although they do not explicitly assume dependence between the objective functions, they claim that such a scenario can be captured, mentioning Bonilla (2007) as an example. Their algorithm, Pareto Active Learning (PAL), is a confidence bound-based method. Given design  $x \in \mathcal{X}$  and the history  $\mathcal{D}$  of actions-observations, the confidence hyper-rectangle of  $x$  is defined as

$$\mathbf{Q}_{\mu, \sigma, \beta}(x) = \{\mathbf{y} \in \mathbb{R}^m : \mu(x) - \beta^{1/2}\sigma(x) \preceq \mathbf{y} \preceq \mu(x) + \beta^{1/2}\sigma(x)\} ,$$

where  $\mu(x)$  and  $\sigma(x)$  are the GP-posterior mean and standard deviation of  $x$  given  $\mathcal{D}$ , respectively, and  $\beta$  is a parameter tailored to yield theoretical guarantees for PAL. The algorithm proceeds in rounds  $t \geq 1$  and partitions the design space into three parts:  $P_t$  (predicted Pareto-optimal designs),  $N_t$  (predicted non-Pareto-optimal designs) and  $U_t$  (undecided designs). Furthermore, each round comprises different phases. The first phase is modeling, where PAL uses the posterior estimates in order to compute the confidence hyper-rectangles of designs which are still up for selection (the ones not in  $N_t$ ). Then, to each such design  $x$ , it associates an uncertainty region  $\mathbf{R}_t(x)$ , which is an intersection of all confidence hyper-rectangles of  $x$  so far. Then, PAL classifies a design as Pareto-optimal if its pessimistic outcome (the bottom-left corner of the rectangle in the two-dimensional case) is not dominated by the optimistic outcome (top-right corner) of any other design in  $U_t$ , where the inequality is considered up to a shift of both by  $\epsilon$ , where  $\mathbf{0} \preceq \epsilon$  represents the inequality error<sup>1</sup>. It then proceeds to discard a design if its optimistic outcome is dominated (up to a shift of both by  $\epsilon$ ) by the pessimistic outcome of some design in  $U_t$ . At the end of the round, PAL decides to evaluate the design  $x$  which maximizes the uncertainty diameter  $\omega_t(x)$  defined as  $\omega_t(x) = \max_{\mathbf{y}, \mathbf{y}' \in \mathbb{R}^m} \|\mathbf{y} - \mathbf{y}'\|_2$ . The sample complexity of PAL (and  $\epsilon$ -PAL (Zuluaga et al., 2016)) depends on the maximum information gain of a single-objective function. PAL terminates in at most  $T$  rounds, where  $T$  is the smallest natural number satisfying  $\sqrt{T}/(C\beta_T\gamma_T) \geq \epsilon$ ,  $C$  is a constant,  $\gamma_T$  is the maximum information gain in  $T$  rounds, and  $\epsilon$  is chosen in such a way that the maximum hypervolume error does not exceed a constant  $\eta$  in (Zuluaga et al., 2013), whereas  $\epsilon = \|\epsilon\|_\infty$  in (Zuluaga et al., 2016).

1. Zuluaga et al. (2013) formalize this rule as  $\epsilon$ -domination. See Definitions 1 and 2.

Table 1: *Comparison with related works.* <sup>(1)</sup>Both the algorithm and the performance analysis take into account dependence between the objectives.

Work	Design space	Function	Dep. <sup>(1)</sup>	Sample complex. bounds	Adaptive discret.
Auer et al. (2016)	Finite	Arbitrary	No	Gap-dependent	Not used
Zuluaga et al. (2013)	Finite	GP sample	No	Inf.-type	Not used
Zuluaga et al. (2016)	Finite	RKHS element	No	Inf.-type	Not used
Hernández-Lobato et al. (2016)	Bounded	GP sample	No	No bound	Not used
Shah and Ghahramani (2016)	Bounded	GP sample	Yes	No bound	Not used
Paria et al. (2020)	Compact	GP sample	No	Bayes Regret	Not used
Belakaria and Deshwal (2019)	General	GP sample	No	Regret norm	Not used
Belakaria et al. (2020)	Continuous	GP sample	No	Regret norm	Not used
Daulton et al. (2020)	Bounded	GP sample	No	Exp. Hypervol.	Not used
<b>Ours</b>	Compact	A GP sample	Yes	Inf. & dim.-type	Used

Apart from Pareto front identification, several works consider identifying designs that satisfy certain performance criteria. For instance, Katz-Samuels and Scott (2018) consider the problem of identifying designs whose objective values lie in a given polyhedron in the fixed confidence setting. On the other hand, Locatelli et al. (2016) consider the problem of identifying designs whose objective values are above a given threshold in the fixed budget setting. In addition, Gotovos (2013) consider level set identification when  $\mathbf{f}$  is a sample from a GP. There also exists a plethora of works developing algorithms for best arm identification in the context of single-objective pure-exploration MAB problems such as the ones by Mannor and Tsitsiklis (2004); Bubeck et al. (2009); Gabillon et al. (2012).

Adaptive discretization is a technique that is mainly used in regret minimization in MAB problems on metric spaces (Kleinberg et al., 2008; Bubeck et al., 2011), including contextual MAB problems (Shekhar et al., 2018), when dealing with large arm and context sets. It consists of adaptively partitioning the ground set along a tree structure into smaller and smaller regions, until, theoretically, the regions converge to a single point (under uniqueness assumptions in the single-objective case). Different from other upper confidence bound-based methods, here, the usual upper confidence bound of a given point  $x$  (in both frequentist and Bayesian approaches) is inflated with a factor times the diameter of the region containing  $x$ , so that the uncertainty coming from the variation of the function values inside the region is also captured. A key efficacy of adaptive discretization comes from the fact that it does not blindly sample the space without first exhaustively partitioning it as long as it is certain. This certainty is formalized by comparing the sample uncertainty diameter with the region diameter. If the latter exceeds the former, then the algorithm decides to partition the given region into smaller subregions. It is known that adaptive discretization can result in a much smaller regret compared to uniform discretization. However, this is significantly different from employing adaptive discretization in the context of PAL. While the regret can be minimized by quickly identifying one design that yields the highest expected reward, PAL requires identifying all designs that can form an  $\epsilon$ -Pareto front together, while at the same

time discarding all designs that are far from being Pareto optimal. Table 1 compares our approach with the related work.

### 1.3 Organization

We explain the properties of the function to be optimized and the structure of the design space in Section 2. This is followed by the description of Adaptive  $\epsilon$ -PAL in Section 3. We give sample complexity bounds for Adaptive  $\epsilon$ -PAL in Section 4, discuss the main aspects of computational complexity analysis in Section 5. We devote Section 6 to the computational experiments, followed by conclusions in Section 7. We present the proof of the main theorem separately in Section A, the appendix. At the end of the paper, we include a table for the frequently used notation.

## 2. Background and formulation

Throughout the paper, let us fix a positive integer  $m \geq 2$  and a compact metric space  $(\mathcal{X}, d)$ . We denote by  $\mathbb{R}^m$  the  $m$ -dimensional Euclidean space and by  $\mathbb{R}_+^m$  the set of all vectors in  $\mathbb{R}^m$  with nonnegative components. We write  $[m] = \{1, \dots, m\}$ . Given a function  $\mathbf{f}: \mathcal{X} \rightarrow \mathbb{R}^m$  and a set  $\mathcal{S} \subseteq \mathcal{X}$ , we denote by  $\mathbf{f}(\mathcal{S}) = \{\mathbf{f}(x): x \in \mathcal{S}\}$  the image of  $\mathcal{S}$  under  $\mathbf{f}$ . Given  $x \in \mathcal{X}$  and  $r \geq 0$ ,  $B(x, r) = \{y \in \mathcal{X}: d(x, y) \leq r\}$  denotes the closed ball centered at  $x$  with radius  $r$ . For a non-empty set  $\mathcal{S} \subseteq \mathbb{R}^m$ , let  $\partial\mathcal{S}$  denote its boundary. If another non-empty set  $\mathcal{S}' \subseteq \mathbb{R}^m$  is given, then we define the Minkowski sum and difference of  $\mathcal{S}$  and  $\mathcal{S}'$  as  $\mathcal{S} + \mathcal{S}' = \{\boldsymbol{\mu} + \boldsymbol{\mu}': \boldsymbol{\mu} \in \mathcal{S}, \boldsymbol{\mu}' \in \mathcal{S}'\}$ ,  $\mathcal{S} - \mathcal{S}' = \{\boldsymbol{\mu} - \boldsymbol{\mu}': \boldsymbol{\mu} \in \mathcal{S}, \boldsymbol{\mu}' \in \mathcal{S}'\}$ , respectively. For a vector  $\boldsymbol{\mu}'' \in \mathbb{R}^m$ , we define  $\boldsymbol{\mu}'' + \mathcal{S} = \{\boldsymbol{\mu}''\} + \mathcal{S}$ .

### 2.1 Multi-objective optimization

A multi-objective optimization problem is an optimization problem that involves multiple objective functions (Hwang and Masud, 2012). Formally, letting  $f^j: \mathcal{X} \rightarrow \mathbb{R}$  be a function for every  $j \in [m]$ , we write

$$\text{maximize } [f^1(x), \dots, f^m(x)]^\top \text{ subject to } x \in \mathcal{X},$$

where  $m \geq 2$  is the number of objectives and  $\mathcal{X}$  is the set of designs. We refer to the vector of all objectives evaluated at design  $x \in \mathcal{X}$  as  $\mathbf{f}(x) = [f^1(x), \dots, f^m(x)]^\top$ . The objective space is given as  $\mathbf{f}(\mathcal{X}) \subseteq \mathbb{R}^m$ . In order to define a set of Pareto optimal designs in  $\mathcal{X}$ , we first describe several order relations on  $\mathbb{R}^m$ .

**Definition 1.** For  $\boldsymbol{\mu}, \boldsymbol{\mu}' \in \mathbb{R}^m$ , we say that: (1)  $\boldsymbol{\mu}$  is weakly dominated by  $\boldsymbol{\mu}'$ , written as  $\boldsymbol{\mu} \preceq \boldsymbol{\mu}'$ , if  $\mu_j \leq \mu'_j$  for every  $j \in [m]$ . (2)  $\boldsymbol{\mu}$  is dominated by  $\boldsymbol{\mu}'$ , written as  $\boldsymbol{\mu} \prec \boldsymbol{\mu}'$ , if  $\boldsymbol{\mu} \preceq \boldsymbol{\mu}'$  and there exists  $j \in [m]$  with  $\mu_j < \mu'_j$ . (3) For  $\boldsymbol{\epsilon} \in \mathbb{R}_+^m$ ,  $\boldsymbol{\mu}$  is  $\boldsymbol{\epsilon}$ -dominated by  $\boldsymbol{\mu}'$ , written as  $\boldsymbol{\mu} \preceq_{\boldsymbol{\epsilon}} \boldsymbol{\mu}'$ , if  $\boldsymbol{\mu} \preceq \boldsymbol{\mu}' + \boldsymbol{\epsilon}$ . (4)  $\boldsymbol{\mu}$  is incomparable with  $\boldsymbol{\mu}'$ , written as  $\boldsymbol{\mu} \parallel \boldsymbol{\mu}'$ , if neither  $\boldsymbol{\mu} \prec \boldsymbol{\mu}'$  nor  $\boldsymbol{\mu}' \prec \boldsymbol{\mu}$  holds.

Based on Definition 1, we define the following induced relations on  $\mathcal{X}$ .

**Definition 2.** For designs  $x, y \in \mathcal{X}$ , we say that: (1)  $x$  is weakly dominated by  $y$ , written as  $x \preceq y$ , if  $\mathbf{f}(x) \preceq \mathbf{f}(y)$ . (2)  $x$  is dominated by  $y$ , written as  $x \prec y$ , if  $\mathbf{f}(x) \prec \mathbf{f}(y)$ . (3) For

$\epsilon \in \mathbb{R}_+^m$ ,  $x$  is  $\epsilon$ -dominated by  $y$ , written as  $x \preceq_\epsilon y$ , if  $\mathbf{f}(x) \preceq_\epsilon \mathbf{f}(y)$ . (4)  $x$  is incomparable with  $y$ , written as  $x \parallel y$ , if  $\mathbf{f}(x) \parallel \mathbf{f}(y)$ .

Note that, while the relation  $\preceq$  on  $\mathbb{R}^m$  (Definition 1) is a partial order, the induced relation  $\preceq$  on  $\mathcal{X}$  (Definition 2) is only a preorder since it does not satisfy antisymmetry in general. If a design  $x \in \mathcal{X}$  is not dominated by any other design, then we say that  $x$  is *Pareto optimal*. The set of all Pareto optimal designs is called the *Pareto set* and is denoted by  $\mathcal{O}(\mathcal{X})$ . The *Pareto front* is defined as  $\mathcal{Z}(\mathcal{X}) = \partial(\mathbf{f}(\mathcal{O}(\mathcal{X})) - \mathbb{R}_+^m)$ .

We assume that  $\mathbf{f}$  is not known beforehand and formalize the goal of identifying  $\mathcal{O}(\mathcal{X})$  as a sequential decision-making problem. In particular, we assume that evaluating  $\mathbf{f}$  at design  $x$  results in a noisy observation of  $\mathbf{f}(x)$ . The exact identification of the Pareto set and the Pareto front using a small number of evaluations is, in general, not possible under this setup, especially when the cardinality of  $\mathcal{X}$  is infinite or a very large finite number. A realistic goal is to identify the Pareto set and the Pareto front in an approximate sense, given a desired level of accuracy that can be specified as an input  $\epsilon$ . Therefore, our goal in this paper is to identify an  $\epsilon$ -accurate Pareto set (see Definition 5) that contains a set of near-Pareto optimal designs by using as few evaluations as possible. Next, we define the  $\epsilon$ -Pareto front and  $\epsilon$ -accurate Pareto set associated with  $\mathcal{X}$ .

**Definition 3.** Given  $\epsilon \in \mathbb{R}_+^m$ , the set  $\mathcal{Z}_\epsilon(\mathcal{X}) = (\mathbf{f}(\mathcal{O}(\mathcal{X})) - \mathbb{R}_+^m) \setminus (\mathbf{f}(\mathcal{O}(\mathcal{X})) - 2\epsilon - \mathbb{R}_+^m)$  is called the  $\epsilon$ -Pareto front of  $\mathcal{X}$ .

Roughly speaking, the  $\epsilon$ -Pareto front can be thought of as the slab of points of width  $2\epsilon$  in  $\mathbb{R}^m$  adjoined to the lower side of the Pareto front.

**Definition 4.** Given  $\epsilon \in \mathbb{R}_+^m$  and  $\mathcal{S} \subseteq \mathbb{R}^m$ , a non-empty subset  $\mathcal{C}$  of  $\mathcal{S}$  is called an  $\epsilon$ -covering of  $\mathcal{S}$  if for every  $\mu \in \mathcal{S}$ , there exists  $\mu' \in \mathcal{C}$  such that  $\mu \preceq_\epsilon \mu'$ .

**Definition 5.** Given  $\epsilon \in \mathbb{R}_+^m$ , a subset  $\mathcal{O}_\epsilon$  of  $\mathcal{X}$  is called an  $\epsilon$ -accurate Pareto set if  $\mathbf{f}(\mathcal{O}_\epsilon)$  is an  $\epsilon$ -covering of  $\mathcal{Z}_\epsilon(\mathcal{X})$ .

Note that the front associated with an  $\epsilon$ -accurate Pareto set is a subset of the  $\epsilon$ -Pareto front. As mentioned in Zuluaga et al. (2016), an  $\epsilon$ -accurate Pareto set is a natural substitute of the Pareto set, since any  $\epsilon$ -accurate Pareto design is guaranteed to be no worse than  $2\epsilon$  of any Pareto optimal design.

## 2.2 Structure and dimensionality of the design space

In order to learn, we need to make use of some concepts which facilitate understanding the structure of the space and ‘navigating’ it. To that end, we will assume that the design space is *well-behaved*. This will allow us to partition the design space  $\mathcal{X}$  along a tree structure, each level  $h$  of which is associated to a partition of  $\mathcal{X}$  into  $N^h$  equal-sized regions  $X_{h,i}$ , centered at a node  $x_{h,i}$ , for all  $0 \leq i \leq N^h$ , where  $N \in \mathbb{N}$ . The formal definition is as follows.

**Definition 6.** (Well-behaved metric space Bubeck et al. (2011)) The compact metric space  $(\mathcal{X}, d)$  is said to be **well-behaved** if there exists a sequence  $(\mathcal{X}_h)_{h \geq 0}$  of subsets of  $\mathcal{X}$  satisfying the following properties:



1. There exists  $N \in \mathbb{N}$  such that for each  $h \geq 0$ , the set  $\mathcal{X}_h$  has  $N^h$  elements. We write  $\mathcal{X}_h = \{x_{h,i} : 1 \leq i \leq N^h\}$  and to each element  $x_{h,i}$  is associated a cell  $X_{h,i} = \{x \in \mathcal{X} : \forall j \neq i : d(x, x_{h,i}) \leq d(x, x_{h,j})\}$ .
2. For all  $h \geq 0$  and  $1 \leq i \leq N^h$ , we have  $X_{h,i} = \bigcup_{j=N(i-1)+1}^{Ni} X_{h+1,j}$ . The nodes  $x_{h+1,j}$  for  $N(i-1)+1 \leq j \leq Ni$  are called the children of  $x_{h,i}$ , which in turn is referred to as the parent of these nodes. We write  $p(x_{h+1,j}) = x_{h,i}$  for every  $N(i-1)+1 \leq j \leq Ni$ .
3. We assume that the cells have geometrically decaying radii, i.e., there exist  $0 < \rho < 1$  and  $0 < v_2 \leq 1 \leq v_1$  such that we have  $B(x_{h,i}, v_2 \rho^h) \subseteq X_{h,i} \subseteq B(x_{h,i}, v_1 \rho^h)$  for every  $h \geq 0$ . Note that we have  $2v_2 \rho^h \leq \text{diam}(X_{h,i}) \leq 2v_1 \rho^h$ , where  $\text{diam}(X_{h,i}) = \sup_{x,y \in X_{h,i}} d(x,y)$ .

The first property implies that, for every  $h \geq 0$ , the cells  $X_{h,i}$ ,  $1 \leq i \leq N^h$  partition  $\mathcal{X}$ . This can be observed trivially by *reductio ad absurdum*. The second property intuitively means that, as  $h$  grows, we get a more refined partition. The third property implies that the nodes  $x_{h,i}$  are evenly spread out in the space.

Additionally, we make use of a notion of dimensionality intrinsic to the design space, namely, the *metric dimension*.

**Definition 7.** (*Packing, Covering and Metric Dimension Shekhar et al. (2018)*) Let  $r \geq 0$ .

- A subset  $\mathcal{X}_1$  of  $\mathcal{X}$  is called an  **$r$ -packing** of  $\mathcal{X}$  if for every  $x, y \in \mathcal{X}_1$  such that  $x \neq y$ , we have  $d(x, y) > r$ . The largest cardinality of such a set is called the  $r$ -packing number of  $\mathcal{X}$  with respect to  $d$ , and is denoted by  $M(\mathcal{X}, r, d)$ .
- A subset  $\mathcal{X}_2$  of  $\mathcal{X}$  is called an  **$r$ -covering**<sup>2</sup> of  $\mathcal{X}$  if for every  $x \in \mathcal{X}$ , there exists  $y \in \mathcal{X}_2$  such that  $d(x, y) \leq r$ . The smallest cardinality of such a set is called the  $r$ -covering number of  $\mathcal{X}$  with respect to  $d$ , and is denoted by  $N(\mathcal{X}, r, d)$ .
- The **metric dimension**  $D_1$  of  $(\mathcal{X}, d)$  is defined as  $D_1 = \inf\{a \geq 0 : \exists C \geq 0, \forall r > 0 : \log(N(\mathcal{X}, r, d)) \leq C - a \log(r)\}$ .

This dimension coincides with the usual dimension of the space when  $\mathcal{X}$  is a subspace of a finite-dimensional Euclidean space. We will upper bound the sample complexity of the algorithm using the metric dimension of  $(\mathcal{X}, d)$ .

### 2.3 Prior knowledge on $f$

We model the vector  $\mathbf{f} = [f^1, \dots, f^m]^\top$  of objective functions as a realization of an  $m$ -output GP with zero mean, i.e.,  $\boldsymbol{\mu}(x) = \mathbf{0}$  for all  $x \in \mathcal{X}$ , and some positive definite covariance function  $\mathbf{k}$ .

**Definition 8.** An  **$m$ -output GP** with index set  $\mathcal{X}$  is a collection  $(\mathbf{f}(x))_{x \in \mathcal{X}}$  of  $m$ -dimensional random vectors which satisfies the property that  $(\mathbf{f}(x_1), \dots, \mathbf{f}(x_n))$  is a Gaussian random vector for all  $\{x_1, \dots, x_n\} \subseteq \mathcal{X}$  and  $n \in \mathbb{N}$ . The probability law of an  $m$ -output GP  $(\mathbf{f}(x))_{x \in \mathcal{X}}$

---

2. Not to be confused with  $\epsilon$ -covering in Definition 4, where  $\epsilon \in \mathbb{R}_+^m$ . The meaning will be clear from the context.

is uniquely specified by its (vector-valued) mean function  $x \mapsto \boldsymbol{\mu}(x) = \mathbb{E}[\mathbf{f}(x)] \in \mathbb{R}^m$  and its (matrix-valued) covariance function  $(x_1, x_2) \mapsto \mathbf{k}(x_1, x_2) = \mathbb{E}[(\mathbf{f}(x_1) - \boldsymbol{\mu}(x_1))(\mathbf{f}(x_2) - \boldsymbol{\mu}(x_2))^\top] \in \mathbb{R}^{m \times m}$ .

Functions generated from a GP naturally satisfy smoothness conditions which are very useful while working with metric spaces, as indicated by the following remark.

**Remark 1.** Let  $g$  be a zero-mean, single-output GP with index set  $\mathcal{X}$  and covariance function  $k$ . The metric  $l$  induced by the GP on  $\mathcal{X}$  is defined as  $l(x_1, x_2) = (\mathbb{E}[(g(x_1) - g(x_2))^2])^{1/2} = (k(x_1, x_1) + k(x_2, x_2) - 2k(x_1, x_2))^{1/2}$ . This gives us the following tail bound for  $x_1, x_2 \in \mathcal{X}$ , and  $a \geq 0$ :  $\mathbb{P}(|g(x_1) - g(x_2)| \geq a) \leq 2\exp(-a^2/(2l^2(x_1, x_2)))$ .

Let us fix an integer  $T \geq 1$ . We consider a finite sequence  $\tilde{x}_{[T]} = [\tilde{x}_1, \dots, \tilde{x}_T]^\top$  of designs with the corresponding vector  $\mathbf{f}_{[T]} = [\mathbf{f}(\tilde{x}_1)^\top, \dots, \mathbf{f}(\tilde{x}_T)^\top]^\top$  of unobserved objective values and the ( $mT$ -dimensional) vector  $\mathbf{y}_{[T]} = [\mathbf{y}_1^\top, \dots, \mathbf{y}_T^\top]^\top$  of observations, where

$$\mathbf{y}_\tau = \mathbf{f}(\tilde{x}_\tau) + \boldsymbol{\kappa}_\tau$$

is the observation that corresponds to  $\tilde{x}_\tau$  and  $\boldsymbol{\kappa}_\tau = [\kappa_\tau^1, \dots, \kappa_\tau^m]^\top$  is the noise vector that corresponds to this particular evaluation for each  $\tau \in [T]$ .

The posterior distribution of  $\mathbf{f}$  given  $\mathbf{y}_{[T]}$  is that of an  $m$ -output GP with mean function  $\boldsymbol{\mu}_T$  and covariance function  $\mathbf{k}_T$  given by

$$\boldsymbol{\mu}_T(x) = \mathbf{k}_{[T]}(x)(\mathbf{K}_{[T]} + \boldsymbol{\Sigma}_{[T]})^{-1}\mathbf{y}_{[T]}^\top$$

and

$$\mathbf{k}_T(x, x') = \mathbf{k}(x, x') - \mathbf{k}_{[T]}(x)(\mathbf{K}_{[T]} + \boldsymbol{\Sigma}_{[T]})^{-1}\mathbf{k}_{[T]}(x')^\top$$

for all  $x, x' \in \mathcal{X}$ , where  $\mathbf{k}_{[T]}(x) = [\mathbf{k}(x, \tilde{x}_1), \dots, \mathbf{k}(x, \tilde{x}_T)] \in \mathbb{R}^{m \times mT}$ ,

$$\mathbf{K}_{[T]} = \begin{bmatrix} \mathbf{k}(\tilde{x}_1, \tilde{x}_1), & \dots, & \mathbf{k}(\tilde{x}_1, \tilde{x}_T) \\ \vdots & & \vdots \\ \mathbf{k}(\tilde{x}_T, \tilde{x}_1), & \dots, & \mathbf{k}(\tilde{x}_T, \tilde{x}_T) \end{bmatrix}, \boldsymbol{\Sigma}_{[T]} = \begin{bmatrix} \sigma^2 \mathbf{I}_m, & \mathbf{0}_m, & \dots, & \mathbf{0}_m \\ \vdots & & & \vdots \\ \mathbf{0}_m, & \mathbf{0}_m, & \dots, & \sigma^2 \mathbf{I}_m \end{bmatrix} \in \mathbb{R}^{mT \times mT},$$

$\mathbf{I}_m$  denotes the  $m \times m$ -dimensional identity matrix, and  $\mathbf{0}_m$  is the  $m \times m$ -dimensional zero matrix. Note that this posterior distribution captures the uncertainty in  $\mathbf{f}(x)$  for all  $x \in \mathcal{X}$ . In particular, the posterior distribution of  $\mathbf{f}(x)$  is  $\mathcal{N}(\boldsymbol{\mu}_T(x), \mathbf{k}_T(x, x))$ ; and for each  $j \in [m]$ , the posterior distribution of  $f^j(x)$  is  $\mathcal{N}(\mu_T^j(x), (\sigma_T^j(x))^2)$ , where  $(\sigma_T^j(x))^2 = k_T^{jj}(x, x)$ . Moreover, the distribution of the corresponding observation  $\mathbf{y}$  is  $\mathcal{N}(\boldsymbol{\mu}_T(x), \mathbf{k}_T(x, x) + \sigma^2 \mathbf{I}_m)$ .

## 2.4 Information gain

Since we aim at finding an  $\epsilon$ -accurate Pareto set in as few evaluations as possible, we need to learn the most informative designs. In order to do that, we will make use of the notion of *information gain*. Our sample complexity result in Theorem 1 depends on the maximum information gain.

In Bayesian experimental design, the informativeness of a finite sequence  $\tilde{x}_{[T]}$  of designs is quantified by  $I(\mathbf{y}_{[T]}; \mathbf{f}_{[T]}) = H(\mathbf{y}_{[T]}) - H(\mathbf{y}_{[T]} | \mathbf{f}_{[T]})$ , where  $H(\cdot)$  denotes the entropy of a random vector and  $H(\cdot | \mathbf{f}_{[T]})$  denotes the conditional entropy of a random vector with respect to  $\mathbf{f}_{[T]}$ . This measure is called the information gain, which gives us the decrease of entropy of  $\mathbf{f}_{[T]}$  given the observations  $\mathbf{y}_{[T]}$ . We define the *maximum information gain* as  $\gamma_T = \max_{\mathbf{y}_{[T]}} I(\mathbf{y}_{[T]}; \mathbf{f}_{[T]})$ .

### 3. Adaptive $\epsilon$ -PAL algorithm

The system operates in rounds  $t \geq 1$ . In each round  $t$ , the algorithm picks a design  $x_t \in \mathcal{X}$ , and assuming that it already had  $\tau$  evaluations, it subsequently decides whether or not to obtain the  $\tau + 1$ st noisy observation  $\mathbf{y}_{\tau+1} = [y_{\tau+1}^1, \dots, y_{\tau+1}^m]^\top$  of the latent function  $\mathbf{f}$  at  $x_t$ . At the end, our algorithm returns a subset  $\hat{P}$  of  $\mathcal{X}$  which is guaranteed to be an  $\epsilon$ -accurate Pareto set with high probability and the associated set  $\hat{\mathcal{P}}$  of nodes which we will define later. The pseudocode is given in Algorithm 1.

#### 3.1 Modeling

We maintain two sets of time indices, one counting the total number of iterations, denoted by  $t$ , and the other counting only the evaluation rounds, denoted by  $\tau$ . The algorithm evaluates a design only in some rounds. For this reason, we also define the following auxiliary time variables which help us understand the chronological connection between the values of  $t$  and  $\tau$ . We let  $\tau_t$  represent the number of evaluations before round  $t \geq 1$  and let  $t_\tau$  denote the round when evaluation  $\tau \geq 0$  is made, with the convention  $t_0 = 0$ . The sequence  $(t_\tau)_{\tau \geq 0}$  is an increasing sequence of stopping times. Note that we have  $\tau_{t_{\tau+1}} = \tau$  for each  $\tau \in \mathbb{N}$ .

Iteration over individual designs may not be feasible when the cardinality of the design space is very large. Thus, we consider partitioning the space into regions of similar designs, i.e., two designs in  $\mathcal{X}$  which are at a close distance have similar outcomes in each objective. This is a natural property of GP-sampled functions as discussed in Remark 1. Since our metric space is well-behaved (see Definition 6), there exist an  $N \in \mathbb{N}$  and a sequence  $(\mathcal{X}_h)_{h \geq 0}$  of subsets of  $\mathcal{X}$  such that for each  $h \geq 0$ , the set  $\mathcal{X}_h$  contains  $N^h$  nodes denoted by  $x_{h,1}, \dots, x_{h,N^h}$ . For each  $i \in [N^h]$ , the associated cell of node  $x_{h,i}$  is denoted by  $X_{h,i}$ .

At each round  $t \in \mathbb{N}$ , the algorithm maintains a set  $\mathcal{S}_t$  of *undecided nodes* and a set  $\mathcal{P}_t$  of *decided nodes*. For an undecided node in  $\mathcal{S}_t$ , its associated cell consists of designs for which we are undecided about including in the  $\epsilon$ -accurate Pareto set. Similarly, for a decided node in  $\mathcal{P}_t$ , its associated cell consists of designs that we decide to include in the  $\epsilon$ -accurate Pareto set. At the beginning of round  $t = 1$  (initialization), we set  $\mathcal{S}_1 = \{x_{0,1}\}$  and  $\mathcal{P}_1 = \emptyset$ . Within each round  $t \in \mathbb{N}$ , the sets  $\mathcal{P}_t$  and  $\mathcal{S}_t$  are updated during the discarding,  $\epsilon$ -covering and refining/evaluating phases of the round; at the end of round  $t$ , their finalized contents are set as  $\mathcal{P}_{t+1}$  and  $\mathcal{S}_{t+1}$ , respectively, as a preparation for round  $t + 1$ . For each  $t \in \mathbb{N}$ , the algorithm performs round  $t$  as long as  $\mathcal{S}_t \neq \emptyset$  at the beginning of round  $t$ ; otherwise, it terminates and returns  $\hat{\mathcal{P}} = \mathcal{P}_t$ .

In addition to the sets of undecided and decided nodes, the algorithm maintains a set  $\mathcal{A}_t$  of *active nodes*, which is defined as the union  $\mathcal{S}_t \cup \mathcal{P}_t$  at the beginning of each round  $t \in \mathbb{N}$ .

While the sets  $\mathcal{S}_t$  and  $\mathcal{P}_t$  are updated within round  $t$  as described above, the set  $\mathcal{A}_t$  is kept fixed throughout the round with its initial content. Note that  $\mathcal{A}_1 = \{x_{0,1}\}$ .

At round  $t \in \mathbb{N}$ , the algorithm considers each node  $x_{h,i} \in \mathcal{A}_t$ . Let  $j \in [m]$ . We define the *lower index* of  $x_{h,i}$  in the  $j$ th objective as  $L_t^j(x_{h,i}) = \underline{B}_t^j(x_{h,i}) - V_h$ , where  $\underline{B}_t^j(x_{h,i})$  is a high probability lower bound on the  $j$ th objective value at  $x_{h,i}$  and is defined as

$$\underline{B}_t^j(x_{h,i}) = \max\{\mu_{\tau_t}^j(x_{h,i}) - \beta_{\tau_t}^{1/2}\sigma_{\tau_t}^j(x_{h,i}), \mu_{\tau_t}^j(p(x_{h,i})) - \beta_{\tau_t}^{1/2}\sigma_{\tau_t}^j(p(x_{h,i})) - V_{h-1}\} .$$

Here,  $\beta_\tau$  is a parameter to be defined later and  $V_h$  is a high probability upper bound on the maximum variation of the objective  $j$  inside region  $X_{h,i}$ , which will also be defined later. Similarly, we define the *upper index* of  $x_{h,i}$  in the  $j$ th objective as  $U_t^j(x_{h,i}) = \bar{B}_t^j(x_{h,i}) + V_h$ , where  $\bar{B}_t^j(x_{h,i})$  is a high probability upper bound on the  $j$ th objective value at  $x_{h,i}$  and is defined as

$$\bar{B}_t^j(x_{h,i}) = \min\{\mu_{\tau_t}^j(x_{h,i}) + \beta_{\tau_t}^{1/2}\sigma_{\tau_t}^j(x_{h,i}), \mu_{\tau_t}^j(p(x_{h,i})) + \beta_{\tau_t}^{1/2}\sigma_{\tau_t}^j(p(x_{h,i})) + V_{h-1}\} .$$

We denote by  $\mathbf{L}_t(x_{h,i}) = [L_t^1(x_{h,i}), \dots, L_t^m(x_{h,i})]^\top$  the *lower index vector* of the node  $x_{h,i}$  at round  $t$  and similarly by  $\mathbf{U}_t(x_{h,i}) = [U_t^1(x_{h,i}), \dots, U_t^m(x_{h,i})]^\top$  the corresponding *upper index vector*. We also let  $\mathbf{V}_h$  denote the  $m$ -dimensional vector with all entries being equal to  $V_h$ . Next, we define the *confidence hyper-rectangle* of node  $x_{h,i}$  at round  $t$  as

$$\mathbf{Q}_t(x_{h,i}) = \{\mathbf{y} \in \mathbb{R}^m : \mathbf{L}_t(x_{h,i}) \preceq \mathbf{y} \preceq \mathbf{U}_t(x_{h,i})\} ,$$

which captures the uncertainty in the learner's prediction of the objective values. Then, the posterior mean vector  $\boldsymbol{\mu}_{\tau_t}(x_{h,i}) = [\mu_{\tau_t}^1(x_{h,i}), \dots, \mu_{\tau_t}^m(x_{h,i})]^\top$  and the variance vector  $\boldsymbol{\sigma}_{\tau_t}(x_{h,i}) = [\sigma_{\tau_t}^1(x_{h,i}), \dots, \sigma_{\tau_t}^m(x_{h,i})]^\top$  are computed by using the GP inference outlined in Section 2. We define the *cumulative confidence hyper-rectangle* of  $x_{h,i}$  at round  $t$  as

$$\mathbf{R}_t(x_{h,i}) = \mathbf{R}_{t-1}(x_{h,i}) \cap \mathbf{Q}_t(x_{h,i}) \tag{1}$$

assuming that  $\mathbf{R}_{t-1}(x_{h,i})$  is well-defined at round  $t-1$  (the case  $t \geq 2$ ) or using the convention that  $\mathbf{R}_0(x_{0,1}) = \mathbb{R}^m$  since  $\mathcal{A}_1 = \{x_{0,1}\}$  (the case  $t = 1$ ). The well-definedness assumption will be verified in the refining/evaluating phase below.

### 3.2 Discarding phase

In order to correctly identify designs to be discarded under uncertainty, we need to compare the pessimistic and optimistic outcomes of designs. First, we define dominance under uncertainty.

**Definition 9.** *Let  $t \in \mathbb{N}$  and let  $x, y \in \mathcal{A}_t$  be two nodes with  $x \neq y$ . We say that  $x$  is  $\epsilon$ -dominated by  $y$  **under uncertainty** at round  $t$  if  $\max(\mathbf{R}_t(x)) \preceq_\epsilon \min(\mathbf{R}_t(y))$ , where we define  $\max(\mathbf{R}_t(x))$  as the unique vector  $\mathbf{v} \in \mathbf{R}_t(x)$  such that  $v^j \geq z^j$  for every  $j \in [m]$  and  $\mathbf{z} = (z^1, \dots, z^m) \in \mathbf{R}_t(x)$ , and we define  $\min(\mathbf{R}_t(y))$  in a similar fashion.*

If a node  $x \in \mathcal{A}_t$  is  $\epsilon$ -dominated by any other node in  $\mathcal{A}_t$  under uncertainty, then the algorithm is confident enough to discard it. To check this, the algorithm compares  $x$  with all of the *pessimistic* available points as introduced next.

**Definition 10. (Pessimistic Pareto set)** Let  $t \geq 1$  and let  $D \subseteq \mathcal{A}_t$  be a set of nodes. We define  $p_{\text{pess},t}(D)$ , called the **pessimistic Pareto set** of  $D$  at round  $t$ , as the set of all nodes  $x \in D$  for which there is no other node  $y \in D \setminus \{x\}$  such that  $\min(\mathbf{R}_t(x)) \preceq \min(\mathbf{R}_t(y))$ . We call a design in  $p_{\text{pess},t}(D)$  a **pessimistic Pareto design** of  $D$  at round  $t$ .

Here we are interested in finding the nodes, say  $x$ , which are Pareto optimal in the most pessimistic scenario when their objective values turn out to be  $\min \mathbf{R}_t(x)$ . We do this in order to identify which nodes (and their associated cells) to discard with overwhelming probability. More precisely, the algorithm calculates  $\mathcal{P}_{\text{pess},t} = p_{\text{pess},t}(\mathcal{A}_t)$  first. For each  $x_{h,i} \in \mathcal{S}_t \setminus \mathcal{P}_{\text{pess},t}$ , it checks if  $\max(\mathbf{R}_t(x_{h,i})) \preceq_\epsilon \min(\mathbf{R}_t(x))$  for some  $x \in \mathcal{P}_{\text{pess},t}$ . In this case, node  $x_{h,i}$  is discarded, that is, it is removed from  $\mathcal{S}_t$ , and will not be considered in the rest of the algorithm; otherwise no change is made in  $\mathcal{S}_t$ .

### 3.3 $\epsilon$ -Covering phase

The overall aim of the learner is to empty the set  $\mathcal{S}_t$  of undecided nodes as fast as possible. A node  $x_{h,i} \in \mathcal{S}_t$  is moved to the decided set  $\mathcal{P}_t$  if it is determined that the associated cell  $X_{h,i}$  belongs to an  $\epsilon$ -accurate Pareto set  $\mathcal{O}_\epsilon$  with high probability. To check this, the notion in the next definition is useful. Let us denote by  $\mathcal{W}_t$  the union  $\mathcal{P}_t \cup \mathcal{S}_t$  at the end of the discarding phase. Note that  $\mathcal{W}_t \subseteq \mathcal{A}_t$  but the two sets do not coincide in general due to the discarding phase.

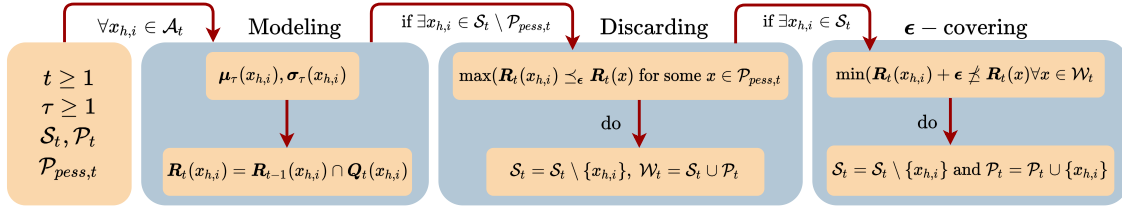


Figure 1: This is an illustration of the modeling, discarding, and  $\epsilon$ -covering phases.

**Definition 11.** Let  $x_{h,i} \in \mathcal{S}_t$ . We say that the cell  $X_{h,i}$  associated to node  $x_{h,i}$  **belongs to an  $\mathcal{O}_\epsilon$  with high probability** if there is no  $x \in \mathcal{W}_t$  such that  $\min(\mathbf{R}_t(x_{h,i})) + \epsilon \preceq \max(\mathbf{R}_t(x))$ .

For each  $x_{h,i} \in \mathcal{S}_t$ , the algorithm checks if  $X_{h,i}$  belongs to an  $\mathcal{O}_\epsilon$  with high probability in view of Definition 11. In this case,  $x_{h,i}$  is removed from the set  $\mathcal{S}_t$  of undecided nodes and is moved to the set  $\mathcal{P}_t$  of decided nodes; otherwise, no change is made. The nodes in  $\mathcal{P}_t$  are never removed from this set; hence, they will be returned by the algorithm as part of the set  $\hat{\mathcal{P}}$  at termination. In the appendix, we show that the union  $\hat{P} = \bigcup_{x_{h,i} \in \hat{\mathcal{P}}} X_{h,i}$  of the cells is an  $\epsilon$ -accurate Pareto cover, according to Definition 5, with high probability.

Note that while the sets  $\mathcal{S}_t, \mathcal{P}_t$  can be modified during this phase, the set  $\mathcal{W}_t$  does not change.

The modeling, discarding, and  $\epsilon$ -covering phases of the algorithm are illustrated in Figure 1.

### 3.4 Refining/evaluating phase

While  $\mathcal{S}_t \neq \emptyset$ , the algorithm selects a design  $x_t = x_{h_t, i_t} \in \mathcal{W}_t$  that corresponds to a node with depth  $h_t$  and index  $i_t$ , according to the following rule. First, for a given node  $x_{h,i} \in \mathcal{W}_t$ , we define

$$\omega_t(x_{h,i}) = \max_{y, y' \in \mathbf{R}_t(x_{h,i})} \|y - y'\|_2, \quad (2)$$

which is the diameter of its cumulative confidence hyper-rectangle in  $\mathbb{R}^m$ . The algorithm picks the most uncertain node for evaluation in order to decrease uncertainty. Hence, among the available points in  $\mathcal{W}_t$ , the node  $x_{h_t, i_t}$  with the maximum such diameter is chosen by the algorithm. We denote the diameter of the cumulative confidence hyper-rectangle associated with the selected node by  $\bar{\omega}_t$  and formally define it as  $\bar{\omega}_t = \max_{x_{h,i} \in \mathcal{W}_t} \omega_t(x_{h,i})$ . Since the learner is not sure about discarding  $x_{h_t, i_t}$  or moving it to  $\mathcal{P}_t$ , he decides whether to refine the associated region  $X_{h_t, i_t}$  or evaluating the objective function at the current node based on the following rule.

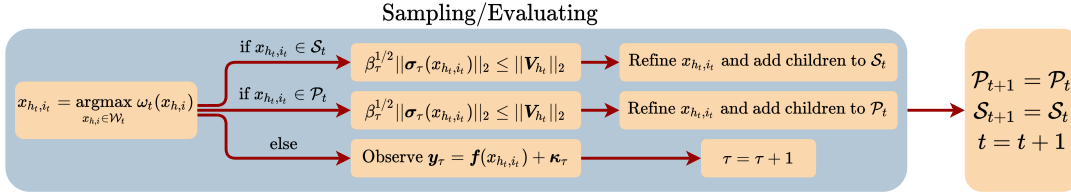


Figure 2: This is an illustration of the sampling and refining phase.

- *Refine*: If  $\beta_{\tau_t}^{1/2} \|\sigma_{\tau_t}(x_{h_t, i_t})\|_2 \leq \|\mathbf{V}_{h_t}\|_2$ , then  $x_{h_t, i_t}$  is expanded, i.e., the  $N$  children nodes  $\{x_{h_t+1, j} : N(i_t - 1) + 1 \leq j \leq i_t\}$  of  $x_{h_t, i_t}$  are generated. If  $x_{h_t, i_t} \in \mathcal{S}_t$ , then these newly generated nodes are added to  $\mathcal{S}_t$  while  $x_{h_t, i_t}$  is removed from  $\mathcal{S}_t$ . An analogous operation is performed if  $x_{h_t, i_t} \in \mathcal{P}_t$ . In each case, for each  $j$  with  $N(i_t - 1) + 1 \leq j \leq i_t$ , the newly generated node  $x_{h_t+1, j}$  inherits the cumulative confidence hyper-rectangle of its parent node  $x_{h_t, i_t} \in \mathcal{A}_t$  as calculated by (1), that is, we define  $\mathbf{R}_t(x_{h_t+1, j}) = \mathbf{R}_t(x_{h_t, i_t}) = \mathbf{R}_{t-1}(x_{h_t, i_t}) \cap \mathbf{Q}_t(x_{h_t, i_t})$ . This way, for every node  $x \in \mathcal{P}_t \cup \mathcal{S}_t$  at the end of refining, the cumulative confidence hyper-rectangles up to round  $t$  are well-defined and we have  $\mathbf{R}_0(x) \supseteq \mathbf{R}_1(x) \supseteq \dots \supseteq \mathbf{R}_t(x)$ . In particular, the well-definedness assumption for (1) is verified for round  $t + 1$  since  $\mathcal{A}_{t+1}$  is defined as  $\mathcal{P}_t \cup \mathcal{S}_t$  at the end of this phase.
- *Evaluate*: If  $\beta_{\tau_t}^{1/2} \|\sigma_{\tau_t}(x_{h_t, i_t})\|_2 > \|\mathbf{V}_{h_t}\|_2$ , then the objective function is evaluated at the point  $x_{h_t, i_t}$ , i.e., we observe the noisy sample  $\mathbf{y}_{\tau_t}$  and update the posterior statistics of  $x_{h_t, i_t}$ . No change is made in  $\mathcal{S}_t$  and  $\mathcal{P}_t$ .

This phase of the algorithm is illustrated in Figure 2. The evolution of the partitioning of the design space is illustrated in Figure 3.

### 3.5 Termination

If  $\mathcal{S}_t = \emptyset$  at the beginning of round  $t$ , then the algorithm terminates. We show in the appendix that at the latest, the algorithm terminates when  $\bar{\omega}_t \leq \min_j \epsilon^j$ . Upon termination,

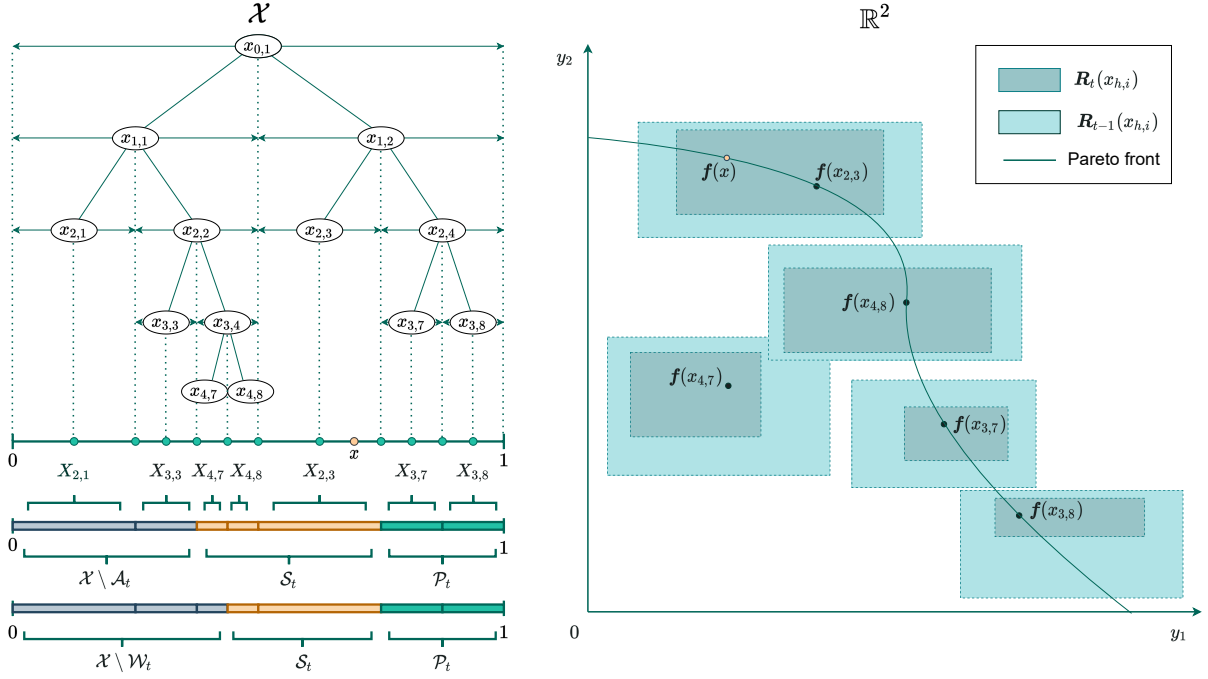


Figure 3: This is an illustration of the structural way of partitioning the design space. In this example we take  $\mathcal{X} = [0, 1]$ ,  $m = 2$  and  $\epsilon = \mathbf{0}$ . On the left, we can see the partition of  $\mathcal{X}$  at the beginning of round  $t$ . Note that  $\mathcal{S}_t = \{x_{4,7}, x_{4,8}, x_{2,3}\}$  and  $\mathcal{P}_t = \{x_{3,7}, x_{3,8}\}$ , while  $x_{2,1}$  and  $x_{3,3}$  have been discarded in some prior round. On the right, we see the corresponding confidence hyper-rectangles of these nodes. At the beginning of round  $t$ , prior to the modeling phase, the hyper-rectangle of node  $x_{h,i}$  is  $\mathbf{R}_{t-1}(x_{h,i})$ . Note that, in the discarding phase, node  $x_{4,8}$  will be discarded since  $\max(\mathbf{R}_t(x_{4,8})) \preceq_{\epsilon} \min(\mathbf{R}_t(x_{4,7}))$ . Thus,  $x_{4,7}$  will be removed from  $\mathcal{S}_t$  by the end of the phase. Furthermore, note that more than one Pareto optimal designs take values in one hyper-rectangle. This is because the node of a region containing Pareto optimal points is not necessarily one of these points. For example, we have  $x \in X_{2,3}$  and  $\mathbf{f}(x) \in \mathbf{R}_t(x_{2,3})$ .

it returns a non-empty set  $\hat{\mathcal{P}}$  of decided nodes together with the corresponding  $\epsilon$ -accurate Pareto set

$$\hat{\mathcal{P}} = \bigcup_{x_{h,i} \in \hat{\mathcal{P}}} X_{h,i},$$

which is the union of the cells corresponding to the nodes in  $\hat{\mathcal{P}}$ .

#### 4. Sample complexity bounds

We state the main result in this section. Its proof is composed of a sequence of lemmas which are given in the appendix. We first state the necessary assumptions (Assumption 1)

---

**Algorithm 1** Adaptive  $\epsilon$ -PAL

---

**Input:**  $\mathcal{X}$ ,  $(\mathcal{X}_h)_{h \geq 0}$ ,  $(V_h)_{h \geq 0}$ ,  $\epsilon$ ,  $\delta$ ,  $(\beta_\tau)_{\tau \geq 1}$ ; GP prior  $\boldsymbol{\mu}_0 = \boldsymbol{\mu}$ ,  $\mathbf{k}_0 = \mathbf{k}$

- 1: **Initialize:**  $\mathcal{P}_1 = \emptyset$ ,  $\mathcal{S}_1 = \{x_{0,1}\}$ ;  $\mathbf{R}_0(x_{0,1}) = \mathbb{R}^m$ ,  $t = 1$ ,  $\tau = 0$ .
- 2: **while**  $\mathcal{S}_t \neq \emptyset$  **do**
- 3:    $\mathcal{A}_t = \mathcal{P}_t \cup \mathcal{S}_t$ ;  $\mathcal{P}_{\text{pess},t} = p_{\text{pess},t}(\mathcal{A}_t)$ .
- 4:   **for**  $x_{h,i} \in \mathcal{A}_t$  **do** ▷ Modeling
- 5:     Obtain  $\boldsymbol{\mu}_\tau(x_{h,i})$  and  $\boldsymbol{\sigma}_\tau(x_{h,i})$  by GP inference.
- 6:      $\mathbf{R}_t(x_{h,i}) = \mathbf{R}_{t-1}(x_{h,i}) \cap \mathbf{Q}_t(x_{h,i})$ .
- 7:   **end for**
- 8:   **for**  $x_{h,i} \in \mathcal{S}_t \setminus \mathcal{P}_{\text{pess},t}$  **do** ▷ Discarding
- 9:     **if**  $\exists x \in \mathcal{P}_{\text{pess},t} : \max(\mathbf{R}_t(x_{h,i})) \preceq_\epsilon \min(\mathbf{R}_t(x))$  **then**
- 10:        $\mathcal{S}_t = \mathcal{S}_t \setminus \{x_{h,i}\}$ .
- 11:     **end if**
- 12:   **end for**
- 13:    $\mathcal{W}_t = \mathcal{S}_t \cup \mathcal{P}_t$ .
- 14:   **for**  $x_{h,i} \in \mathcal{S}_t$  **do** ▷  $\epsilon$ -Covering
- 15:     **if**  $\nexists x \in \mathcal{W}_t : \min(\mathbf{R}_t(x_{h,i})) + \epsilon \preceq \max(\mathbf{R}_t(x))$  **then**
- 16:        $\mathcal{S}_t = \mathcal{S}_t \setminus \{x_{h,i}\}$ ;  $\mathcal{P}_t = \mathcal{P}_t \cup \{x_{h,i}\}$ .
- 17:     **end if**
- 18:   **end for**
- 19:   **if**  $\mathcal{S}_t \neq \emptyset$  **then** ▷ Refining/Evaluating
- 20:     Select node  $x_{h_t, i_t} = \operatorname{argmax}_{x_{h,i} \in \mathcal{W}_t} \omega_t(x_{h,i})$ .
- 21:     **if**  $\beta_\tau^{1/2} \|\boldsymbol{\sigma}_\tau(x_{h_t, i_t})\|_2 \leq \|\mathbf{V}_{h_t}\|_2$  AND  $x_{h_t, i_t} \in \mathcal{S}_t$  **then**
- 22:        $\mathcal{S}_t = \mathcal{S}_t \setminus \{x_{h_t, i_t}\}$ ;  $\mathcal{S}_t = \mathcal{S}_t \cup \{x_{h_{t+1}, i} : N(i_t - 1) + 1 \leq i \leq N i_t\}$ .
- 23:        $\mathbf{R}_t(x_{h_{t+1}, i}) = \mathbf{R}_t(x_{h_t, i_t})$  for each  $i$  with  $N(i_t - 1) + 1 \leq i \leq N i_t$ .
- 24:     **else if**  $\beta_\tau^{1/2} \|\boldsymbol{\sigma}_\tau(x_{h_t, i_t})\|_2 \leq \|\mathbf{V}_{h_t}\|_2$  AND  $x_{h_t, i_t} \in \mathcal{P}_t$  **then**
- 25:        $\mathcal{P}_t = \mathcal{P}_t \setminus \{x_{h_t, i_t}\}$ ;  $\mathcal{P}_t = \mathcal{P}_t \cup \{x_{h_{t+1}, i} : N(i_t - 1) + 1 \leq i \leq N i_t\}$ .
- 26:        $\mathbf{R}_t(x_{h_{t+1}, i}) = \mathbf{R}_t(x_{h_t, i_t})$  for each  $i$  with  $N(i_t - 1) + 1 \leq i \leq N i_t$ .
- 27:     **else**
- 28:       Evaluate design  $x_t = x_{h_t, i_t}$  and observe  $\mathbf{y}_\tau = \mathbf{f}(x_{h_t, i_t}) + \boldsymbol{\kappa}_\tau$ .
- 29:        $\tau = \tau + 1$ .
- 30:     **end if**
- 31:   **end if**
- 32:    $\mathcal{P}_{t+1} = \mathcal{P}_t$ ;  $\mathcal{S}_{t+1} = \mathcal{S}_t$ .
- 33:    $t = t + 1$ .
- 34: **end while**
- 35: **return**  $\hat{\mathcal{P}} = \mathcal{P}_t$  and  $\hat{P} = \bigcup_{x_{h,i} \in \mathcal{P}_t} X_{h,i}$ .

---



on the metric and the kernel under which the result holds. Then, we provide a sketch of its proof and subsequently give an example of an  $m$ -output GP for which the maximum information gain is linear in  $T$ .

#### 4.1 The main result

**Assumption 1.** *The class  $\mathcal{K}$  of covariance functions to which we restrict our focus satisfies the following criteria for any  $\mathbf{k} \in \mathcal{K}$ : (1) For any  $x, y \in \mathcal{X}$  and  $j \in [m]$ , we have  $l_j(x, y) \leq C_{\mathbf{k}} d(x, y)^\alpha$ , for suitable  $C_{\mathbf{k}} > 0$  and  $0 < \alpha \leq 1$ . Here,  $l_j$  is the natural metric induced on  $\mathcal{X}$  by the  $j$ th component of the GP in Definition 8 as given in Remark 1 with covariance function  $k^{jj}$ . (2) We assume bounded variance, that is, for any  $x \in \mathcal{X}$  and  $j \in [m]$ , we have  $k^{jj}(x, x) \leq 1$ .*

**Theorem 1.** *Let  $\epsilon = [\epsilon^1, \dots, \epsilon^m]^\top$  be given with  $\epsilon = \min_{j \in [m]} \epsilon^j > 0$ . Let  $\delta \in (0, 1)$  and  $\bar{D} > D_1$ . For each  $h \geq 0$ , let  $V_h \in \tilde{O}(\rho^{\alpha h})$ ; for each  $\tau \in \mathbb{N}$ , let  $\beta_\tau \in O(\log(\tau^2/\delta))$ ; the exact definitions are given in the appendix. When we run Adaptive  $\epsilon$ -PAL with prior GP(0,  $\mathbf{k}$ ) and noise  $\mathcal{N}(0, \sigma^2)$ , the following holds with probability at least  $1 - \delta$ .*

*An  $\epsilon$ -accurate Pareto set can be found with at most  $T$  function evaluations, where  $T$  is the smallest natural number satisfying*

$$\min \left\{ K_1 \beta_T T^{\frac{-\alpha}{\bar{D}+2\alpha}} (\log T)^{\frac{-(\bar{D}+\alpha)}{\bar{D}+2\alpha}} + K_2 T^{\frac{-\alpha}{\bar{D}+2\alpha}} (\log T)^{\frac{\alpha}{\bar{D}+2\alpha}}, \sqrt{\frac{C \beta_T \gamma_T}{T}} \right\} \leq \epsilon,$$

where  $C$  and  $K_1$  are constants that are defined in the appendix and do not depend on  $T$ ,  $K_2$  is logarithmic in  $T$ , and  $\gamma_T$  is the maximum information gain which depends on the choice of  $\mathbf{k}$ .

Note that we minimize over two different bounds in Theorem 1. The term that involves  $\gamma_T$  corresponds to the information-type bound, while the other term corresponds to the metric dimension-type bound. Equivalently, we can express our information-type bound as  $\tilde{O}(g(\epsilon))$  where  $g(\epsilon) = \min\{T \geq 1 : \sqrt{\gamma_T/T} \leq \epsilon\}$  and our metric dimension-type bound as  $\tilde{O}(\epsilon^{-(\frac{\bar{D}}{\alpha}+2)})$  for any  $\bar{D} > D_1$ . For certain kernels, such as squared exponential and Matérn kernels,  $\gamma_T$  can be upper bounded by a sublinear function of  $T$  (see Srinivas et al. (2012)). Our information type-bound is of the same form as in Zuluaga et al. (2016). When  $\mathcal{X}$  is a finite subset of the Euclidean space, we have  $D_1 = 0$ , and thus, our metric-dimension type bound becomes near- $O(1/\epsilon^2)$ , which is along the same lines with the almost optimal, gap-dependent near- $O(1/\text{gap}^2)$  bound for Pareto front identification in Auer et al. (2016).

*Sketch of the proof of Theorem 1:* We divide the proof of Theorem 1 into three essential parts. First, we prove that the algorithm terminates in finite time, and examine the events that necessitate and the ones that follow termination. Here, it is important to note that if the largest uncertainty diameter in a given round  $t$  is less than or equal to  $\epsilon$ , then the algorithm terminates. This introduces a way on how to proceed on upper bounding sample complexity, namely, we can upper bound the sum of these uncertainty diameters over all rounds. Then, by observing that i) the term  $V_h$  decays to 0 as  $h$  grows indefinitely, which means that the algorithm refines up until a finite number of tree levels, and that ii) a node cannot be refined more than a finite number of times before expansion, we can conclude

that the algorithm terminates in finite time. After this point we prove, using Hoeffding bounds, that the true function values live inside the uncertainty hyper-rectangles with high probability. We then proceed on first proving the dimension-type sample complexity bounds and then the information-type bounds. We use the aforementioned termination condition and upper bound the sum of the uncertainty diameters over all rounds. We use Cauchy-Schwarz inequality to manipulate the expression as we desire and then upper bound it in terms of information gain using an already established result in the paper. For the dimension-type bounds, we consider expressing the sum over rounds as a sum over levels  $h$  of the tree of partitions and upper bound it using the notion of metric dimension. We take the minimum of the two bounds, thus achieving the bound stated in Theorem 1.

In order to prove the bounds in Theorem 1, even for infinite  $\mathcal{X}$ , we propose a novel way of defining the confidence hyper-rectangles and refining them. Since Adaptive  $\epsilon$ -PAL discards,  $\epsilon$ -covers and refines/evaluates in ways different than  $\epsilon$ -PAL in Zuluaga et al. (2016), we use different arguments in the proof to show when the algorithm converges and what it returns when it converges. In particular, for the information-type bound, we exploit the dependence structure between the objectives. Moreover, having two different bounds allows us to use the best of both, as it is known that for certain kernels, the metric dimension-type bound can be tighter than the information-type bound. We provide such an example in the next section.

## 4.2 An example of a multi-output GP where the information gain is linear in $T$

The following example illustrates a case of an  $m$ -output GP which yields linear maximum information gain.

**Example 1.** (The multi-output version of Example 1 in Shekhar et al. (2018)) Let  $\mathcal{X} = [0, 1]$ . Let  $j \in [m]$ ,  $x \in \mathcal{X}$ , and let us define

$$\tilde{f}^j(x) = \sum_{i=1}^{\infty} 4\bar{a}_{ij} X_{ij} \left( (3^i x - 1)(2 - 3^i x)\mathbb{I}(x \in L_i) - (3^i x - 2)(3 - 3^i x)\mathbb{I}(x \in R_i) \right) ,$$

where, for each  $j \in [m]$ ,  $(\bar{a}_{ij})_{i=1}^{\infty}$  is a non-increasing sequence of positive real numbers with  $\bar{a}_{1j} \leq 1$ ;  $(X_{ij})_{i=1, j=1}^{\infty, m}$  is a sequence of independent and identically distributed standard Gaussian random variables; and we let  $L_i := [3^{-i}, 2 \cdot 3^{-i})$  for all  $i \geq 1$ ,  $R_i := [2 \cdot 3^{-i}, 3^{-i+1})$  for all  $i \geq 2$ , and  $R_i = [2 \cdot 3^{-i}, 3^{-i+1}]$  for  $i = 1$ . Note that we have

$$\mathcal{X} = \bigcup_{i=1}^{\infty} (L_i \cup R_i) ,$$

and moreover,  $L_1, R_1, L_2, R_2, \dots$  do not overlap, thus they partition  $\mathcal{X}$ . Therefore, for any  $x \in \mathcal{X}$ , there exists  $i(x) \geq 1$  such that  $x \in L_{i(x)} \cup R_{i(x)}$  and  $x \notin L_l \cup R_l$ , for any  $l \neq i$ . So we have

$$\tilde{f}^j(x) = 4\bar{a}_{ij} X_{ij} \left( (3^{i(x)} x - 1)(2 - 3^{i(x)} x)\mathbb{I}(x \in L_{i(x)}) - (3^{i(x)} x - 2)(3 - 3^{i(x)} x)\mathbb{I}(x \in R_{i(x)}) \right) .$$

Let  $x, x' \in \mathcal{X}$  and  $j, l \in [m]$ . We define  $\tilde{\mathbf{f}}(x) = [\tilde{f}^1(x), \dots, \tilde{f}^m(x)]^{\top}$ . Note that we have  $\mathbb{E}[\tilde{\mathbf{f}}(x)] = [0, \dots, 0]^{\top}$ . Moreover, we let  $\tilde{\mathbf{k}}(x, x')$  denote the covariance matrix of the  $m$ -output

GP  $(\tilde{\mathbf{f}}(x))_{x \in \mathcal{X}}$ . Note that we have

$$\mathbb{E}[\tilde{f}^j(x)\tilde{f}^l(x)] = 0, \text{ for } j \neq l,$$

due to independence of  $X_{ij}$  across objectives which implies that

$$\tilde{\mathbf{k}}(x, x) = \begin{bmatrix} \tilde{k}^{11}(x, x) & \dots & 0 \\ \vdots & & \vdots \\ 0 & \dots & \tilde{k}^{mm}(x, x) \end{bmatrix}$$

Now let  $A = (a_{pq})_{p,q \in [m]} \in \mathbb{R}^{m \times m}$  be a square matrix such that  $\|A_j\|_2 = 1$ , for all  $j \in [m]$ , where  $A_j$  denotes the  $j$ th row of  $A$ . Furthermore, let us define  $\mathbf{f}(x) = A\tilde{\mathbf{f}}$ . Let  $\mathbf{k}$  be the covariance function associated with the  $m$ -output GP  $(\mathbf{f}(x))_{x \in \mathcal{X}}$ . Assume that  $T$  designs of the form  $x_i = 1/3^i + 1/(2 \cdot 3^i)$  are selected for evaluation and subsequently the noisy observations  $\mathbf{y}_i$  are obtained, for  $i \leq T$ . Note that in this case we have  $i(x_i) = i$ . Now we explicitly calculate the variances of these evaluated points at all objectives. Let  $j \leq m$  and  $i \leq T$ . We have

$$k^{jj}(x_i, x_i) = \mathbb{E}[(A\tilde{\mathbf{f}}(x_i))(A\tilde{\mathbf{f}}(x_i))^\top] = A_j \tilde{\mathbf{k}}(x_i, x_i) A_j^\top = \sum_{l=1}^m \tilde{k}^{ll}(x_i, x_i) a_{jl}^2,$$

where the third equality follows from the fact that  $\tilde{\mathbf{k}}(x, x)$  is diagonal. Now we have

$$\begin{aligned} \tilde{f}^j(x_i) &= 4\bar{a}_{ij}X_{ij} \left( (3^i x - 1) (2 - 3^i x) \mathbb{I}(x \in L_i) - (3^i x - 2) (3 - 3^i x) \mathbb{I}(x \in R_i) \right) \\ &= 4\bar{a}_{ij}X_{ij} \left( 3^i \left( \frac{1}{3^i} + \frac{1}{2 \cdot 3^i} \right) - 1 \right) \left( 2 - 3^i \left( \frac{1}{3^i} + \frac{1}{2 \cdot 3^i} \right) \right) \\ &= 4\bar{a}_{ij}X_{ij} \frac{1}{4} \\ &= \bar{a}_{ij}X_{ij}. \end{aligned}$$

Therefore, we have that  $\tilde{k}^{ll}(x_i, x_i) = \mathbb{E}[(\tilde{f}^l(x_i))^2] = \bar{a}_{il}^2$ , from which we obtain

$$k^{jj}(x_i, x_i) = \sum_{l=1}^m \bar{a}_{il}^2 a_{jl}^2 \leq \sum_{l=1}^m \bar{a}_{1l}^2 a_{jl}^2 \leq \|A_j\|_2^2 = 1 \quad (3)$$

using the assumptions on the sequence  $(\bar{a}_{il})$  and the matrix  $A$ . The observations at different designs are uncorrelated, hence independent, by the choice of the designs, and this implies that the posterior distribution is the same as the prior distribution. This, together with

*Proposition 1 implies*

$$\begin{aligned}
\gamma_T \geq I(\mathbf{y}_{[T]}; \mathbf{f}_{[T]}) &\geq \frac{1}{m} \sum_{i=1}^T \sum_{j=1}^m \frac{1}{2} \log \left( 1 + \sigma^{-2} (\sigma_{i-1}^j(x_i))^2 \right) \\
&= \frac{1}{m} \sum_{i=1}^T \sum_{j=1}^m \frac{1}{2} \log \left( 1 + \sigma^{-2} (\bar{a}_{ij}^2) \right) \\
&\geq \frac{T}{2m} \sum_{j=1}^m \log \left( 1 + \frac{\bar{a}_{Tj}^2}{\sigma^2} \right) \\
&\geq T \frac{1}{2m} \sum_{j=1}^m \frac{\bar{a}_{Tj}^2 / \sigma^2}{1 + \bar{a}_{Tj}^2 / \sigma^2} \\
&= T \frac{1}{2m} \sum_{j=1}^m \frac{\bar{a}_{Tj}^2}{\bar{a}_{Tj}^2 + \sigma^2} ,
\end{aligned}$$

where in the third inequality we have used the fact that the sequence  $(a_{ij})_{i=1}^\infty$  is decreasing and in the fourth inequality we use the fact that  $\log(1+x) \geq x/(1+x)$ . Thus, we obtain

$$\gamma_T = \Omega(T) .$$

By Theorem 1, we see that the information-type quantity  $\sqrt{C\beta_T\gamma_T/T}$  increases logarithmically in  $T$  and the metric dimension-type quantity  $K_1\beta_T T^{-\frac{\alpha}{D+2\alpha}} (\log T)^{\frac{-(D+\alpha)}{D+2\alpha}} + K_2 T^{-\frac{\alpha}{D+2\alpha}} (\log T)^{\frac{\alpha}{D+2\alpha}}$  decreases exponentially in  $T$ , for any choice of  $\bar{D} > D_1$  and  $0 < \alpha \leq 1$ .

On the other hand, for a suitably chosen metric  $d$ , the first part of Assumption 1 holds. Similar to (3), it can also be checked that  $k^{jj}(x, x) \leq 1$  for all  $x \in \mathcal{X}$ . Hence, the second part of Assumption 1 holds as well.

## 5. Computational complexity analysis

The most significant subroutines of Adaptive  $\epsilon$ -PAL in terms of computational complexity are the modeling, discarding, and  $\epsilon$ -covering phases. Below, we inspect the computational complexity of these three phases separately.

**Modeling.** In the modeling phase, mean and variance values of the GP surrogate are computed for every node point in the leaf set. This results in a complexity of  $\mathcal{O}(\tau^3 + n\tau^2)$ , where  $\tau$  is the number of evaluations and  $n$  is the number of node points at a particular round. Note that the bound on  $n$  depends on the maximum depth of the search tree.

**Discarding.** This phase can be further separated into two substeps. In the first substep, the pessimistic Pareto front is determined by choosing the leaf nodes whose lower confidence bounds are not dominated by any other point in the leaf set. In the second phase, the leaf points whose upper confidence bounds are  $\epsilon$ -dominated by pessimistic Pareto set points are discarded. If done naively by comparing each point with all the other points, both of the phases can result in  $\mathcal{O}(n^2)$  complexity. However, there are efficient methods that achieve

lower computational complexity. In our implementation, we adopt an efficient algorithm in Kung et al. (1975) to reduce computational complexity to  $\mathcal{O}(n \log n)$  when  $m = 2$  or  $m = 3$ . Another algorithm proposed by Kung et al. (1975) can be implemented and it achieves  $\mathcal{O}(n(\log n)^{m-2} + n \log n)$  complexity for  $m > 3$ .

**$\epsilon$ -Covering.** In the  $\epsilon$ -covering phase, the algorithm moves the nodes that are not dominated by any other node to  $\hat{\mathcal{P}}$ . Similar to the discarding phase, when implemented naively, the  $\epsilon$ -covering phase results in  $\mathcal{O}(n^2)$  complexity. An adaptation of Kung et al. (1975) algorithm can be implemented as in the case of discarding phase to achieve sub-quadratic complexity which results in  $\mathcal{O}(n \log n)$  for  $m = 2$  and  $m = 3$  and  $\mathcal{O}(n(\log n)^{m-2} + n \log n)$  for  $m > 3$ .

In general, we observed that the number of evaluations was much smaller than the number of nodes throughout a run. Therefore we can say that discarding and  $\epsilon$ -covering phases are the main bottlenecks in our implementation which scale sub-quadratically with the number of points.

## 6. Experiments

We test Adaptive  $\epsilon$ -PAL on five different synthetic setups and compared the results with well-known Multi-Objective-Bayesian Optimization (MOBO) methods from the literature using four different performance metrics <sup>3</sup>. We proceed by explaining our used metrics, followed by the algorithms used, and finally the simulation setups and results.

### 6.1 Performance metrics

We use a combination of three different performance metrics, namely hypervolume,  $\epsilon$ -accuracy, and  $\epsilon$ -coverage. Since all of the objective functions tested are continuous, so is the Pareto front, and thus it contains infinitely many points. Then, to compute the metrics, we sample 10000 sample points from the input space, evaluating the objective function at each of these points, and then computing the Pareto front. Notice that we keep the difference between two consecutive sampled points less than  $\frac{\epsilon}{10}$  so that we can reasonably use the Pareto front computed from the discretized objective function as the true Pareto front. Below we describe the performance metrics.

#### 6.1.1 HYPERVOLUME

Hypervolume is a popular performance metric used in the multi-objective Bayesian optimization literature (Zitzler, 1999) to assess the performance of competing algorithms. It is computed by setting an arbitrary reference point and calculating the volume enclosed between this reference and the predicted Pareto front points.

#### 6.1.2 $\epsilon$ -ACCURACY RATIO

This metric is computed by finding the ratio between the  $\epsilon$ -accurate points and the predicted Pareto set. More specifically, we count the number of predicted Pareto points that are inside

---

3. The code for the implementation of Adaptive  $\epsilon$ -PAL is available online at:  
<https://github.com/KeremBozgann/adaptive-epsilon-pal>

the  $\epsilon$ -Pareto front (i.e., predicted Pareto points that are at most  $2\epsilon$  away from the closest true Pareto point), and divide this number by the total number of predicted Pareto points.

Our theoretical results for Adaptive  $\epsilon$ -PAL guarantee 100%  $\epsilon$ -accuracy with high probability, given there is no mismatch between surrogate model and real objective functions.

Although it is desirable to achieve a high  $\epsilon$ -accuracy, it is on its own not enough to assess the performance of a multi-objective Bayesian optimization algorithm. In addition to the predicted Pareto points being close to the true Pareto points, which is measured by  $\epsilon$ -accuracy, we want the predicted Pareto points to cover as many true Pareto points as possible. The latter is measured by the  $\epsilon$ -coverage metric.

### 6.1.3 $\epsilon$ -COVERAGE RATIO

This metric is computed the same way as the  $\epsilon$ -accuracy ratio, with the only difference being that we iterate over the true Pareto front points. In other words, we count the number of true Pareto front points that are within  $2\epsilon$  of the closest predicted Pareto front point and divide this count by the total number of true Pareto front points.

### 6.1.4 AVERAGE MEAN-SQUARED ERROR

This metric is computed by averaging the mean-squared error between each true Pareto point and the closest predicted Pareto point. Notice that this metric is alike  $\epsilon$ -coverage ratio. Thus, when  $\epsilon$ -accuracy is high, the predicted Pareto points are close to the true Pareto points; and when  $\epsilon$ -coverage is high, the predicted Pareto points cover the true Pareto points. Ideally, we want both metrics to simultaneously be high.

## 6.2 Multi-objective Bayesian optimization algorithms

We compare Adaptive  $\epsilon$ -PAL with PESMO (Hernández-Lobato et al., 2016), ParEGO (Knowles, 2006b), and USeMO (Belakaria et al., 2020), which are some of the state-of-the-art multi-objective Bayesian optimization methods.

Since all algorithms except Adaptive  $\epsilon$ -PAL require a pre-specified evaluation budget rather than an  $\epsilon$  value, we set the evaluation budget to be at least as large as the number of observations that Adaptive  $\epsilon$ -PAL made before its termination. We used the codes for PESMO and ParEGO methods from the Bayesian optimization library *Spearmint*<sup>4</sup> and for USeMO from the authors' open source code available on Github<sup>5</sup>.

## 6.3 Simulation setups & results

In all setups, we sample a function from a GP with known kernels and use it as the multi-objective function to maximize. Then, we run the algorithms that use GPs, adaptive  $\epsilon$ -PAL, USeMO, and PESMO, with the known kernels of the GP from which the objective function was sampled.

---

4. <https://github.com/HIPS/Spearmint/tree/PESM>

5. <https://github.com/belakaria/USEMO>

## 6.3.1 SIMULATION I

**Setup.** In this simulation, we sample a 1-dimensional input and 2-dimensional output function, concisely written as a  $(1, 2)$ -function, from a GP with a zero mean function and two independent squared exponential kernels with variances 0.5 and 0.1, and lengthscales 0.1 and 0.06.

**Adaptive  $\epsilon$ -PAL.** We run Adaptive  $\epsilon$ -PAL until it terminates. Moreover, we run Adaptive  $\epsilon$ -PAL with three different  $h_{\max}$  values. We use  $h_{\max} = 24$ , which is computed using Lemma 4 in the appendix,  $h_{\max} = 10$ , and  $h_{\max} = 9$ . When we set a non-theoretical  $h_{\max}$ , we have to force the algorithm to not refine beyond  $h_{\max}$  and thus we set  $V_h$  to zero when  $h \geq h_{\max}$ . Reducing  $h_{\max}$  greatly improves the running time of Adaptive  $\epsilon$ -PAL, and, as we will see, only marginally reduces its performance. Furthermore, we set  $v_1 = v_2 = 1$ ,  $N = 2$ ,  $\rho = 1/2$ ,  $\delta = 0.05$ , and  $\epsilon = (\epsilon, \epsilon)$  with  $\epsilon = 0.05$ .

**PESMO and ParEGO.** We run PESMO and ParEGO for 100 iterations. We use the same confidence ratio  $\delta = 0.05$  with Adaptive  $\epsilon$ -PAL. The acquisition function is optimized on a grid with size 1000 to find an initial starting point. Then the acquisition function is optimized with L-BFGS method.

**USeMO.** We run USeMO for 100 iterations. EI (Expected Improvement) is used as the acquisition function.

**Results.** We use the predicted Pareto front points returned by each algorithm and use them to compute the  $\epsilon$ -accuracy,  $\epsilon$ -coverage, and average mean-squared error. Figure 4 shows the predicted Pareto points returned by each algorithm as well as the true Pareto points. Visually, it is clear that ParEGO and PESMO perform badly, as they predicted a trail of points (purple and bottom right for PESMO; brown and center for ParEGO) far away from the true Pareto front. Furthermore, it appears that the predicted Pareto points of Adaptive  $\epsilon$ -PAL for both  $h_{\max} = 24$  and  $h_{\max} = 10$  are lying right on top of the true Pareto points.

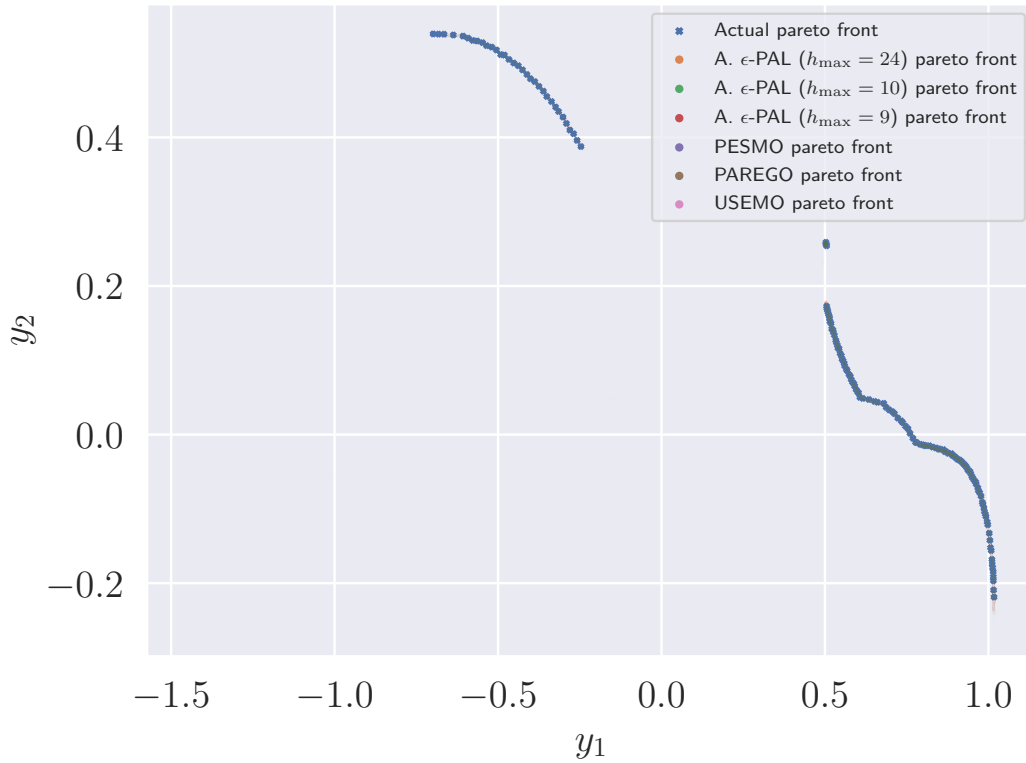


Figure 4: The true and predicted Pareto fronts of each algorithm in Simulation I

To better understand the performance of the other algorithms and compare them, we look at the  $\epsilon$ -accuracy and  $\epsilon$ -coverage metrics provided in Figures 5 and 6, respectively. Notice that we use different  $\epsilon$  values to compute the accuracy and coverage. The smaller the  $\epsilon$  value (i.e.,  $y$ -axis in the figures), the stricter the metric.

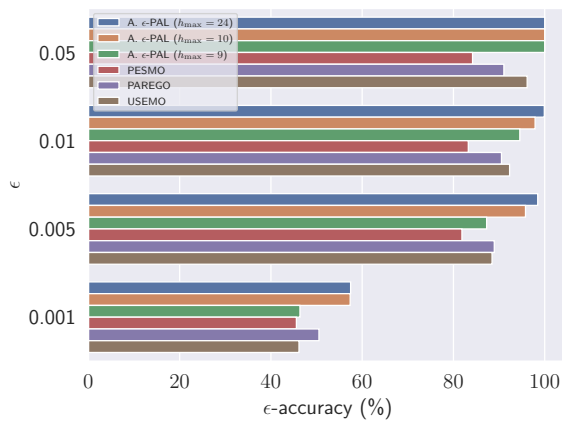


Figure 5:  $\epsilon$ -accuracy of the algorithms in Simulation I

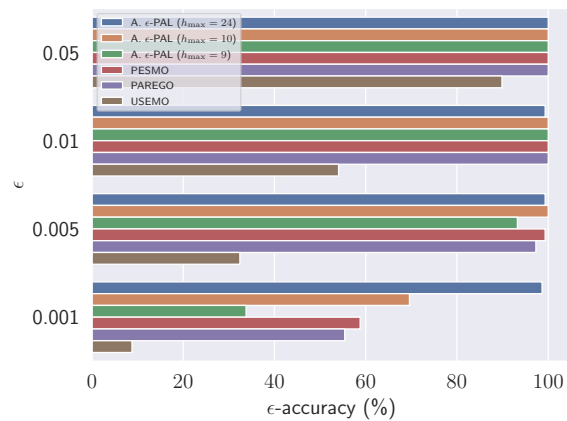


Figure 6:  $\epsilon$ -coverage of the algorithms in Simulation I



Unsurprisingly, Adaptive  $\epsilon$ -PAL with its theoretical parameters ( $h_{\max} = 24$ ) gets 100%  $\epsilon$ -accuracy and coverage when we use  $\epsilon = 0.05$ , which was the  $\epsilon$  value that we provided to the algorithm. Notice that reducing  $h_{\max}$  to 10 or 9 does not affect the  $\epsilon$  accuracy or coverage at  $\epsilon = 0.05$ , but it does affect both the  $\epsilon$ -accuracy and coverage at smaller  $\epsilon$ s. This is because when  $h_{\max}$  is smaller than its theoretical value, the algorithm will be less accurate when discarding a node or adding it to the decided set.

Looking at the other algorithms, we see that no algorithm surpasses the  $\epsilon$ -accuracy or coverage of Adaptive  $\epsilon$ -PAL, even with  $h_{\max}$  set to 10. Interestingly, USEMO performs the best after Adaptive  $\epsilon$ -PAL when it comes to  $\epsilon$ -accuracy, but it performs the worst when it comes to  $\epsilon$ -coverage. This is because USEMO returned very few Pareto points. In fact, looking at Figure 4, we see that there are very few predicted USEMO points (in pink) compared to the other algorithms. On the other hand, PESMO achieves high  $\epsilon$ -coverage ratios, but performs very badly with  $\epsilon$ -accuracy. This is due to the erroneous trail of points returned by PESMO, as seen in purple in Figure 4. Combining the two metrics, we present the average of the  $\epsilon$ -accuracy and coverage of each algorithm in Figure 7. We also present the average mean-squared error of each algorithm in Figure 8. Both figures corroborate our findings, namely that even with a limited  $h_{\max}$  of 10, Adaptive  $\epsilon$ -PAL outperforms the other multi-objective Bayesian optimization algorithms and trades blows with the Adaptive  $\epsilon$ -PAL that uses the theoretical parameters.

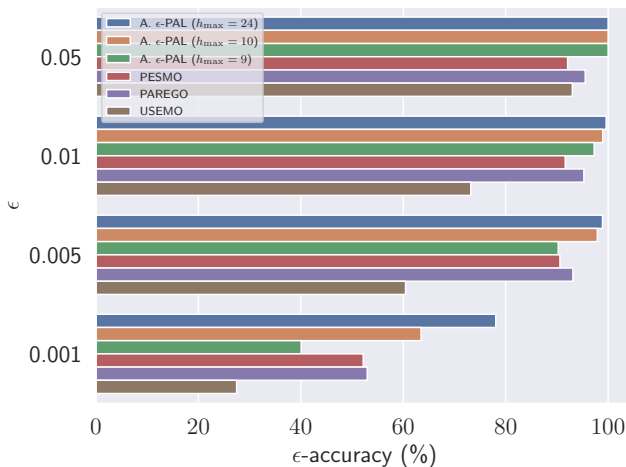


Figure 7: Average of the  $\epsilon$ -accuracy and coverage of the algorithms in Simulation I

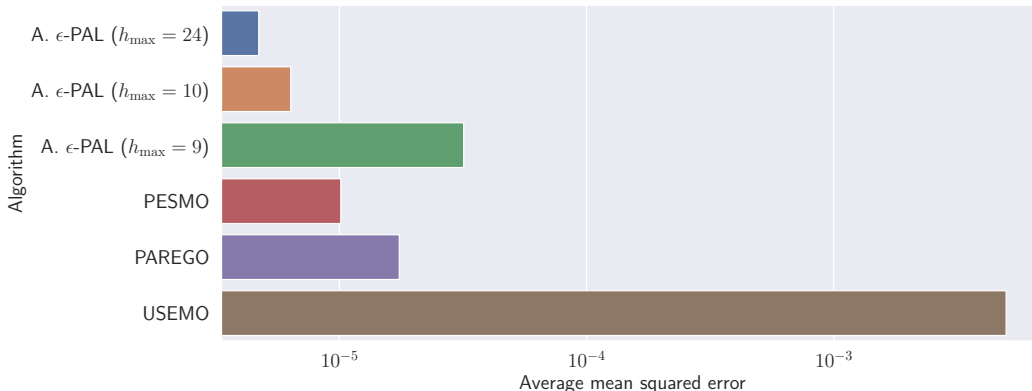


Figure 8: Average mean-squared error of the algorithms in Simulation I

Lastly, we look at the running time of the three different Adaptive  $\epsilon$ -PAL configurations, given in Table 2. Notice that by reducing  $h_{\max}$  from 24 to 10, we speed up the running time of the algorithm by more than 900 times, whereas there was no performance loss, as measured by  $\epsilon$ -accuracy and coverage, at the  $\epsilon = 0.05$  level. Therefore, we can conclude that running Adaptive  $\epsilon$ -PAL with a reduced  $h_{\max}$  significantly reduces the running time while practically maintaining the same performance.

Table 2: Total running times of adaptive  $\epsilon$ -PAL using different optimizations

Algorithm	Total running time (hh:mm:ss)
Adaptive $\epsilon$ -PAL with $h_{\max} = 24$	15:15:24
Adaptive $\epsilon$ -PAL with $h_{\max} = 10$	00:01:00
Adaptive $\epsilon$ -PAL with $h_{\max} = 9$	00:00:27
ParEGO	00:07:30
PESMO	00:09:20
USEMO	00:23:40

### 6.3.2 SIMULATIONS II-V

We validate our theoretical results by conducting further experiments on 1-dimensional and 2-dimensional synthetic Gaussian samples with squared exponential (sqexp) and Matérn-52 type kernels. We produce all the samples from a GP kernel with lengthscale 0.2 and variance 0.6. In Figure 10, we display the results belonging to a single run and Figure 11, we display the average results over 10 independent runs.

We were curious to see how the other methods would perform on these tasks since these methods do not provide any strict theoretical guarantee for the quality of the Pareto set they return. We observed that on all the synthetic GP sample functions we experimented with, these algorithms fail to find a good prediction for the true Pareto front and they often

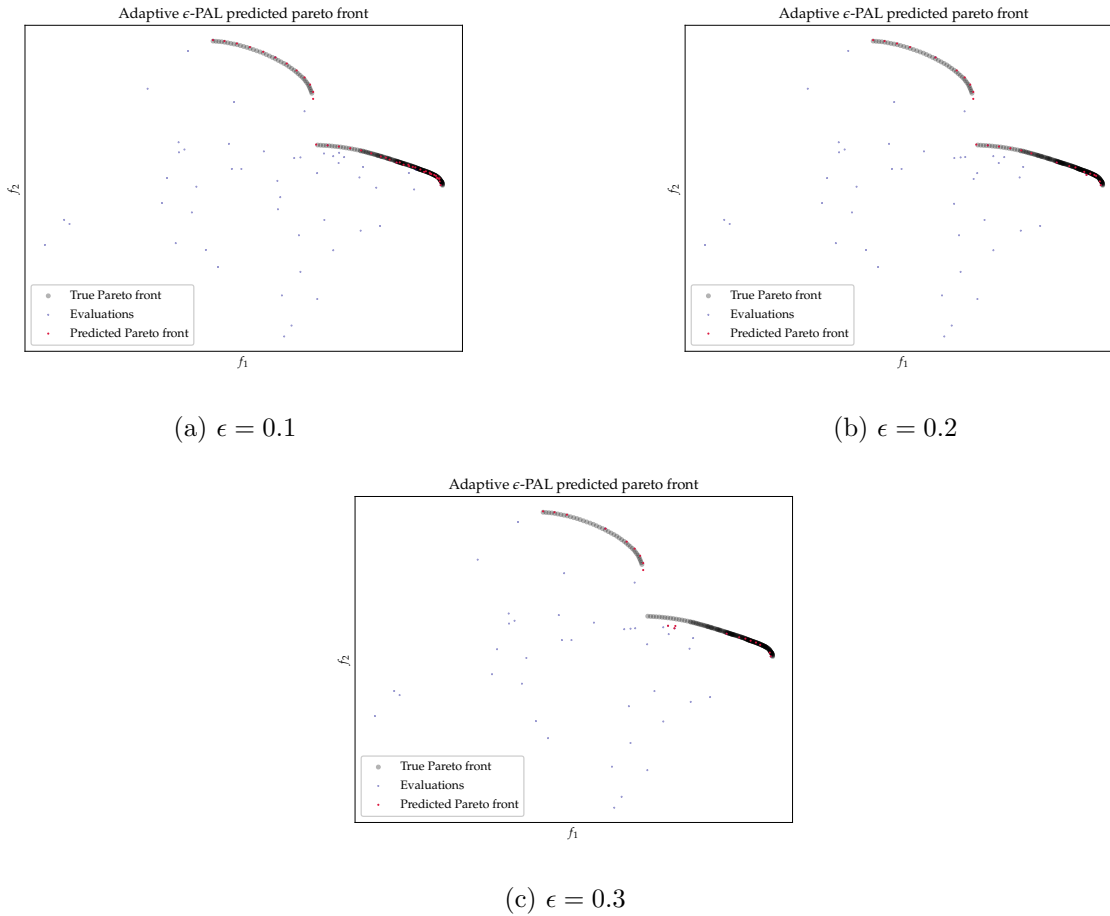


Figure 9: Predicted Pareto front returned by Adaptive  $\epsilon$ -PAL for different  $\epsilon$  accuracy values

returned points that are far away from the true Pareto front. On the contrary, Adaptive  $\epsilon$ -PAL always succeeded in returning a Pareto front that is inside the specified  $\epsilon$  range, and most of the time it returned points that are exactly from the true Pareto set. For all the experiments and for all the  $\epsilon$  values we specified, Adaptive  $\epsilon$ -PAL was able to return an  $\epsilon$ -accurate Pareto front as predicted by the theoretical results. An example Pareto front returned by Adaptive  $\epsilon$ -PAL on a GP sample with the sqrexp kernel for runs with three different  $\epsilon$  values are displayed in Figure 9. As can be observed from the results displayed in Figure 10a and 10b, Adaptive  $\epsilon$ -PAL scores 100 percent on both the  $\epsilon$ -accuracy and  $\epsilon$ -coverage metrics while the competing methods often score below 100 percent in both these metrics, which supports the observations made previously. Furthermore, it can be seen that Adaptive  $\epsilon$ -PAL scores the highest in hypervolume for the Matérn-52-1D, sqrexp-2D and Matérn-52-2D examples and scores comparable with the other methods on the sqrexp-1D

example.

The change of hypervolume with evaluations is displayed in Figure 11 for all the algorithms on different synthetic GP samples. It can be observed that Adaptive  $\epsilon$ -PAL returns a prediction that scores higher in hypervolume at the end than the competing methods for the Matérn52-1D, sqrexp-2d and Matérn52-2D type GP samples while performing comparable with other methods on the sqrexp-1d example. Although sometimes competing methods perform better in the early phases, in general they seemed to get stuck at a non-optimal prediction.

We conclude that, the theoretical strictness of Adaptive  $\epsilon$ -PAL allows it to make significantly better predictions than the heuristic methods.

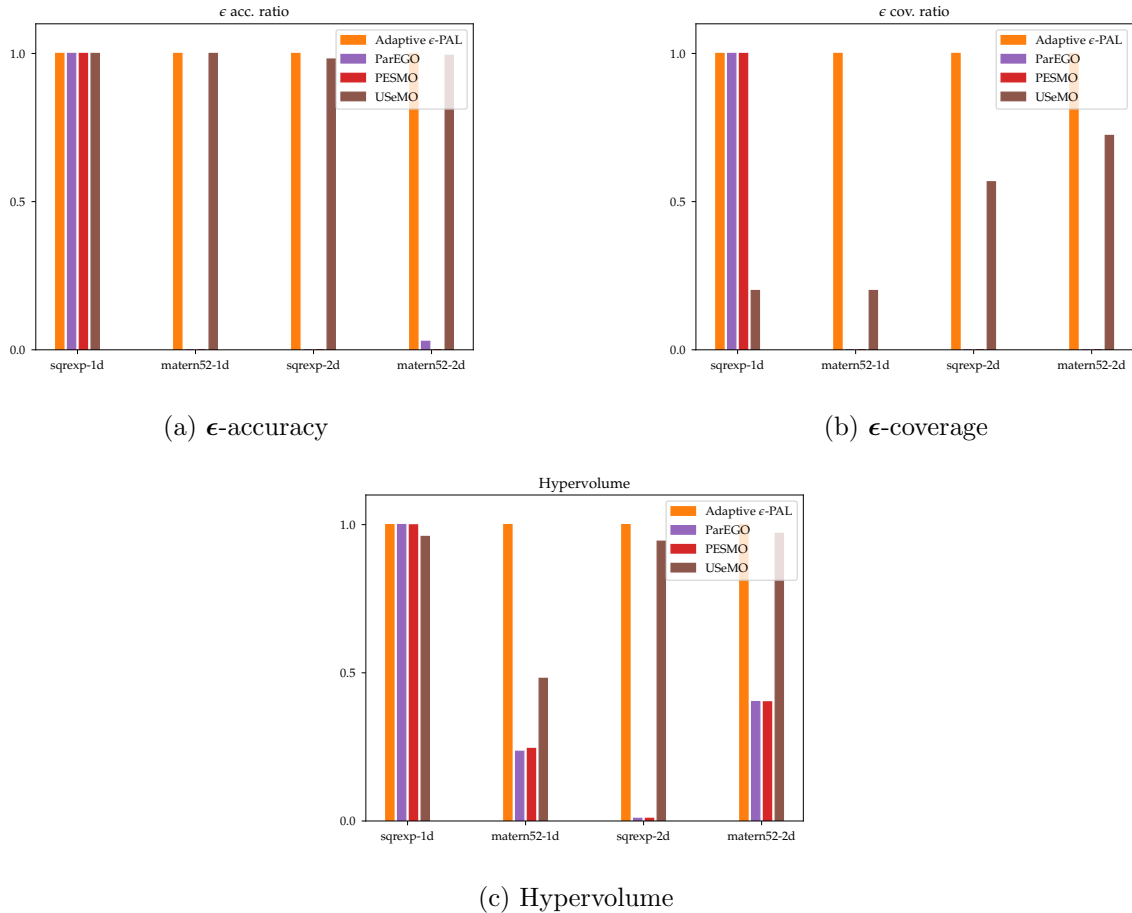


Figure 10:  $\epsilon$ -accuracy and coverage ratios of Adaptive  $\epsilon$ -PAL for different types of kernels

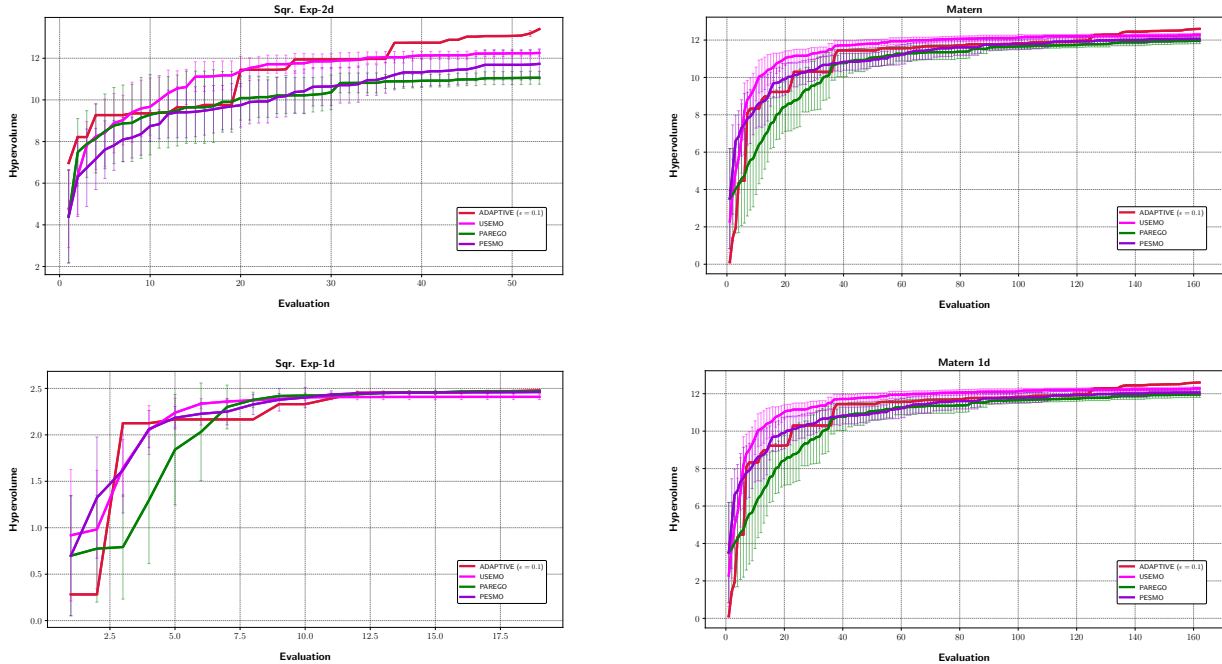


Figure 11: Hypervolume change with evaluations is displayed for competing methods on different benchmarks.

## 7. Conclusion

In this paper, we proposed a new algorithm for PAL in large design spaces. Our algorithm learns an  $\epsilon$ -accurate Pareto set of designs in as few evaluations as possible by combining an adaptive discretization strategy with GP inference of the objective values. We proved both information-type and metric-dimension type bounds on the sample complexity of our algorithm. To the best of our knowledge, this is the first sample complexity result for PAL that (i) involves an information gain term, which captures the dependence between objectives and (ii) explains how sample complexity depends on the metric dimension of the design space.

## Acknowledgments

This work was supported in part by the Scientific and Technological Research Council of Turkey under Grant 215E342 and by the BAGEP Award of the Science Academy.

## Appendix A. The proof of Theorem 1

The proof of Theorem 1 is composed of a series of sophisticated steps, and is divided into multiple subsections. First, we describe in Section A.1 a set of preliminary results that will be utilized in obtaining dimension-type and information-type bounds on the sample complexity. Then, in Section A.2, we prove a key result that provides a sufficient condition for the termination of Adaptive  $\epsilon$ -PAL. We also show in this section that Adaptive  $\epsilon$ -PAL returns an  $\epsilon$ -accurate Pareto set when it terminates and bound the maximum depth node that can be created by the algorithm before it terminates. In the proof,  $\tau_s$  represents the number of evaluations performed by the algorithm until termination, and  $t_s$  represents the round (iteration) at which the algorithm terminates. Throughout the proof, for a given  $\epsilon$ , we let  $\epsilon = \min_j \epsilon^j$ , and assume that  $\epsilon$  is such that  $\epsilon > 0$ . Unless noted otherwise, all inequalities that involve random variables hold with probability one.

### A.1 Preliminary results

We start by formulating the relationship between packing number, covering number, and metric dimension, which will help us in obtaining dimension-type bounds on the sample complexity. Recall that  $(\mathcal{X}, d)$  is a compact well-behaved metric space with metric dimension  $D_1 < +\infty$ .

**Lemma 1.** *For every constant  $r > 0$ , we have*

$$M(\mathcal{X}, 2r, d) \leq N(\mathcal{X}, r, d).$$

Moreover, for every  $\bar{D} > D_1$ , there exists  $Q > 0$  such that

$$M(\mathcal{X}, 2r, d) \leq N(\mathcal{X}, r, d) \leq Qr^{-\bar{D}}.$$

*Proof.* We argue by contradiction. Suppose that we have a  $2r$ -packing  $\{x_1, \dots, x_M\}$  and an  $r$ -covering  $\{y_1, \dots, y_M\}$  of  $\mathcal{X}$  such that  $M \geq N + 1$ . Then, by the pigeon-hole principle, we must have that both  $x_i$  and  $x_j$  lie in the same ball  $B(y_k, r)$ , for some  $i \neq j$  and some  $k$ , meaning that  $d(x_i, x_j) \leq r$ , which contradicts the definition of  $r$ -packing. Thus, the size of any  $2r$ -packing is less than or equal to the size of any  $r$ -covering and the first claim of the lemma follows. The second claim is an immediate consequence of Definition 7 and the fact that  $D_1 < +\infty$ .  $\blacksquare$

Our next result gives a relation between the metric dimension of  $\mathcal{X}$  with respect to  $d$  and the one of  $\mathcal{X}$  with respect to the metrics induced by the GP, which holds under Assumption 1.

**Lemma 2.** *Part 1 of Assumption 1 implies that if  $(\mathcal{X}, d)$  has a finite metric dimension  $D_1$ , then  $(\mathcal{X}, l_j)$  has a metric dimension  $D_1^j$  such that  $D_1^j \leq D_1/\alpha$ .*

*Proof.* We will proceed in two steps.

We first claim that  $N(\mathcal{X}, r, l_j) \leq N(\mathcal{X}, (\frac{r}{C_K})^{\frac{1}{\alpha}}, d)$ . In order to show this, let  $\tilde{X}$  be an  $(\frac{r}{C_K})^{\frac{1}{\alpha}}$ -covering of  $(\mathcal{X}, d)$ . Then, it is an  $r$ -covering of  $(\mathcal{X}, l_j)$ . Indeed, let  $x \in \mathcal{X}$ . Then, there exists  $y \in \tilde{X}$ , such that

$$d(x, y) \leq \left( \frac{r}{C_K} \right)^{\frac{1}{\alpha}}.$$

Table 3: *Notation.*

Symbol	Description
$\mathcal{X}$	The design space
$\mathbf{f}$	The latent function drawn from an $m$ -output GP
$\epsilon$	Accuracy level given as input to the algorithm
$\mathcal{Z}(\mathcal{X})$	The Pareto front of $\mathcal{X}$
$\mathcal{Z}_\epsilon(\mathcal{X})$	The $\epsilon$ -Pareto front of $\mathcal{X}$
$\mathbf{y}_\tau = \mathbf{f}(\tilde{x}_\tau) + \boldsymbol{\kappa}_\tau$	$\tau$ th noisy observation of $\mathbf{f}$
$\mathbf{y}_{[\tau]}$	Vector that represents the first $\tau$ noisy observations
$x_{h,i}$	The node with index $i$ in depth $h$ of the tree
$X_{h,i}$	The cell associated to node $x_{h,i}$
$p(x_{h,i})$	Parent of node $x_{h,i}$
$\boldsymbol{\mu}_\tau(x_{h,i})$	The posterior mean after $\tau$ evaluations of $x_{h,i}$ with $j$ th component $\mu_\tau^j(x_{h,i})$
$\boldsymbol{\sigma}_\tau(x_{h,i})$	The posterior variance after $\tau$ evaluations of $x_{h,i}$ with $j$ th component $\sigma_\tau^j(x_{h,i})$
$\beta_\tau$	The confidence term
$\mathbf{k}$	The covariance function of the GP
$d$	The metric associated with the design space
$l_j$	The metric on $\mathcal{X}$ induced by the $j$ th component of the GP
$\mathcal{P}_t$ and $P_t$	The predicted $\epsilon$ -accurate Pareto sets of nodes and regions, respectively, at round $t$
$\mathcal{S}_t$ and $S_t$	The undecided sets of nodes and regions, respectively, at round $t$
$\hat{\mathcal{P}}$	The $\epsilon$ -accurate Pareto set of nodes returned by Algorithm 1
$\mathcal{A}_t$	The union of sets $\mathcal{S}_t$ and $\mathcal{P}_t$ at the beginning of round $t$
$\mathcal{W}_t$	The union of sets $\mathcal{S}_t$ and $\mathcal{P}_t$ at the end of the discarding phase of round $t$
$\mathbf{L}_t(x_{h,i})$ and $\mathbf{U}_t(x_{h,i})$	The lower and upper vector-valued indices of node $x_{h,i}$ at time $t$ , whose $j$ th components are $L_t^j(x_{h,i})$ and $U_t^j(x_{h,i})$
$\overline{\mathbf{B}}_t^j(x_{h,i})$ and $\underline{\mathbf{B}}_t^j(x_{h,i})$	The auxiliary indices of the lower and upper index of node $x_{h,i}$ at time $t$
$\mathbf{V}_h$	The $m$ -dimensional vector with components are equal to $V_h$ , which appears in high probability bounds on the variation of $\mathbf{f}$
$\mathbf{Q}_t(x_{h,i})$	The confidence hyper-rectangle associated with node $x_{h,i}$ at round $t$
$\mathbf{R}_t(x_{h,i})$	The cumulative confidence hyper-rectangle associated with node $x_{h,i}$ at round $t$
$\omega_t(x_{h,i})$	The diameter of the cumulative confidence hyper-rectangle of $x_{h,i}$ at round $t$
$\overline{\omega}_t$	The maximum $\omega_t(x_{h,i})$ over all active nodes at round $t$
$D_1$	The metric dimension of $\mathcal{X}$
$\gamma_T$	The maximum information gain in $T$ evaluations of $\mathbf{f}$
$\tau_s$	The number of evaluations performed by the algorithm until termination
$t_s$	The round in which the algorithm terminates

Thus,  $l_j(x, y) \leq C_{\mathbf{k}} d(x, y)^\alpha \leq r$ , which implies that  $\tilde{X}$  is an  $r$ -covering of  $(\mathcal{X}, l_j)$ . By the definition of the covering number, we have

$$N(\mathcal{X}, r, l_j) \leq |\tilde{X}|,$$

and since this holds for any  $(\frac{r}{C_{\mathbf{k}}})^{\frac{1}{\alpha}}$ -covering of  $(\mathcal{X}, d)$ , we conclude that

$$N(\mathcal{X}, r, l_j) \leq N\left(\mathcal{X}, \left(\frac{r}{C_{\mathbf{k}}}\right)^{\frac{1}{\alpha}}, d\right).$$

Next, we will show that  $D_1^j \leq D_1/\alpha$ . For this, it is enough to show that  $D_1^j \leq \bar{D}_1/\alpha$  for every  $\bar{D}_1 > D_1$ . By Lemma 1, there exists a constant  $Q_1 \geq 1$  such that  $N(\mathcal{X}, r, d) \leq Q_1 r^{-\bar{D}_1}$  for all  $r > 0$ . In particular, for every  $r > 0$ , we have

$$N(\mathcal{X}, r, l_j) \leq N\left(\mathcal{X}, \left(\frac{r}{C_{\mathbf{k}}}\right)^{\frac{1}{\alpha}}, d\right) \leq Q_1 \left(\frac{r}{C_{\mathbf{k}}}\right)^{\frac{-\bar{D}_1}{\alpha}} \leq \left(\frac{Q_1}{(C_{\mathbf{k}})^{-\bar{D}_1/\alpha}}\right) r^{\bar{D}_1/\alpha}.$$

For all  $r > 0$ , assuming  $C_{\mathbf{k}} \geq 1$ , we have

$$\log N(\mathcal{X}, r, l_j) \leq \log Q_1 + (\bar{D}_1/\alpha) \log(C_{\mathbf{k}}) - (\bar{D}_1/\alpha) \log(r).$$

Therefore, there exists  $Q_2 > 0$ , such that for all  $r > 0$ , we have  $\log N(\mathcal{X}, r, l_j) \leq Q_2 - (\bar{D}_1/\alpha) \log r$ , with  $Q_2 = \log Q_1 + (\bar{D}_1/\alpha) \log(C_{\mathbf{k}})$ . Hence, we conclude that  $D_1^j \leq D_1/\alpha$ . ■

Next, we state a proposition that relates the information gain with the posterior variance of the GP after each evaluation. This proposition will help us in obtaining information-type bounds on the sample complexity. Since its proof is lengthy, we defer it to Section A.9.

**Proposition 1.** *Let  $T \in \mathbb{N}$  and  $\tilde{x}_{[T]} = [\tilde{x}_1, \dots, \tilde{x}_T]^\top$  be the finite sequence of designs that are evaluated. Consider the corresponding vector  $\mathbf{f}_{[T]} = [\mathbf{f}(\tilde{x}_1)^\top, \dots, \mathbf{f}(\tilde{x}_T)^\top]^\top$  of unobserved objective values and the vector  $\mathbf{y}_{[T]} = [\mathbf{y}_1^\top, \dots, \mathbf{y}_T^\top]^\top$  of noisy observations. Then, we have*

$$I(\mathbf{y}_{[T]}; \mathbf{f}_{[T]}) \geq \frac{1}{2m} \sum_{\tau=1}^T \sum_{j=1}^m \log(1 + \sigma^{-2}(\sigma_{\tau-1}^j(\tilde{x}_\tau))^2).$$

## A.2 Termination condition

In this section, we derive a sufficient condition under which Adaptive  $\epsilon$ -PAL terminates. We also give an upper bound on the maximum depth node that can be created by Adaptive  $\epsilon$ -PAL until it terminates.

In the lemma given below, we show that the algorithm terminates at latest when the diameter of the most uncertain node has fallen below  $\min_j \epsilon^j$ .

**Lemma 3. (Termination condition for Adaptive  $\epsilon$ -PAL)** *Let  $\epsilon = \min_j \epsilon^j > 0$ , where  $(\epsilon^1, \dots, \epsilon^m) = \boldsymbol{\epsilon}$ . When running Adaptive  $\epsilon$ -PAL, if  $\bar{\omega}_t \leq \epsilon$  holds at round  $t$ , then the algorithm terminates without further sampling.*



*Proof.* Since Adaptive  $\epsilon$ -PAL updates  $\mathcal{S}_t$  and  $\mathcal{P}_t$  at the end of discarding and  $\epsilon$ -covering phases, contents of these sets might change within round  $t$ . Thus, we let  $\mathcal{S}_{t,0}$  ( $\mathcal{P}_{t,0}$ ),  $\mathcal{S}_{t,1}$  ( $\mathcal{P}_{t,1}$ ) and  $\mathcal{S}_{t,2}$  ( $\mathcal{P}_{t,2}$ ) represent the elements in  $\mathcal{S}_t$  ( $\mathcal{P}_t$ ) at the end of modeling, discarding and covering phases, respectively. These sets are related in the following ways:  $\mathcal{S}_{t,0} \supseteq \mathcal{S}_{t,1} \supseteq \mathcal{S}_{t,2}$ ,  $\mathcal{P}_{t,0} = \mathcal{P}_{t,1} \subseteq \mathcal{P}_{t,2}$  and  $\mathcal{S}_{t,1} \cup \mathcal{P}_{t,1} = \mathcal{S}_{t,2} \cup \mathcal{P}_{t,2}$ .

Next, we state a claim from which termination immediately follows.

**Claim 1.** *If  $\bar{\omega}_t \leq \epsilon$  holds at iteration  $t$ , then for all  $x_{h,i} \in \mathcal{S}_{t,0} \setminus \mathcal{P}_{t,2}$ , we have  $x_{h,i} \notin \mathcal{S}_{t,1}$ .*

If Claim 1 holds, then any  $x_{h,i} \in \mathcal{S}_{t,0} \setminus \mathcal{P}_{t,2}$  must be discarded by the end of the discarding phase of Adaptive  $\epsilon$ -PAL. This implies that any  $x_{h,i} \in \mathcal{S}_{t,0}$  is either discarded or moved to  $\mathcal{P}_{t,2}$  by the end of the  $\epsilon$ -covering phase of round  $t$ , thereby completing the proof.

Next, we prove Claim 1. Note that  $\bar{\omega}_t$  is an upper bound on  $\|\max(\mathbf{R}_t(x_{h,i})) - \min(\mathbf{R}_t(x_{h,i}))\|_2$ , for all  $x_{h,i} \in \mathcal{S}_{t,2} \cup \mathcal{P}_{t,2}$ . For each  $x_{h,i} \in \mathcal{S}_{t,2} \cup \mathcal{P}_{t,2}$  define

$$\omega_{h,i} = \max(\mathbf{R}_t(x_{h,i})) - \min(\mathbf{R}_t(x_{h,i})) .$$

We have  $\|\omega_{h,i}\|_2 \leq \bar{\omega}_t \leq \epsilon$ , which implies that  $\omega_{h,i} \preceq \epsilon$  since  $\omega_{h,i}^j \leq \sqrt{\sum_{j'=1}^m (\omega_{h,i}^{j'})^2} \leq \epsilon \leq \epsilon^j$  for all  $j \in [m]$ .

We will show that if  $x_{h,i} \in \mathcal{S}_{t,0} \setminus \mathcal{P}_{t,2}$  holds, then  $x_{h,i}$  cannot belong to  $\mathcal{S}_{t,1}$ . To prove this, assume that  $x_{h,i} \in \mathcal{S}_{t,1}$ . Since  $x_{h,i} \notin \mathcal{P}_{t,2}$ , then by the  $\epsilon$ -covering rule of Adaptive  $\epsilon$ -PAL specified in line 15 of Algorithm 1, there exists some  $y^* \in \mathcal{S}_{t,1} \cup \mathcal{P}_{t,1}$  for which

$$\min(\mathbf{R}_t(x_{h,i})) + \epsilon \preceq \max(\mathbf{R}_t(y^*)) . \quad (4)$$

Since  $\mathcal{S}_{t,1} \cup \mathcal{P}_{t,1} = \mathcal{S}_{t,2} \cup \mathcal{P}_{t,2}$ , we have for all  $y \in \mathcal{S}_{t,1} \cup \mathcal{P}_{t,1}$

$$\max(\mathbf{R}_t(y)) - \min(\mathbf{R}_t(y)) \preceq \epsilon . \quad (5)$$

Combining (4) and (5), we obtain

$$\begin{aligned} \max(\mathbf{R}_t(x_{h,i})) &= \min(\mathbf{R}_t(x_{h,i})) + \omega_{h,i} \preceq \min(\mathbf{R}_t(x_{h,i})) + \epsilon \\ &\preceq \max(\mathbf{R}_t(y^*)) \\ &\preceq \min(\mathbf{R}_t(y^*)) + \epsilon . \end{aligned} \quad (6)$$

An immediate consequence of (6) is that

$$\min(\mathbf{R}_t(x_{h,i})) \preceq \min(\mathbf{R}_t(y^*)) . \quad (7)$$

Since  $y^* \in \mathcal{S}_{t,0} \cup \mathcal{P}_{t,0}$ , by Definition 10 and (7), we conclude that  $x_{h,i} \notin \mathcal{P}_{\text{pess},t}$ . Thus, we must have  $x_{h,i} \in \mathcal{S}_{t,0} \setminus \mathcal{P}_{\text{pess},t}$ . Finally, we claim that  $\max(\mathbf{R}_t(x_{h,i})) \preceq_{\epsilon} \min(\mathbf{R}_t(y^{**}))$  for some  $y^{**} \in \mathcal{P}_{\text{pess},t}$ . Since (6) implies that  $\max(\mathbf{R}_t(x_{h,i})) \preceq_{\epsilon} \min(\mathbf{R}_t(y^*))$ , if  $y^* \in \mathcal{P}_{\text{pess},t}$ , then we can simply set  $y^{**} = y^*$ . Else if  $y^* \notin \mathcal{P}_{\text{pess},t}$ , then this will imply by Definition 10 existence of  $y^{**} \in \mathcal{P}_{\text{pess},t}$  such that  $\min(\mathbf{R}_t(y^*)) \preceq \min(\mathbf{R}_t(y^{**}))$ , which in turn together with (6) implies that  $\max(\mathbf{R}_t(x_{h,i})) \preceq_{\epsilon} \min(\mathbf{R}_t(y^{**}))$ . Then, by the discarding rule of Adaptive  $\epsilon$ -PAL specified in line 9 of Algorithm 1, we must have  $x_{h,i}$  discarded by the end of the discarding phase, which implies that  $x_{h,i}$  cannot be in  $\mathcal{S}_{t,1}$ . This proves that all  $x_{h,i} \in \mathcal{S}_{t,0} \setminus \mathcal{P}_{t,2}$  must be discarded.

We will prove information-type and dimension-type sample complexity bounds by making use of the termination condition given in Lemma 3.

### A.3 Guarantees on the termination of Adaptive $\epsilon$ -PAL

We start by stating a bound on the maximum depth node that can be created by Adaptive  $\epsilon$ -PAL before it terminates for a given  $\epsilon$ . This result will be used in defining “good” events that hold with high probability under which  $\mathbf{f}(x_{h,i})$  lies in the confidence hyper-rectangle of  $x_{h,i}$  formed by Adaptive  $\epsilon$ -PAL, for all possible nodes that can be created by the algorithm (see Section A.4). Our bounds on sample complexity will hold given that these “good” events happen.

**Lemma 4.** *Given  $\epsilon$ , there exists  $h_{max} \in \mathbb{N}$  (dependent on  $\epsilon$ ) such that Adaptive  $\epsilon$ -PAL stops refining at level  $h_{max}$ .*

*Proof.* By Lemma 3, at the latest, the algorithm terminates at round  $t$  for which  $\bar{\omega}_t \leq \epsilon$ , i.e.,  $\bar{\omega}_t^2 \leq \epsilon^2$ . By definition, at a refining round we have

$$\begin{aligned}
\bar{\omega}_t^2 &\leq \max_{y, y' \in \mathbf{Q}_t(x_{h_t, i_t})} \|y - y'\|_2^2 \\
&= \|\mathbf{U}_t(x_{h_t, i_t}) - \mathbf{L}_t(x_{h_t, i_t})\|_2^2 \\
&= \sum_{j=1}^m \left( U_t^j(x_{h_t, i_t}) - L_t^j(x_{h_t, i_t}) \right)^2 \\
&= \sum_{j=1}^m \left( \bar{B}_t^j(x_{h_t, i_t}) - \underline{B}_t^j(x_{h_t, i_t}) + 2V_{h_t} \right)^2 \\
&\leq \sum_{j=1}^m \left( 2\beta_{\tau_t}^{1/2} \sigma_{\tau_t}^j(x_{h_t, i_t}) + 2V_{h_t} \right)^2 \\
&= \left( 4 \sum_{j=1}^m \beta_{\tau_t} (\sigma_{\tau_t}^j(x_{h_t, i_t}))^2 + 8 \sum_{j=1}^m V_{h_t} \beta_{\tau_t}^{1/2} \sigma_{\tau_t}^j(x_{h_t, i_t}) + 4 \sum_{j=1}^m (V_{h_t})^2 \right) \\
&\leq \left( 4 \sum_{j=1}^m (V_{h_t})^2 + 8 \left( \sum_{j=1}^m (V_{h_t})^2 \right)^{1/2} \left( \sum_{j=1}^m (V_{h_t})^2 \right)^{1/2} + 4 \sum_{j=1}^m (V_{h_t})^2 \right) \quad (8) \\
&= 16mV_{h_t}^2,
\end{aligned}$$

where (8) follows from the fact that we refine at round  $t$  and from the Cauchy-Schwarz inequality. Thus, if at round  $t$ , we have

$$16mV_{h_t}^2 \leq \epsilon^2,$$

then we guarantee termination of the algorithm. We let

$$V_h = 4C_{\mathbf{k}}(v_1\rho^h)^\alpha \left( \sqrt{C_2 + 2\log(2h^2\pi^2m/6\delta) + h\log N + \max\{0, -4(D_1/\alpha)\log(C_{\mathbf{k}}(v_1\rho^h)^\alpha)\}} + C_3 \right),$$

for positive constants  $C_2$  and  $C_3$  defined in Corollary 1. Obviously,  $V_h$  decays to 0 exponentially in  $h$ . Thus, by letting  $h_{max} = h_{max}(\epsilon)$  to be the smallest  $h \geq 0$ , for which  $16mV_{h_{max}}^2 \leq \epsilon^2$  holds, it is observed that the algorithm stops refining at level  $h_{max}$ .  $\blacksquare$

Our next result gives an upper bound on the maximum number of times a node can be evaluated before it is expanded.

**Lemma 5.** *Let  $h \geq 0$  and  $i \in [N^h]$ . Let  $\tau_s$  be the number of evaluations performed by Adaptive  $\epsilon$ -PAL until termination. Any active node  $x_{h,i}$  may be evaluated no more than  $q_h$  times before it is expanded, where*

$$q_h = \frac{\sigma^2 \beta_{\tau_s}}{V_h^2} .$$

Furthermore, we have

$$q_h \leq \frac{\sigma^2 \beta_{\tau_s}}{g(v_1 \rho^h)^2 C_3} .$$

*Proof.* The proof is similar to the proof of (Shekhar et al., 2018, Lemma 1). Fix  $t \geq 1$ . By definition, the vector  $\mathbf{y}_{[\tau_t]}$  denotes the evaluations made prior to round  $t$ . Let  $\mathbf{y}_{x_{h,i}}$  be the vector that represents the subset of evaluations in  $\mathbf{y}_{[\tau_t]}$  made at node  $x_{h,i}$  prior to round  $t$ , and let  $n_t(x_{h,i})$  represent the number of evaluations in  $\mathbf{y}_{x_{h,i}}$ . Similarly, let  $\bar{\mathbf{y}}_{x_{h,i}}$  be the vector that represents the subset of evaluations in  $\mathbf{y}_{[\tau_t]}$  made at nodes other than node  $x_{h,i}$  prior to round  $t$ . For any  $j \in [m]$ , by non-negativity of the information gain, we have

$$I(f^j(x_{h,i}); \mathbf{y}_{x_{h,i}} | \bar{\mathbf{y}}_{x_{h,i}}) = H(f^j(x_{h,i}) | \mathbf{y}_{x_{h,i}}) - H(f^j(x_{h,i}) | \mathbf{y}_{x_{h,i}}, \bar{\mathbf{y}}_{x_{h,i}}) \geq 0 .$$

Furthermore, let  $y_{x_{h,i}}^j$  be the vector of evaluations that corresponds to the  $j$ th objective at node  $x_{h,i}$ , and  $\bar{y}_{x_{h,i}}^j$  be the vector of evaluations that corresponds to the  $j$ th objective at nodes other than node  $x_{h,i}$  prior to round  $t$ . Since conditioning on more variables reduces the entropy, we have  $H(f^j(x_{h,i}) | \mathbf{y}_{x_{h,i}}) \leq H(f^j(x_{h,i}) | y_{x_{h,i}}^j)$ , and thus,

$$H(f^j(x_{h,i}) | y_{x_{h,i}}^j) - H(f^j(x_{h,i}) | \mathbf{y}_{x_{h,i}}, \bar{\mathbf{y}}_{x_{h,i}}) \geq 0 .$$

Using the definition of conditional entropy for Gaussian random variables, after a short algebraic calculation, we get

$$\frac{1}{2} \log \left( \left| \frac{2\pi e}{n_t(x_{h,i})/\sigma^2 + (k^{jj}(x_{h,i}, x_{h,i}))^{-1}} \right| \right) - \frac{1}{2} \log(|2\pi e(\sigma_{\tau_t}^j(x_{h,i}))^2|) \geq 0 .$$

Since  $\mathbf{k}(x_{h,i}, x_{h,i})$  is positive definite, we have  $k^{jj}(x_{h,i}, x_{h,i}) > 0$ , and as a result we obtain the following.

$$(\sigma_{\tau_t}^j(x_{h,i}))^{-2} \geq \frac{n_t(x_{h,i})}{\sigma^2} + \frac{1}{k^{jj}(x_{h,i}, x_{h,i})} \geq \frac{n_t(x_{h,i})}{\sigma^2}$$

Thus, we have that  $(\sigma_{\tau_t}^j(x_{h,i}))^2 \leq \sigma^2/n_t(x_{h,i})$ . If the algorithm has not yet refined, then it means that we have

$$mV_h^2 < \beta_{\tau_t} \sum_{j=1}^m (\sigma_{\tau_t}^j)^2 \leq \beta_{\tau_s} m\sigma^2/n_t(x_{h,i}) .$$

Therefore, we obtain

$$n_t(x_{h,i}) \leq q_h = \frac{\sigma^2 \beta_{\tau_s}}{V_h^2} .$$

The second statement of the result follows from the trivial observation that

$$\frac{\sigma^2 \beta_{\tau_s}}{V_h^2} \leq \frac{\sigma^2 \beta_{\tau_t}}{g(v_1 \rho^h)^2 C_3}.$$

■

Next, we show that Adaptive  $\epsilon$ -PAL terminates in finite time.

**Proposition 2.** *Given  $\epsilon$  such that  $\min_j \epsilon^j > 0$ , Adaptive  $\epsilon$ -PAL terminates in finite time.*

*Proof.* By Lemma 4, the algorithm refines no deeper than  $h_{max}(\epsilon)$  until termination. Moreover, the algorithm cannot evaluate a node  $x_{h,i}$  indefinitely, since there must exist some finite  $\tau_t$  for which  $\beta_{\tau_t}^{1/2} \|\sigma_{\tau_t}(x_{h,i})\|_2 \leq \|\mathbf{V}_h\|_2$  holds. This observation is a consequence of the fact that  $(\sigma_{\tau_t}^j(x_{h,i}))^2 \leq \sigma^2/n_t(x_{h,i})$ , given in the proof of Lemma 5, where  $n_t(x_{h,i})$  represents the number of evaluations made at node  $x_{h,i}$  prior to round  $t$ . Let  $t'_s$  be the round that comes just after the round in which  $s$  evaluations are made at node  $x_{h,i}$ . Since  $(\sigma_{\tau_{t'_s}}^j(x_{h,i}))^2 \leq \sigma^2/s$ , we conclude by observing that there exists  $s \in \mathbb{N}$  such that  $\beta_{\tau_{t'_s}}^{1/2} \|\sigma_{\tau_{t'_s}}(x_{h,i})\|_2 \leq \|\mathbf{V}_h\|_2$  holds. ■

#### A.4 Two “good” events under which the sample complexity will be bounded

First, we show that the indices of all possible nodes that could be created by Adaptive  $\epsilon$ -PAL do not deviate too much from the true mean objective values in all objectives, and that similar designs yield similar outcomes with high probability. To that end let us denote by  $\mathcal{T}_{h_{max}}$  the set of all nodes that can be created until the level  $h_{max}$ , where  $h_{max}$  comes from Lemma 4. Note that we have

$$\mathcal{T}_{h_{max}} = \bigcup_{h=0}^{h_{max}} \mathcal{X}_h.$$

**Lemma 6. (The first “good” event)** *For any  $\delta \in (0, 1)$ , the probability of the following event is at least  $1 - \delta/2$ :*

$$\mathcal{F}_1 = \{\forall j \in [m], \forall \tau \geq 0, \forall x \in \mathcal{T}_{h_{max}} : |f^j(x) - \mu_\tau^j(x)| \leq \beta_\tau^{1/2} \sigma_\tau^j\},$$

where  $\beta_\tau = 2 \log(2m\pi^2 N^{h_{max}+1} (\tau+1)^2 / (3\delta))$  with  $h_{max}$  being the deepest level of the tree before termination.

*Proof.* We have:

$$\begin{aligned}
 1 - \mathbb{P}(\mathcal{F}_1) &= \mathbb{E} \left[ \mathbb{I} \left( \exists j \in [m], \exists \tau \geq 0, \exists x \in \mathcal{T}_{h_{max}} : |f^j(x) - \mu_\tau^j(x)| > \beta_\tau^{1/2} \sigma_\tau^j(x) \right) \right] \\
 &\leq \mathbb{E} \left[ \sum_{j=1}^m \sum_{\tau \geq 0} \sum_{x \in \mathcal{T}_{h_{max}}} \mathbb{I} \left( |f^j(x) - \mu_\tau^j(x)| > \beta_\tau^{1/2} \sigma_\tau^j(x) \right) \right] \\
 &= \sum_{j=1}^m \sum_{\tau \geq 0} \sum_{x \in \mathcal{T}_{h_{max}}} \mathbb{E} \left[ \mathbb{E} \left[ \mathbb{I} \left( |f^j(x) - \mu_\tau^j(x)| > \beta_\tau^{1/2} \sigma_\tau^j(x) \right) \mid \mathbf{y}_{[\tau]} \right] \right] \tag{9}
 \end{aligned}$$

$$\begin{aligned}
 &= \sum_{j=1}^m \sum_{\tau \geq 0} \sum_{x \in \mathcal{T}_{h_{max}}} \mathbb{E} \left[ \mathbb{P} \left\{ |f^j(x) - \mu_\tau^j(x)| > \beta_\tau^{1/2} \sigma_\tau^j(x) \mid \mathbf{y}_{[\tau]} \right\} \right] \\
 &\leq \sum_{j=1}^m \sum_{\tau \geq 0} \sum_{x \in \mathcal{T}_{h_{max}}} 2e^{-\beta_\tau/2} \tag{10}
 \end{aligned}$$

$$\begin{aligned}
 &\leq 2mN^{h_{max}+1} \sum_{\tau \geq 0} e^{-\beta_\tau/2} \tag{11} \\
 &= 2mN^{h_{max}+1} \sum_{\tau \geq 0} (2m\pi^2 N^{h_{max}+1} (\tau+1)^2 / (3\delta))^{-1} \\
 &= \frac{\delta}{2} \frac{6}{\pi^2} \sum_{\tau \geq 0} (\tau+1)^{-2} = \frac{\delta}{2},
 \end{aligned}$$

where (9) uses the tower rule and linearity of expectation; (10) uses Gaussian tail bounds (note that  $f^j(x) \sim \mathcal{N}(\mu_{\tau_t}^j(x), \sigma_{\tau_t}^j(x))$  conditioned on  $\mathbf{y}_{[\tau_t]}$ ) and (11) uses the fact that for any  $t \geq 1$ , the cardinality of  $\mathcal{T}_{h_{max}}$  is  $1+N+N^2+\dots+N^{h_{max}} = (N^{h_{max}+1}-1)/(N-1) \leq N^{h_{max}+1}$ , since  $N \geq 2$ .  $\blacksquare$

Next, we introduce a bound on the maximum variation of the function inside a region. First, we state a result taken from Shekhar et al. (2018) on which this bound is based. Suppose  $\{g(x); x \in \mathcal{X}\}$  is a separable zero mean single output Gaussian Process  $GP(0, k)$  and let  $l$  be the GP-induced metric on  $\mathcal{X}$ . Let  $D'_1$  be the metric dimension of  $\mathcal{X}$  with respect to  $l$ . By Lemma 1, we have that if  $D'_1 < \infty$ , then there exists a positive constant  $\tilde{C}_1$  depending on  $2D'_1$  such that for any  $z \leq \text{diam}(\mathcal{X})$  we have  $N(\mathcal{X}, z, l) \leq \tilde{C}_1 z^{-2D'_1}$ . Let  $\eta_1 = \sum_{n \geq 1} 2^{-(n-1)} \sqrt{\log n}$ ,  $\eta_2 = \sum_{n \geq 1} 2^{-(n-1)} \sqrt{n}$ , and define

$$\tilde{C}_2 = 2 \log(2\tilde{C}_1^2 \pi^2 / 6) \quad \text{and} \quad \tilde{C}_3 = \eta_1 + \eta_2 \sqrt{2D'_1 \log 2}.$$

**Lemma 7.** (*Proposition 1, Section 6, Shekhar et al. (2018)*) Let  $x_0 \in \mathcal{X}$  and  $B(x_0, b, l) \subset \mathcal{X}$  be an  $l$ -ball of radius  $b > 0$ , where  $l$  is the GP-induced metric on  $\mathcal{X}$ . Then, we have for any  $u > 0$

$$\mathbb{P} \left\{ \sup_{x \in B(x_0, b, l)} |g(x) - g(x_0)| > \omega(b) \right\} \leq e^{-u},$$

where  $\omega(b) = 4b \left( \sqrt{\tilde{C}_2 + 2u + \max\{0, 4D'_1 \log(1/b)\}} + \tilde{C}_3 \right)$ .

**Remark 2.** Note that by Remark 1, for every  $j \in [m]$ , the covariance function  $k^{jj}(x, x)$  is continuous with respect to the metric  $l_j$ , and thus, the process  $\{f^j(x); x \in \mathcal{X}\}$  is separable.

**Corollary 1. (The second “good” event)** For any  $\delta \in (0, 1)$ , the probability of the following event is at least  $1 - \delta/2$ :

$$\mathcal{F}_2 = \left\{ \forall h \geq 0, \forall i \in [N^h], \forall j \in [m] : \sup_{x \in B(x_{h,i}, v_1 \rho^h, d)} |f^j(x) - f^j(x_{h,i})| \leq V_h \right\},$$

where

$$V_h = 4C_{\mathbf{k}}(v_1 \rho^h)^\alpha \left( \sqrt{C_2 + 2 \log(2h^2 \pi^2 m / 6\delta) + h \log N + \max\{0, -4(D_1/\alpha) \log(C_{\mathbf{k}}(v_1 \rho^h)^\alpha)\}} + C_3 \right),$$

and  $C_2$  and  $C_3$  are the positive constants defined below which depend on the metric dimension  $D_1$  of  $\mathcal{X}$  with respect to metric  $d$ .

*Proof.* Let  $D_1$  be the metric dimension of  $\mathcal{X}$  with respect to  $d$ . By Lemma 2, we have that  $D_1^j \leq D_1/\alpha$ , where  $D_1^j$  is the metric dimension of  $\mathcal{X}$  with respect to  $l_j$ , for all  $j \in [m]$ . We also have constants  $C_1^j$  associated with  $D_1^j$ , such that  $N(\mathcal{X}, r^\alpha, d) \leq N(\mathcal{X}, r, l_j) \leq C_1^j r^{2D_1^j}$ . Let  $C_1 = \max_j C_1^j$ . Also, let

$$C_2 = 2 \log(2C_1^2 \pi^2 / 6) \text{ and } C_3 = \eta_1 + \eta_2 \sqrt{2D_1 \alpha \log 2}.$$

Using Lemma 7 and Remark 2 we let

$$\omega(b) = 4b \left( \sqrt{C_2 + 2u + \max\{0, 4D_1 \log(1/b)\}} + C_3 \right).$$

Now let  $u = -\log \delta + \log m + h \log N + \log(2h^2 \pi^2 / 6)$ . We have

$$\begin{aligned} & 1 - \mathbb{P}(\mathcal{F}_2) \\ &= \mathbb{P} \left\{ \exists h \geq 0, \exists i \in [N^h], \exists j \in [m] : \sup_{x \in B(x_{h,i}, v_1 \rho^h, d)} |f^j(x) - f^j(x_{h,i})| > \omega(C_{\mathbf{k}}(v_1 \rho^h)^\alpha) \right\} \\ &\leq \sum_{h \geq 0} \sum_{1 \leq i \leq N^h} \sum_{j=1}^m \mathbb{P} \left\{ \sup_{x \in B(x_{h,i}, v_1 \rho^h, d)} |f^j(x) - f^j(x_{h,i})| > \omega(C_{\mathbf{k}}(v_1 \rho^h)^\alpha) \right\} \\ &\leq \sum_{h \geq 0} \sum_{1 \leq i \leq N^h} \sum_{j=1}^m \mathbb{P} \left\{ \sup_{x \in B(x_{h,i}, C_{\mathbf{k}}(v_1 \rho^h)^\alpha, l)} |f^j(x) - f^j(x_{h,i})| > \omega(C_{\mathbf{k}}(v_1 \rho^h)^\alpha) \right\} \quad (12) \\ &\leq \sum_{h \geq 0} \sum_{1 \leq i \leq N^h} \sum_{j=1}^m e^{-u} \\ &\leq \delta \frac{\pi^2}{6} \sum_{h \geq 0} \frac{1}{2} m N^h (m N^h)^{-1} h^{-2} \\ &\leq \frac{\delta}{2}, \end{aligned}$$

where for (12) we argue as follows. Note that by Assumption 1, given  $x, y \in \mathcal{X}$  and  $j \in [m]$ , we have  $l_j(x, y) \leq C_{\mathbf{k}} d(x, y)^\alpha$ . In particular, letting  $y$  be any design which is  $v_1 \rho^h$  away from  $x_{h,i}$  under  $d$ , we have  $l_j(x_{h,i}, y) \leq C_{\mathbf{k}} d(x_{h,i}, y)^\alpha = C_{\mathbf{k}} (v_1 \rho^h)^\alpha$ . This implies that  $B(x_{h,i}, r, l_j) \subseteq B(x_{h,i}, C_{\mathbf{k}} (v_1 \rho^h)^\alpha, l_j)$ , where  $r := l_j(x_{h,i}, y)$ . Note that we have  $B(x_{h,i}, r, l_j) = B(x_{h,i}, v_1 \rho^h, d)$ . The result follows from observing that the probability that the variation of the function exceeds  $\omega(C_{\mathbf{k}} (v_1 \rho^h)^\alpha)$  is higher in  $B(x_{h,i}, C_{\mathbf{k}} (v_1 \rho^h)^\alpha, l_j)$  than in  $B(x_{h,i}, v_1 \rho^h, d)$ , since  $B(x_{h,i}, v_1 \rho^h, d) \subseteq B(x_{h,i}, C_{\mathbf{k}} (v_1 \rho^h)^\alpha, l_j)$ .  $\blacksquare$

### A.5 Key results that hold under the “good” events

Our next result shows that the objective values of all designs  $x \in \mathcal{X}$  belong to the uncertainty hyper-rectangles of the nodes associated to the regions containing them in a given round. To that end, let us denote by  $c_t(x)$  the node associated to the cell  $C_t(x)$  containing  $x$  at the beginning of round  $t$ . Also, let us denote by  $h_t(x)$  the depth of the tree where  $c_t(x)$  is located.

**Lemma 8.** *Under events  $\mathcal{F}_1$  and  $\mathcal{F}_2$ , for any round  $t \geq 1$  before Adaptive  $\epsilon$ -PAL terminates and for any  $x \in \mathcal{X}$ , we have*

$$\mathbf{f}(x) \in \mathbf{R}_t(c_t(x)) .$$

*Proof.* First, let us denote by  $1 = s_0 < s_1 < s_2 < \dots < s_n$  the sequence of stopping times up to round  $t$  in which the original node containing design  $x$  was refined into children nodes, so that we have  $C_{s_n+1}(x) \subseteq C_{s_n}(x) \subseteq \dots \subseteq C_0(x)$ . By the definition of the cumulative confidence hyper-rectangle, for  $c_{s_0}(x)$ , we have

$$\begin{aligned} \mathbf{R}_{s_1}(c_{s_0}(x)) &= \mathbf{R}_{s_1-1}(c_{s_0}(x)) \cap \mathbf{Q}_{t_1}(c_{s_0}(x)) \\ &= \mathbf{R}_{s_1-2}(c_{s_0}(x)) \cap \mathbf{Q}_{s_1-1}(c_{s_0}(x)) \cap \mathbf{Q}_{s_1}(c_{s_0}(x)) \\ &= \mathbf{R}_0(c_{s_0}(x)) \cap \mathbf{Q}_{s_0}(c_{s_0}(x)) \cap \dots \cap \mathbf{Q}_{s_1}(c_{s_0}(x)) , \end{aligned}$$

and since  $\mathbf{R}_0(c_{s_0}(x)) = \mathbb{R}^m$ , we obtain

$$\mathbf{R}_{s_1}(c_{s_0}(x)) = \bigcap_{s=1}^{s_1} \mathbf{Q}_s(c_{s_0}(x)) .$$

Similarly, for  $c_{s_1}(x)$  we have

$$\begin{aligned} \mathbf{R}_{s_2}(c_{s_1}(x)) &= \mathbf{R}_{s_2-1}(c_{s_1}(x)) \cap \mathbf{Q}_{s_2}(c_{s_1}(x)) \\ &= \mathbf{R}_{s_1}(c_{s_1}(x)) \cap \mathbf{Q}_{s_1+1}(c_{s_1}(x)) \cap \dots \cap \mathbf{Q}_{s_2}(c_{s_1}(x)) , \end{aligned}$$

where

$$\mathbf{R}_{s_1}(c_{s_1}(x)) = \mathbf{R}_{s_1}(p(c_{s_1}(x))) = \mathbf{R}_{s_1}(c_{s_0}(x)) .$$

Thus, we obtain

$$\mathbf{R}_{s_2}(c_{s_1}(x)) = \left( \bigcap_{s=1}^{s_1} \mathbf{Q}_s(c_{s_0}(x)) \right) \cap \left( \bigcap_{s=s_1+1}^{s_2} \mathbf{Q}_s(c_{s_1}(x)) \right) .$$

Note that  $c_s(x) = c_{s_i}(x)$  for all  $s$  such that  $s_i < s \leq s_{i+1}$  for each  $i \in \{0, \dots, n-1\}$ ; and  $c_s(x) = c_{s_n}(x)$  for all  $s$  such that  $s_{n+1} < s \leq t$ . Thus, continuing as above, we can write

$$\begin{aligned} \mathbf{R}_t(c_t(x)) &= \left( \bigcap_{s=1}^{s_1} \mathbf{Q}_s(c_{s_0}(x)) \right) \cap \dots \cap \left( \bigcap_{s=s_{n-1}+1}^{s_n} \mathbf{Q}_s(c_{s_{n-1}}(x)) \right) \cap \left( \bigcap_{s=s_n+1}^t \mathbf{Q}_s(c_{s_n}(x)) \right) \\ &= \bigcap_{s=1}^t \mathbf{Q}_s(c_s(x)) . \end{aligned}$$

Based on the above display, to prove that  $\mathbf{f}(x) \in \mathbf{R}_t(c_t(x))$ , it is enough to show that  $\mathbf{f}(x) \in \mathbf{Q}_s(c_s(x))$ , for all  $s \leq t$ . Next, we prove that this is indeed the case, by showing that for any  $s \leq t$  and  $j \in [m]$ , it holds that

$$L_s^j(c_s(x)) = \underline{B}_s^j(c_s(x)) - V_{h_s(x)} \leq f^j(x) \leq \overline{B}_s^j(c_s(x)) + V_{h_s(x)} = U_s^j(c_s(x)) . \quad (13)$$

To show this, we first note that by definition

$$\underline{B}_s^j(c_s(x)) = \max\{\mu_{\tau_s}^j(c_s(x)) - \beta_{\tau_s}^{1/2} \sigma_{\tau_s}^j(c_s(x)), \mu_{\tau_s}^j(p(c_s(x))) - \beta_{\tau_s}^{1/2} \sigma_{\tau_s}^j(p(c_s(x))) - V_{h_s(x)-1}\} ,$$

and

$$\overline{B}_s^j(c_s(x)) = \min\{\mu_{\tau_s}^j(c_s(x)) + \beta_{\tau_s}^{1/2} \sigma_{\tau_s}^j(c_s(x)), \mu_{\tau_s}^j(p(c_s(x))) + \beta_{\tau_s}^{1/2} \sigma_{\tau_s}^j(p(c_s(x))) + V_{h_s(x)-1}\} .$$

Hence, we need to consider four cases: two cases for  $\underline{B}_s^j(c_s(x))$  and two cases for  $\overline{B}_s^j(c_s(x))$ . Let  $j \in [m]$ . Note that under events  $\mathcal{F}_1$  and  $\mathcal{F}_2$ , we have

$$\mu_{\tau_s}^j(c_s(x)) - \beta_{\tau_s}^{1/2} \sigma_{\tau_s}^j(c_s(x)) \leq f^j(c_t(x)) \leq \mu_{\tau_s}^j(c_s(x)) + \beta_{\tau_s}^{1/2} \sigma_{\tau_s}^j(c_s(x)) , \quad (14)$$

and

$$f^j(c_s(x)) - V_{h_s(x)} \leq f^j(x) \leq f^j(c_s(x)) + V_{h_s(x)} . \quad (15)$$

The following inequalities hold under  $\mathcal{F}_1$  and  $\mathcal{F}_2$ .

**Case 1:** If we have  $L_s^j(c_s(x)) = \mu_{\tau_s}^j(c_s(x)) - \beta_{\tau_s}^{1/2} \sigma_{\tau_s}^j(c_s(x)) - V_{h_s(x)}$ , then

$$\begin{aligned} L_t^j(c_s(x)) &= \mu_{\tau_s}^j(c_s(x)) - \beta_{\tau_s}^{1/2} \sigma_{\tau_s}^j(c_s(x)) - V_{h_s(x)} \\ &\leq f^j(c_s(x)) - V_{h_s(x)} \\ &\leq f^j(x) , \end{aligned}$$

where the first inequality follows from (14) and the second inequality follows from (15).

**Case 2:** If we have  $L_s^j(c_s(x)) = \mu_{\tau_s}^j(p(c_s(x))) - \beta_{\tau_s}^{1/2} \sigma_{\tau_s}^j(p(c_s(x))) - V_{h_s(x)-1} - V_{h_s(x)}$ , then

$$\begin{aligned} L_s^j(c_s(x)) &= \mu_{\tau_s}^j(p(c_s(x))) - \beta_{\tau_s}^{1/2} \sigma_{\tau_s}^j(p(c_s(x))) - V_{h_s(x)-1} - V_{h_s(x)} \\ &\leq f^j(p(c_s(x))) - V_{h_s(x)-1} - V_{h_s(x)} \\ &\leq f^j(c_s(x)) - V_{h_s(x)} \\ &\leq f^j(x) , \end{aligned}$$



where the first inequality follows from (14); for the second inequality we use the fact that  $c_s(x)$  belongs to the cell associated to  $p(c_s(x))$ , and thus we have that  $f^j(p(c_s(x))) \leq f^j(c_s(x)) + V_{h_s(x)-1}$ ; the third inequality follows from (15).

**Case 3:** If we have  $U_s^j(c_s(x)) = \mu_{\tau_s}^j(c_s(x)) + \beta_{\tau_s}^{1/2} \sigma_{\tau_s}^j(c_s(x)) + V_{h_s(x)}$ , then

$$\begin{aligned} f^j(x) &\leq f^j(c_s(x)) + V_{h_s(x)} \\ &\leq \mu_{\tau_s}^j(c_s(x)) + \beta_{\tau_s}^{1/2} \sigma_{\tau_s}^j(c_s(x)) + V_{h_s(x)} \\ &= U_s^j(c_s(x)) , \end{aligned}$$

where the first inequality follows from (15) and the second inequality follows from (14).

**Case 4:** If we have  $U_s^j(c_s(x)) = \mu_{\tau_s}^j(p(c_s(x))) + \beta_{\tau_s}^{1/2} \sigma_{\tau_s}^j(p(c_s(x))) + V_{h_s(x)-1} + V_{h_s(x)}$ , then

$$\begin{aligned} f^j(x) &\leq f^j(c_s(x)) + V_{h_s(x)} \\ &\leq f^j(p(c_s(x))) + V_{h_s(x)-1} + V_{h_s(x)} \\ &\leq \mu_{\tau_s}^j(p(c_s(x))) + \beta_{\tau_s}^{1/2} \sigma_{\tau_s}^j(p(c_s(x))) + V_{h_s(x)-1} + V_{h_s(x)} \\ &= U_s^j(c_s(x)) . \end{aligned}$$

The analysis of this case follows the same argument as the one of Case 2. This proves that (13) holds, and thus, the result follows.  $\blacksquare$

Our next result ensures that Adaptive  $\epsilon$ -PAL does not return "bad" nodes.

**Lemma 9.** *Let  $x \in \mathcal{X}$ . Under events  $\mathcal{F}_1$  and  $\mathcal{F}_2$ , if  $\mathbf{f}(x) \notin \mathcal{Z}_\epsilon(\mathcal{X})$ , then  $x \notin \hat{P}$ .*

*Proof.* Suppose that  $\mathbf{f}(x) \notin \mathcal{Z}_\epsilon(\mathcal{X})$ . Then, by Definition 3, we have  $\mathbf{f}(x) \in \mathbf{f}(\mathcal{O}(\mathcal{X})) - 2\epsilon - \mathbb{R}_+^m$ , that is, there exists  $x^* \in \mathcal{O}(\mathcal{X})$  such that we have

$$\mathbf{f}(x) + 2\epsilon \preceq \mathbf{f}(x^*) . \quad (16)$$

To get a contradiction, let us assume that  $x \in \hat{P}$ . This implies that there exists  $t \geq 1$  such that  $c_t(x)$  is added to  $\mathcal{P}_t$  by line 16 of the algorithm pseudocode. Thus, by the  $\epsilon$ -Pareto front covering rule in line 15 of the algorithm pseudocode, for each  $x_{h,i} \in \mathcal{W}_t$ , we have

$$\min(\mathbf{R}_t(c_t(x))) + \epsilon \not\leq \max(\mathbf{R}_t(x_{h,i})) . \quad (17)$$

In particular, we have that  $\min(\mathbf{R}_t(c_t(x))) + \epsilon \not\leq \max(\mathbf{R}_t(c_t(x^*)))$  (note that we may even have  $c_t(x) = c_t(x^*)$  and this would yield the same result), which, together with Lemma 8, implies that  $\mathbf{f}(x) + \epsilon \not\leq \mathbf{f}(x^*)$ . This contradicts (16).

Now since we have  $x, x^* \in C_t(x)$ , we must have  $\min(\mathbf{R}_t(c_t(x))) \preceq \mathbf{f}(x)$  and  $\mathbf{f}(x^*) \preceq \max(\mathbf{R}_t(c_t(x)))$  by Lemma 8, which implies that  $\mathbf{f}(x) + \epsilon \not\leq \mathbf{f}(x^*)$ , thereby contradicting (16).

Next, let us assume that  $c_t(x^*) \notin \mathcal{W}_t$ . This means that there exists a round  $s_1 \leq t$  at which  $c_{s_1}(x^*)$  is discarded. By line 9 of the Algorithm 1, there exists  $y_1 \in \mathcal{P}_{\text{pess}, s_1}$  such that we have

$$\max(\mathbf{R}_{s_1}(c_{s_1}(x^*))) - \epsilon \preceq \min(\mathbf{R}_{s_1}(y_1)) . \quad (18)$$

Assume that the child node  $c_t(y_1)$  of  $y_1$  at round  $t$  (due to possible refining in the middle rounds) is still not discarded by round  $t$ , i.e.  $c_t(y_1) \in \mathcal{W}_t$ . Then, by (17), we have

$$\min(\mathbf{R}_t(c_t(x))) + \epsilon \not\leq \max(\mathbf{R}_t(c_t(y_1))) ,$$

which implies that

$$\min(\mathbf{R}_t(c_t(x))) + \epsilon \not\leq \min(\mathbf{R}_t(c_t(y_1))) ,$$

which in return implies that

$$\min(\mathbf{R}_t(c_t(x))) + \epsilon \not\leq \min(\mathbf{R}_{s_1}(y_1))$$

due to the fact that  $\min(\mathbf{R}_{s_1}(y_1)) = \min(\mathbf{R}_{s_1}(c_t(y_1))) \preceq \min(\mathbf{R}_t(c_t(y_1)))$ . Thus, by (18), we obtain

$$\min(\mathbf{R}_t(c_t(x))) + \epsilon \not\leq \max(\mathbf{R}_{s_1}(c_{s_1}(x^*))) - \epsilon ,$$

or equivalently,

$$\min(\mathbf{R}_t(c_t(x))) + 2\epsilon \not\leq \max(\mathbf{R}_{s_1}(c_{s_1}(x^*))) .$$

By Lemma 8, this implies that  $\mathbf{f}(x) + 2\epsilon \not\leq \mathbf{f}(x^*)$ , contradicting (16). Hence, it remains to consider the case  $c_t(y_1) \notin \mathcal{W}_t$ .

In general, let the finite sequence of nodes  $[y_1, y_2, \dots, y_n]^\top$  be such that all the nodes  $y_1$  to  $y_{n-1}$  are discarded, meaning that, for each  $i \in [n-1]$ , the node  $y_i$  stopped being part of  $\mathcal{P}_{\text{pess}, s_{i+1}}$  at some round  $s_{i+1}$  by satisfying

$$\min(\mathbf{R}_{s_{i+1}}(c_{s_{i+1}}(y_i))) \preceq \min(\mathbf{R}_{s_{i+1}}(y_{i+1})) .$$

Suppose that  $c_t(y_n)$  is active in round  $t$ , meaning that  $c_t(y_n) \in \mathcal{W}_t$  (note that we can always find such an  $n$  since the algorithm terminates and that we choose the sequence such that it satisfies that condition; furthermore, we have  $s_1 < s_2 < \dots < s_n \leq t$ ). Since we have  $c_t(y_n) \in \mathcal{W}_t$ , by (17), we obtain

$$\min(\mathbf{R}_t(c_t(x))) + \epsilon \not\leq \max(\mathbf{R}_t(c_t(y_n))) . \quad (19)$$

Note that (18) implies

$$\begin{aligned} \max(\mathbf{R}_{s_1}(c_{s_1}(x^*))) - \epsilon &\preceq \min(\mathbf{R}_{s_1}(y_1)) \preceq \min(\mathbf{R}_{s_2}(c_{s_2}(y_1))) \\ &\preceq \min(\mathbf{R}_{s_2}(y_2)) \preceq \min(\mathbf{R}_{s_3}(c_{s_3}(y_2))) \\ &\preceq \dots \\ &\preceq \min(\mathbf{R}_{s_n}(y_n)) \preceq \min(\mathbf{R}_t(c_t(y_n))) , \end{aligned}$$

which in turn implies that

$$\max(\mathbf{R}_{s_1}(c_{s_1}(x^*))) - \epsilon \preceq \min(\mathbf{R}_t(c_t(y_n))) \preceq \max(\mathbf{R}_t(c_t(y_n))) .$$

This, combined with (19) implies

$$\min(\mathbf{R}_t(c_t(x))) + 2\epsilon \not\leq \max(\mathbf{R}_{s_1}(c_{s_1}(x^*))) .$$

Thus, in all cases we have that  $\mathbf{f}(x) + 2\epsilon \not\leq \mathbf{f}(x^*)$ , contradicting our assumption. We conclude that  $x \notin \hat{P}$ .  $\blacksquare$

Next, we show that Adaptive  $\epsilon$ -PAL returns an  $\epsilon$ -accurate Pareto set when it terminates.

**Lemma 10. (*Adaptive  $\epsilon$ -PAL returns an  $\epsilon$ -accurate Pareto set*)** Under events  $\mathcal{F}_1$  and  $\mathcal{F}_2$ , the set  $\hat{P}$  returned by Adaptive  $\epsilon$ -PAL is an  $\epsilon$ -accurate Pareto set.

*Proof.* Let  $x \in \mathcal{O}(\mathcal{X})$ . We claim that there exists  $z \in \hat{P}$  such that  $\mathbf{f}(x) \preceq_{\epsilon} \mathbf{f}(z)$ . Note that if  $x \in \hat{P}$ , then the claim holds trivially. Let us assume that  $x \notin \hat{P}$ . Then, there exists some round  $s_1 \in \mathbb{N}$  at which Adaptive  $\epsilon$ -PAL discards the node  $c_{s_1}(x)$ . By line 9 of the algorithm pseudocode, there exists a node  $z_1 \in \mathcal{P}_{\text{pess},s_1}$  such that

$$\max(\mathbf{R}_{s_1}(c_{s_1}(x))) \preceq \min(\mathbf{R}_{s_1}(z_1)) + \epsilon .$$

By Lemma 8, we have

$$\mathbf{f}(x) \preceq \max(\mathbf{R}_{s_1}(c_{s_1}(x))) \preceq \min(\mathbf{R}_{s_1}(z_1)) + \epsilon \preceq \mathbf{f}(z_1) + \epsilon . \quad (20)$$

Hence, if  $z_1 \in \hat{P}$ , then the claim holds with  $z = z_1$ .

Now, suppose that  $z_1 \notin \hat{P}$ . Hence, at some round  $s_2 \geq s_1$ , the node  $c_{s_2}(z_1)$  associated with  $z_1$  must be discarded by Adaptive  $\epsilon$ -PAL. By line 8 of the algorithm pseudocode, we know that a node in  $\mathcal{P}_{\text{pess},s_2}$  cannot be discarded at round  $s_2$ . Hence,  $c_{s_2}(z_1) \notin \mathcal{P}_{\text{pess},s_2}$ . Then, by Definition 10, there exists a node  $z_2 \in \mathcal{A}_{s_2}$  such that

$$\min(\mathbf{R}_{s_2}(c_{s_2}(z_1))) \preceq \min(\mathbf{R}_{s_2}(z_2)) ,$$

which, by (20), implies that

$$\begin{aligned} \mathbf{f}(x) &\preceq \min(\mathbf{R}_{s_1}(z_1)) + \epsilon \\ &= \min(\mathbf{R}_{s_1}(c_{s_2}(z_1))) + \epsilon \\ &\preceq \min(\mathbf{R}_{s_2}(c_{s_2}(z_1))) + \epsilon \\ &\preceq \min(\mathbf{R}_{s_2}(z_2)) + \epsilon \\ &\preceq \mathbf{f}(z_2) + \epsilon . \end{aligned}$$

Here, the equality follows since the child node inherits the cumulative confidence hyper-rectangles of its parents at prior rounds (see refining/evaluating phase in Section 3), and the second inequality follows from the fact that the cumulative confidence hyper-rectangles shrink with time. Hence,  $\mathbf{f}(x) \preceq_{\epsilon} \mathbf{f}(z_2)$ . If  $z_2 \in \hat{P}$ , then the claim holds with  $z = z_2$ .

Suppose that  $z_2 \notin \hat{P}$ . Then, the above process continues in a similar fashion. Suppose that the process never yields a node in  $\hat{P}$ . Since the algorithm is guaranteed to terminate by Lemma 3, the process stops and yields a finite sequence  $[z_1, \dots, z_n]^{\top}$  of designs such that  $z_1 \notin \hat{P}, \dots, z_n \notin \hat{P}$ . For each  $i \in [n-1]$ , let  $s_{i+1} \in \mathbb{N}$  be the round at which  $c_{s_{i+1}}(z_i)$  is discarded; by the above process, we have

$$\mathbf{f}(x) \preceq \min(\mathbf{R}_{s_{i+1}}(z_{i+1})) + \epsilon .$$

In particular,  $\mathbf{f}(x) \preceq \min(\mathbf{R}_{s_n}(z_n)) + \epsilon$ . Since  $z_n \notin \hat{P}$ , there exists a round  $s_{n+1} \geq s_n$  at which the node  $c_{s_{n+1}}(z_n)$  is discarded. Consequently, the node  $c_{s_{n+1}}(z_n) \notin \mathcal{P}_{\text{pess},s_{n+1}}$ . This implies that the condition of Definition 10 is violated at round  $s_{n+1}$ , that is, there exists  $z_{n+1} \in \mathcal{A}_{s_{n+1}}$  such that

$$\min(\mathbf{R}_{s_{n+1}}(c_{s_{n+1}}(z_n))) \preceq \min(\mathbf{R}_{s_{n+1}}(z_{n+1})) . \quad (21)$$

Hence, (21) and the earlier inequalities imply that

$$\begin{aligned}
\mathbf{f}(x) &\preceq \min(\mathbf{R}_{s_n}(z_n)) + \epsilon \\
&= \min(\mathbf{R}_{s_n}(c_{s_{n+1}}(z_n))) + \epsilon \\
&\preceq \min(\mathbf{R}_{s_{n+1}}(c_{s_{n+1}}(z_n))) + \epsilon \\
&\preceq \min(\mathbf{R}_{s_{n+1}}(z_{n+1})) + \epsilon \\
&\preceq \mathbf{f}(z_{n+1}) + \epsilon,
\end{aligned}$$

where we have again used the shrinking property of the cumulative confidence hyperrectangles in the second inequality. This means that  $z_{n+1}$  is another node that  $\epsilon$ -dominates  $x$  but it is not in the finite sequence  $[z_1, \dots, z_n]^\top$ . This contradicts our assumption that the process stops after finding  $n$  designs. Hence, at least one of the designs in  $[z_1, \dots, z_n]^\top$  is in  $\hat{P}$ ; let us call it  $z$ . This completes the proof of the claim.

Next, let  $\boldsymbol{\mu} \in \mathbf{f}(\mathcal{O}(\mathcal{X})) - \mathbb{R}_+^m$ . Then, there exist  $x \in \mathcal{O}(\mathcal{X})$  and  $\boldsymbol{\mu}' \in \mathbb{R}_+^m$  such that  $\boldsymbol{\mu} = \mathbf{f}(x) - \boldsymbol{\mu}'$ . By the above claim, there exists  $z \in \hat{P}$  such that  $\mathbf{f}(x) \preceq \mathbf{f}(z) + \epsilon$ . Hence,

$$\boldsymbol{\mu} \preceq \boldsymbol{\mu} + \boldsymbol{\mu}' = \mathbf{f}(x) \preceq \mathbf{f}(z) + \epsilon.$$

This shows that for every  $\boldsymbol{\mu} \in \mathbf{f}(\mathcal{O}(\mathcal{X})) - \mathbb{R}_+^m$ , there exists  $z \in \hat{P}$  such that  $\boldsymbol{\mu} \preceq_\epsilon \mathbf{f}(z)$ . By Definition 3, we have  $\mathcal{Z}_\epsilon(\mathcal{X}) \subseteq \mathbf{f}(\mathcal{O}(\mathcal{X})) - \mathbb{R}_+^m$ . Hence, for every  $\boldsymbol{\mu} \in \mathcal{Z}_\epsilon(\mathcal{X})$ , there exists  $\boldsymbol{\mu}'' \in \mathbf{f}(\hat{P})$  such that  $\boldsymbol{\mu} \preceq_\epsilon \boldsymbol{\mu}''$ . On the other hand, since we work under  $\mathcal{F}_1 \cap \mathcal{F}_2$ , Lemma 9 implies that  $\mathbf{f}(\hat{P}) \subseteq \mathcal{Z}_\epsilon(\mathcal{X})$ . Therefore,  $\mathbf{f}(\hat{P})$  is an  $\epsilon$ -covering of  $\mathcal{Z}_\epsilon(\mathcal{X})$  (Definition 4), that is,  $\hat{P}$  is an  $\epsilon$ -accurate Pareto set (Definition 5).  $\blacksquare$

## A.6 Derivation of the information-type sample complexity bound

In this section, we provide sample complexity upper bounds that depend on the maximum information gain from observing the evaluated designs.

We begin with an auxiliary lemma whose statement is straightforward for the case  $m = 1$ .

**Lemma 11.** *Let  $T \geq 1$ ,  $x \in \mathcal{X}$ . The matrices  $\mathbf{K}_{[T]} + \boldsymbol{\Sigma}_{[T]}$  and  $\mathbf{k}_{[T]}(x)(\mathbf{K}_{[T]} + \boldsymbol{\Sigma}_{[T]})^{-1}\mathbf{k}_{[T]}(x)^\top$  are symmetric and positive definite. In particular,  $(\mathbf{k}_{[T]}(x)(\mathbf{K}_{[T]} + \boldsymbol{\Sigma}_{[T]})^{-1}\mathbf{k}_{[T]}(x)^\top)^{jj} > 0$  for each  $j \in [m]$ .*

**Proof** Note that  $\mathbf{K}_{[T]}$  is the covariance matrix of the random vector  $\mathbf{f}_{[T]} = [\mathbf{f}(\tilde{x}_1)^\top, \dots, \mathbf{f}(\tilde{x}_T)^\top]^\top$ ; hence, it is symmetric and positive semidefinite. Being a diagonal matrix with positive entries,  $\boldsymbol{\Sigma}_{[T]}$  is symmetric and positive definite. Hence,  $\mathbf{K}_{[T]} + \boldsymbol{\Sigma}_{[T]}$  is symmetric and positive definite; and so is  $(\mathbf{K}_{[T]} + \boldsymbol{\Sigma}_{[T]})^{-1}$ . The latter implies that  $\mathbf{k}_{[T]}(x)(\mathbf{K}_{[T]} + \boldsymbol{\Sigma}_{[T]})^{-1}\mathbf{k}_{[T]}(x)^\top$  is symmetric and that

$$\mathbf{w}^\top \left( \mathbf{k}_{[T]}(x)(\mathbf{K}_{[T]} + \boldsymbol{\Sigma}_{[T]})^{-1}\mathbf{k}_{[T]}(x)^\top \right) \mathbf{w} = (\mathbf{k}_{[T]}(x)^\top \mathbf{w})^\top (\mathbf{K}_{[T]} + \boldsymbol{\Sigma}_{[T]})^{-1} (\mathbf{k}_{[T]}(x)^\top \mathbf{w}) > 0$$

for every  $\mathbf{w} \in \mathbb{R}^m$  with  $\mathbf{w} \neq 0$ . Therefore,  $\mathbf{a} = \mathbf{k}_{[T]}(x)(\mathbf{K}_{[T]} + \boldsymbol{\Sigma}_{[T]})^{-1}\mathbf{k}_{[T]}(x)^\top$  is positive definite. Let  $\lambda_{(1)} > 0$  be its minimum eigenvalue. Let  $j \in [m]$ . By the variational characterization of minimum eigenvalue, we have

$$a^{jj} = \mathbf{e}_j^\top \mathbf{a} \mathbf{e}_j \geq \min_{\mathbf{w} \in \mathbb{R}^m: \|\mathbf{w}\|_2=1} \mathbf{w}^\top \mathbf{a} \mathbf{w} = \lambda_{(1)} > 0,$$

where  $a^{jj} = (\mathbf{k}_{[T]}(x)(\mathbf{K}_{[T]} + \mathbf{\Sigma}_{[T]})^{-1}\mathbf{k}_{[T]}(x))^\top)^{jj}$  and  $\mathbf{e}_j$  is the  $j^{\text{th}}$  unit vector in  $\mathbb{R}^m$ . This completes the proof.  $\blacksquare$

Recall from (2) that, for each  $t \geq 1$  such that  $S_t \neq \emptyset$ ,  $\bar{\omega}_t = \omega_t(x_{h_t, i_t})$  denotes the diameter of the selected node  $x_{h_t, i_t} \in \mathcal{A}_t$  at round  $t$ .

**Lemma 12.** *Let  $\delta \in (0, 1)$ . We have*

$$\sum_{\tau=1}^{\tau_s} \bar{\omega}_{t_\tau} \leq \sqrt{\tau_s (16\beta_{\tau_s} \sigma^2 C m \gamma_{\tau_s})},$$

where  $C = \sigma^{-2} / \log(1 + \sigma^{-2})$  and  $\gamma_{\tau_s}$  is the maximum information gain in  $\tau_s$  evaluations as defined at the end of Section 2.

**Proof** Let  $\tau \in [\tau_s]$  and  $j \in [m]$ . Note that the  $\tau$ th evaluation is made at round  $t_\tau$  and we have  $\tau_{t_\tau} = \tau - 1$ . Hence, we have

$$\begin{aligned} & \bar{B}_{t_\tau}^j(x_{h_{t_\tau}, i_{t_\tau}}) - \underline{B}_{t_\tau}^j(x_{h_{t_\tau}, i_{t_\tau}}) \\ &= \min\{\mu_{\tau_{t_\tau}}^j(x_{h_{t_\tau}, i_{t_\tau}}) + \beta_{\tau_{t_\tau}}^{1/2} \sigma_{\tau_{t_\tau}}^j(x_{h_{t_\tau}, i_{t_\tau}}), \mu_{\tau_{t_\tau}}^j(p(x_{h_{t_\tau}, i_{t_\tau}})) + \beta_{\tau_{t_\tau}}^{1/2} \sigma_{\tau_{t_\tau}}^j(p(x_{h_{t_\tau}, i_{t_\tau}})) + V_{h_{t_\tau-1}}\} \\ & \quad - \max\{\mu_{\tau_{t_\tau}}^j(x_{h_{t_\tau}, i_{t_\tau}}) - \beta_{\tau_{t_\tau}}^{1/2} \sigma_{\tau_{t_\tau}}^j(x_{h_{t_\tau}, i_{t_\tau}}), \mu_{\tau_{t_\tau}}^j(p(x_{h_{t_\tau}, i_{t_\tau}})) - \beta_{\tau_{t_\tau}}^{1/2} \sigma_{\tau_{t_\tau}}^j(p(x_{h_{t_\tau}, i_{t_\tau}})) - V_{h_{t_\tau-1}}\} \\ &= \min\{\mu_{\tau-1}^j(x_{h_{t_\tau}, i_{t_\tau}}) + \beta_{\tau-1}^{1/2} \sigma_{\tau-1}^j(x_{h_{t_\tau}, i_{t_\tau}}), \mu_{\tau-1}^j(p(x_{h_{t_\tau}, i_{t_\tau}})) + \beta_{\tau-1}^{1/2} \sigma_{\tau-1}^j(p(x_{h_{t_\tau}, i_{t_\tau}})) + V_{h_{t_\tau-1}}\} \\ & \quad - \max\{\mu_{\tau-1}^j(x_{h_{t_\tau}, i_{t_\tau}}) - \beta_{\tau-1}^{1/2} \sigma_{\tau-1}^j(x_{h_{t_\tau}, i_{t_\tau}}), \mu_{\tau-1}^j(p(x_{h_{t_\tau}, i_{t_\tau}})) - \beta_{\tau-1}^{1/2} \sigma_{\tau-1}^j(p(x_{h_{t_\tau}, i_{t_\tau}})) - V_{h_{t_\tau-1}}\}. \end{aligned}$$

We can bound this difference in two ways, so that we can use information-type bounds and dimension-type bounds. In this result, we focus on the information-type bounds and write

$$\begin{aligned} & \bar{B}_{t_\tau}^j(x_{h_{t_\tau}, i_{t_\tau}}) - \underline{B}_{t_\tau}^j(x_{h_{t_\tau}, i_{t_\tau}}) \\ & \leq \mu_{\tau-1}^j(x_{h_{t_\tau}, i_{t_\tau}}) + \beta_{\tau-1}^{1/2} \sigma_{\tau-1}^j(x_{h_{t_\tau}, i_{t_\tau}}) - \mu_{\tau-1}^j(p(x_{h_{t_\tau}, i_{t_\tau}})) + \beta_{\tau-1}^{1/2} \sigma_{\tau-1}^j(p(x_{h_{t_\tau}, i_{t_\tau}})) \\ & = 2\beta_{\tau-1}^{1/2} \sigma_{\tau-1}^j(x_{h_{t_\tau}, i_{t_\tau}}). \end{aligned} \tag{22}$$

Since the diagonal distance of the hyper-rectangle  $\mathbf{Q}_{t_\tau}(x_{h_{t_\tau}}, i_{t_\tau})$  is the largest distance between any two points in the hyper-rectangle, we have

$$\begin{aligned}
& \sum_{\tau=1}^{\tau_s} \bar{\omega}_{t_\tau}^2 \\
&= \sum_{\tau=1}^{\tau_s} \max_{y, y' \in \mathbf{R}_{t_\tau}(x_{h_{t_\tau}}, i_{t_\tau})} \|y - y'\|_2^2 \\
&\leq \sum_{\tau=1}^{\tau_s} \max_{y, y' \in \mathbf{Q}_{t_\tau}(x_{h_{t_\tau}}, i_{t_\tau})} \|y - y'\|_2^2 \\
&= \sum_{\tau=1}^{\tau_s} \|\mathbf{U}_{t_\tau}(x_{h_{t_\tau}}, i_{t_\tau}) - \mathbf{L}_{t_\tau}(x_{h_{t_\tau}}, i_{t_\tau})\|_2^2 \\
&= \sum_{\tau=1}^{\tau_s} \sum_{j=1}^m \left( U_{t_\tau}^j(x_{h_{t_\tau}}, i_{t_\tau}) - L_{t_\tau}^j(x_{h_{t_\tau}}, i_{t_\tau}) \right)^2 \\
&= \sum_{\tau=1}^{\tau_s} \sum_{j=1}^m \left( \bar{B}_{t_\tau}^j(x_{h_{t_\tau}}, i_{t_\tau}) - \underline{B}_{t_\tau}^j(x_{h_{t_\tau}}, i_{t_\tau}) + 2V_{h_{t_\tau}} \right)^2 \tag{23}
\end{aligned}$$

$$\leq \sum_{\tau=1}^{\tau_s} \sum_{j=1}^m \left( 2\beta_{\tau-1}^{1/2} \sigma_{\tau-1}^j(x_{h_{t_\tau}}, i_{t_\tau}) + 2V_{h_{t_\tau}} \right)^2 \tag{24}$$

$$\begin{aligned}
&= 4 \sum_{\tau=1}^{\tau_s} \left( \sum_{j=1}^m \beta_{\tau-1} (\sigma_{\tau-1}^j(x_{h_{t_\tau}}, i_{t_\tau}))^2 + 2 \sum_{j=1}^m V_{h_{t_\tau}} \beta_{\tau-1}^{1/2} \sigma_{\tau-1}^j(x_{h_{t_\tau}}, i_{t_\tau}) + \sum_{j=1}^m (V_{h_{t_\tau}})^2 \right) \\
&\leq 4 \sum_{\tau=1}^{\tau_s} \left( \sum_{j=1}^m \beta_{\tau-1} (\sigma_{\tau-1}^j(x_{h_{t_\tau}}, i_{t_\tau}))^2 \right. \\
&\quad \left. + 2 \left( \sum_{j=1}^m (V_{h_{t_\tau}})^2 \right)^{1/2} \left( \sum_{j=1}^m \beta_{\tau-1} (\sigma_{\tau-1}^j(x_{h_{t_\tau}}, i_{t_\tau}))^2 \right)^{1/2} + \sum_{j=1}^m (V_{h_{t_\tau}})^2 \right) \tag{25}
\end{aligned}$$

$$\begin{aligned}
&\leq 4 \sum_{\tau=1}^{\tau_s} \left( \sum_{j=1}^m \beta_{\tau-1} (\sigma_{\tau-1}^j(x_{h_{t_\tau}}, i_{t_\tau}))^2 + 2 \sum_{j=1}^m \beta_{\tau-1} (\sigma_{\tau-1}^j(x_{h_{t_\tau}}, i_{t_\tau}))^2 \right. \\
&\quad \left. + \sum_{j=1}^m \beta_{\tau-1} (\sigma_{\tau-1}^j(x_{h_{t_\tau}}, i_{t_\tau}))^2 \right) \tag{26}
\end{aligned}$$

$$\leq 16\beta_{\tau_s} \sum_{\tau=1}^{\tau_s} \sum_{j=1}^m (\sigma_{\tau-1}^j(x_{h_{t_\tau}}, i_{t_\tau}))^2 \tag{27}$$

$$\begin{aligned}
&= 16\beta_{\tau_s} \sigma^2 \sum_{\tau=1}^{\tau_s} \sum_{j=1}^m \sigma^{-2} (\sigma_{\tau-1}^j(x_{h_{t_\tau}}, i_{t_\tau}))^2 \\
&\leq 16\beta_{\tau_s} \sigma^2 C \left( \sum_{\tau=1}^{\tau_s} \sum_{j=1}^m \log(1 + \sigma^{-2} (\sigma_{\tau-1}^j(x_{h_{t_\tau}}, i_{t_\tau}))^2) \right) \tag{28}
\end{aligned}$$

$$\leq 16\beta_{\tau_s} \sigma^2 C m I(\mathbf{y}_{[\tau_s]}, \mathbf{f}_{[\tau_s]}) \tag{29}$$

$$\leq 16\beta_{\tau_s} \sigma^2 C m \gamma_{\tau_s}, \tag{30}$$

where  $C = \sigma^{-2}/\log(1 + \sigma^{-2})$ . In this calculation, (23) follows by definitions; (24) follows by (22); (25) follows from Cauchy-Schwarz inequality; (26) follows from the fact that we make evaluation at round  $t_\tau$  so that we have

$$\beta_{\tau-1}^{1/2} \|\boldsymbol{\sigma}_{\tau-1}(x_{h_{t_\tau}, i_{t_\tau}})\|_2 = \beta_{\tau_\tau}^{1/2} \|\boldsymbol{\sigma}_{\tau_\tau}(x_{h_{t_\tau}, i_{t_\tau}})\|_2 > \|\mathbf{V}_{h_{t_\tau}}\|_2$$

by the structure of the algorithm; (27) holds since  $\beta_\tau$  is monotonically non-decreasing in  $\tau$  (see the definition of  $\beta_\tau$  in Theorem 1); (28) follows from the fact that  $s \leq C \log(1 + s)$  for all  $0 \leq s \leq \sigma^{-2}$  and that we have

$$\begin{aligned} & \sigma^{-2} (\boldsymbol{\sigma}_{\tau-1}^j(x_{h_{t_\tau}, i_{t_\tau}}))^2 \\ &= \sigma^{-2} \left( k^{jj}(x_{h_{t_\tau}, i_{t_\tau}}, x_{h_{t_\tau}, i_{t_\tau}}) - (\mathbf{k}_{[\tau-1]}(x_{h_{t_\tau}, i_{t_\tau}})(\mathbf{K}_{[\tau-1]} + \boldsymbol{\Sigma}_{[\tau-1]})^{-1} \mathbf{k}_{[\tau-1]}(x_{h_{t_\tau}, i_{t_\tau}})^{\tau_s})^{jj} \right) \\ &\leq \sigma^{-2} k^{jj}(x_{h_t, i_t}, x_{h_t, i_t}) \\ &\leq \sigma^{-2} \end{aligned}$$

thanks to Lemma 11 and Assumption 1; (29) follows from Proposition 1; and (30) follows from definition of the maximum information gain.

Finally, by Cauchy-Schwarz inequality, we have

$$\sum_{\tau=1}^{\tau_s} \bar{\omega}_{t_\tau} \leq \sqrt{\tau_s \sum_{\tau=1}^{\tau_s} \bar{\omega}_{t_\tau}^2} \leq \sqrt{\tau_s (16\beta_{\tau_s} \sigma^2 C m \gamma_{\tau_s})},$$

which completes the proof. ■

**Lemma 13.** *Running Adaptive  $\epsilon$ -PAL with  $(\beta_\tau)_{\tau \in \mathbb{N}}$  as defined in Lemma 6, we have*

$$\bar{\omega}_{t_s} \leq \sqrt{\frac{16\beta_{\tau_s} \sigma^2 C m \gamma_{\tau_s}}{\tau_s}}.$$

**Proof** First we show that the sequence  $(\bar{\omega}_t)_{t \in \mathbb{N}}$  is a monotonically non-increasing sequence. To that end, note that by the principle of selection we have that  $\omega_{t-1}(x_{h_t, i_t}) \leq \bar{\omega}_{t-1}$ . On the other hand, for every  $x \in \mathcal{X}$ , we have  $\omega_t(x) \leq \omega_{t-1}(x)$  since  $\mathbf{R}_t(x) \subseteq \mathbf{R}_{t-1}(x)$ . Thus,  $\bar{\omega}_t = \omega_t(x_{h_t, i_t}) \leq \omega_{t-1}(x_{h_t, i_t})$ . So we obtain  $\bar{\omega}_t \leq \bar{\omega}_{t-1}$ .

By above and by Lemma 12, we have

$$\bar{\omega}_{t_s} \leq \frac{\sum_{\tau=1}^{\tau_s} \bar{\omega}_{t_\tau}}{\tau_s} \leq \sqrt{\frac{16\beta_{\tau_s} \sigma^2 C m \gamma_{\tau_s}}{\tau_s}}.$$

Finally, we are ready to state the information-type bound on the sample complexity. ■

**Proposition 3.** *Let  $\boldsymbol{\epsilon} = [\epsilon^1, \dots, \epsilon^m]^\top$  be given with  $\epsilon = \min_{j \in [m]} \epsilon^j > 0$ . Let  $\delta \in (0, 1)$  and  $\bar{D} > D_1$ . For each  $h \geq 0$ , let  $V_h$  be defined as in Corollary 1; for each  $\tau \in \mathbb{N}$ , let  $\beta_\tau$  be defined as in Lemma 6. When we run Adaptive  $\boldsymbol{\epsilon}$ -PAL with prior  $GP(0, \mathbf{k})$  and noise  $\mathcal{N}(0, \sigma^2)$ , the following holds with probability at least  $1 - \delta$ . An  $\boldsymbol{\epsilon}$ -accurate Pareto set can be found with at most  $T$  function evaluations, where  $T$  is the smallest natural number satisfying*

$$\sqrt{\frac{16\beta_T\sigma^2 C m \gamma_T}{T}} \leq \epsilon .$$

In the above expression,  $C$  represents the constant defined in Lemma 12.

*Proof.* According to Lemma 3, we have  $\bar{w}_{t_s} \leq \epsilon$ . In addition, Lemma 13 says that

$$\omega_{\tau_s} \leq \frac{\sum_{\tau=1}^{\tau_s} \bar{w}_{t_\tau}}{\tau_s} \leq \sqrt{\frac{16\beta_{\tau_s}\sigma^2 C m \gamma_{\tau_s}}{\tau_s}} .$$

We use these two facts to find an upper bound on  $\tau_s$  that holds with probability one. Let

$$T = \min \left\{ \tau \in \mathbb{N} : \sqrt{\frac{16\beta_\tau\sigma^2 C m \gamma_\tau}{\tau}} \leq \epsilon \right\} .$$

Since the event  $\{\tau_s = T\}$  implies that  $\{\bar{w}_{t_s} \leq \epsilon\}$ , we have  $\Pr(\tau_s > T) = 0$ . ■

### A.7 Derivation of the dimension-type sample complexity bound

In order to bound the diameter, we make use of the following observation.

**Remark 3.** *We have*

$$V_h/V_{h+1} \leq N_1 := \rho^{-\alpha} .$$

The next lemma bounds diameters of confidence hyper-rectangles of the nodes in  $\mathcal{A}_t$  for all rounds  $t$ .

**Lemma 14.** *In any round  $t \geq 1$  before Adaptive  $\boldsymbol{\epsilon}$ -PAL terminates, we have*

$$\bar{\omega}_t^2 \leq L V_{h_t}^2 ,$$

where  $L = m (4N_1^2 + 4N_1^2(2N_1 + 2) + (2N_1 + 2)^2)$ .



*Proof.* We have

$$\begin{aligned}
 \bar{\omega}_t^2 &= \omega_t^2(x_{h_t, i_t}) \\
 &= \left( \max_{y, y' \in \mathbf{R}_t(x_{h_t, i_t})} \|y - y'\|_2 \right)^2 \\
 &\leq \left( \max_{y, y' \in \mathbf{Q}_t(x_{h_t, i_t})} \|y - y'\|_2 \right)^2 \\
 &= \left( \|\mathbf{U}_t(x_{h_t, i_t}) - \mathbf{L}_t(x_{h_t, i_t})\|_2 \right)^2 \\
 &= \sum_{j=1}^m \left( \bar{B}_t^j(x_{h_t, i_t}) - \underline{B}_t^j(x_{h_t, i_t}) + 2V_{h_t} \right)^2 \\
 &\leq \sum_{j=1}^m \left( 2\beta_{\tau_t}^{1/2} \sigma_{\tau_t}^j(p(x_{h_t, i_t})) + (2N_1 + 2)V_{h_t} \right)^2 \tag{31}
 \end{aligned}$$

$$\begin{aligned}
 &= 4\beta_{\tau_t} \sum_{j=1}^m \left( \sigma_{\tau_t}^j(p(x_{h_t, i_t})) \right)^2 + 4(2N_1 + 2) \sum_{j=1}^m \beta_{\tau_t}^{1/2} \sigma_{\tau_t}^j(p(x_{h_t, i_t})) V_{h_t} \\
 &\quad + (2N_1 + 2)^2 \sum_{j=1}^m (V_{h_t})^2 \\
 &\leq 4 \sum_{j=1}^m (V_{h_{t-1}})^2 + 4(2N_1 + 2) \sum_{j=1}^m \beta_{\tau_t}^{1/2} \sigma_{\tau_t}^j(p(x_{h_t, i_t})) V_{h_t} + (2N_1 + 2)^2 \sum_{j=1}^m (V_{h_t})^2 \tag{32}
 \end{aligned}$$

$$\begin{aligned}
 &\leq 4 \sum_{j=1}^m (V_{h_{t-1}})^2 + 4(2N_1 + 2) \left( \sum_{j=1}^m \beta_{\tau_t} \left( \sigma_{\tau_t}^j(p(x_{h_t, i_t})) \right)^2 \right)^{1/2} \left( \sum_{j=1}^m (V_{h_t})^2 \right)^{1/2} \\
 &\quad + (2N_1 + 2)^2 \sum_{j=1}^m (V_{h_t})^2 \tag{33}
 \end{aligned}$$

$$\begin{aligned}
 &\leq 4 \sum_{j=1}^m (V_{h_{t-1}})^2 + 4(2N_1 + 2) N_1 \left( \sum_{j=1}^m (V_{h_{t-1}})^2 \right)^{1/2} \left( \sum_{j=1}^m (V_{h_t})^2 \right)^{1/2} \\
 &\quad + (2N_1 + 2)^2 \sum_{j=1}^m (V_{h_t})^2 \tag{34}
 \end{aligned}$$

$$\leq m (4N_1^2 + 4N_1^2(2N_1 + 2) + (2N_1 + 2)^2) (V_{h_t})^2 = LV_{h_t}^2 . \tag{35}$$

In the above expression, (31) follows from the fact that for  $j \in [m]$  and  $t \geq 1$

$$\begin{aligned}
& \overline{B}_t^j(x_{h_t, i_t}) - \underline{B}_t^j(x_{h_t, i_t}) \\
&= \min\{\mu_{\tau_t}^j(x_{h_t, i_t}) + \beta_{\tau_t}^{1/2} \sigma_{\tau_t}^j(x_{h_t, i_t}), \mu_{\tau_t}^j(p(x_{h_t, i_t})) + \beta_{\tau_t}^{1/2} \sigma_{\tau_t}^j(p(x_{h_t, i_t})) + V_{h_t-1}\} \\
&\quad - \max\{\mu_{\tau_t}^j(x_{h_t, i_t}) - \beta_{\tau_t}^{1/2} \sigma_{\tau_t}^j(x_{h_t, i_t}), \mu_{\tau_t}^j(p(x_{h_t, i_t})) - \beta_{\tau_t}^{1/2} \sigma_{\tau_t}^j(p(x_{h_t, i_t})) - V_{h_t-1}\} \\
&\leq \mu_{\tau_t}^j(p(x_{h_t, i_t})) + \beta_{\tau_t}^{1/2} \sigma_{\tau_t}^j(p(x_{h_t, i_t})) + V_{h_t-1} - \mu_{\tau_t}^j(p(x_{h_t, i_t})) + \beta_{\tau_t}^{1/2} \sigma_{\tau_t}^j(p(x_{h_t, i_t})) + V_{h_t-1} \\
&\leq 2\beta_{\tau_t}^{1/2} \sigma_{\tau_t}^j(p(x_{h_t, i_t})) + 2V_{h_t-1} \\
&\leq 2\beta_{\tau_t}^{1/2} \sigma_{\tau_t}^j(p(x_{h_t, i_t})) + 2N_1 V_{h_t} , \tag{36}
\end{aligned}$$

where (36) follows from Remark 3. (32) is obtained by observing that the node  $p(x_{h_t, i_t})$  has been refined, and hence, it holds that  $\beta_{\tau_t}^{1/2} \|\sigma_{\tau_t}(p(x_{h_t, i_t}))\|_2 \leq \|\mathbf{V}_{h_t-1}\|_2$ . (33) follows from application of the Cauchy-Schwarz inequality. (34) follows again from the fact that  $\beta_{\tau_t}^{1/2} \|\sigma_{\tau_t}(p(x_{h_t, i_t}))\|_2 \leq \|\mathbf{V}_{h_t-1}\|_2$ , and (35) follows from Remark 3.  $\blacksquare$

Let  $\mathcal{E}$  denote the set of rounds in which Adaptive  $\epsilon$ -PAL performs design evaluations. Note that  $|\mathcal{E}| = \tau_s$ . Let  $t_s$  denote the round in which the algorithm terminates. Next, we use Lemma 1 together with Lemma 14 to upper bound  $\overline{\omega}_{t_s}$  as a function of the number evaluations until termination.

**Lemma 15.** *Let  $\delta \in (0, 1)$  and  $\bar{D} > D_1$ . Running Adaptive  $\epsilon$ -PAL with  $\beta_\tau$  defined in Lemma 6, there exists a constant  $Q > 0$  such that the following event holds almost surely.*

$$\overline{\omega}_{t_s} \leq K_1 \tau_s^{-\frac{\alpha}{\bar{D}+2\alpha}} (\log \tau_s)^{-\frac{-(\bar{D}+\alpha)}{\bar{D}+2\alpha}} + K_2 \tau_s^{-\frac{\alpha}{\bar{D}+2\alpha}} (\log \tau_s)^{\frac{\alpha}{\bar{D}+2\alpha}} ,$$

where

$$\begin{aligned}
K_1 &= \frac{\sqrt{L} Q \sigma^2 \beta_{\tau_s}}{C_{\mathbf{k}} v_1^\alpha v_2^{\bar{D}} (\rho^{-(\bar{D}+\alpha)} - 1)} , \\
K_2 &= 4\sqrt{L} C_{\mathbf{k}} v_1^\alpha \left( \sqrt{C_2 + 2 \log(2H^2 \pi^2 m / 6\delta) + H \log N + \max\{0, -4(D_1/\alpha) \log(C_{\mathbf{k}}(v_1 \rho^H)^\alpha)\}} + C_3 \right) , \\
H &= \left\lfloor \frac{\log \tau_s - \log(\log \tau_s)}{\log(1/\rho)(\bar{D} + 2\alpha)} \right\rfloor .
\end{aligned}$$

*Proof.* We have

$$\overline{\omega}_{t_s} \leq \frac{\sum_{t \in \mathcal{E}} \overline{\omega}_t}{\tau_s} \leq \frac{\sqrt{L} \sum_{t \in \mathcal{E}} V_{h_t}}{\tau_s} , \tag{37}$$

where the first inequality follows from the fact that  $\overline{\omega}_t \leq \overline{\omega}_{t-1}$  for all  $t \geq 1$  and the second inequality is the result of Lemma 14. We will bound  $\sum_{t \in \mathcal{E}} V_{h_t}$  and use it to obtain a bound for (37). First, we define

$$S_1 = \sum_{\substack{t \in \mathcal{E}: \\ h_t < H}} V_{h_t} \text{ and } S_2 = \sum_{\substack{t \in \mathcal{E}: \\ h_t \geq H}} V_{h_t} ,$$

and write  $\sum_{t \in \mathcal{E}} V_{h_t} = S_1 + S_2$ . We have

$$\begin{aligned}
 S_1 &= \sum_{\substack{t \geq 1: \\ h_t < H}} V_{h_t} \mathbb{I}(t \in \mathcal{E}) \\
 &= \sum_{t \geq 1} \sum_{h < H} V_h \mathbb{I}(h_t = h) \mathbb{I}(t \in \mathcal{E}) \\
 &= \sum_{h < H} \sum_{t \geq 1} V_h \mathbb{I}(h_t = h) \mathbb{I}(t \in \mathcal{E}) \\
 &\leq \sum_{h < H} V_h Q (v_2 \rho^h)^{-\bar{D}} q_h \tag{38}
 \end{aligned}$$

$$\leq \sum_{h < H} V_h Q (v_2 \rho^h)^{-\bar{D}} \frac{\sigma^2 \beta_T}{V_h^2} \tag{39}$$

$$\leq \sum_{h < H} Q (v_2 \rho^h)^{-\bar{D}} \frac{\sigma^2 \beta_T}{C_{\mathbf{k}} (v_1 \rho^h)^\alpha} \tag{40}$$

$$\begin{aligned}
 &\leq \frac{Q \sigma^2 \beta_T}{C_{\mathbf{k}} v_1^\alpha v_2^{\bar{D}}} \sum_{h < H} \rho^{-(\bar{D} + \alpha)h} \\
 &\leq \frac{Q \sigma^2 \beta_T}{C_{\mathbf{k}} v_1^\alpha v_2^{\bar{D}}} \frac{\rho^{-(\bar{D} + \alpha)H}}{\rho^{-(\bar{D} + \alpha)} - 1}. \tag{41}
 \end{aligned}$$

In the above display, to obtain (38), we note that for a fixed  $h$  the cells  $X_{h,i}$  are disjoint, a ball of radius  $v_2 \rho^h$  should be able to fit in each cell, and thus, the number of depth  $h$  cells is upper bounded by the number of radius  $v_2 \rho^h$  balls we can pack in  $(\mathcal{X}, d)$ , which is in turn upper bounded by  $M(\mathcal{X}, 2v_2 \rho^h, d)$ . The rest follows from Lemma 1, which states that there exists a positive constant  $Q$ , such that  $M(\mathcal{X}, 2v_2 \rho^h, d) \leq N(\mathcal{X}, v_2 \rho^h, d) \leq Q (v_2 \rho^h)^{-\bar{D}}$ . For (39), we upper bound  $q_h$  using Lemma 5, and (40) follows by observing that  $V_h \geq C_{\mathbf{k}} (v_1 \rho^h)^\alpha$ .

Since  $V_h$  is decreasing in  $h$ , the remainder of the sum can be bounded as

$$\begin{aligned}
 S_2 &= \sum_{\substack{t \geq 1: \\ h_t \geq H}} V_{h_t} \mathbb{I}(t \in \mathcal{E}) \\
 &\leq \sum_{t \in \mathcal{E}} V_H = \tau_s V_H = (K_2 / \sqrt{L}) \tau_s \rho^{H\alpha}. \tag{42}
 \end{aligned}$$

Combining (41) and (42), we obtain

$$\sum_{t \in \mathcal{E}} V_{h_t} \leq \frac{Q \sigma^2 \beta_{\tau_s}}{C_{\mathbf{k}} v_1^\alpha v_2^{\bar{D}}} \frac{\rho^{-(\bar{D} + \alpha)H}}{\rho^{-(\bar{D} + \alpha)} - 1} + (K_2 / \sqrt{L}) \tau_s \rho^{H\alpha}. \tag{43}$$

Since

$$H = \left\lceil \frac{\log \tau_s - \log(\log \tau_s)}{\log(1/\rho)(\bar{D} + 2\alpha)} \right\rceil = \left\lceil -\log_\rho \left( \frac{\tau_s}{\log \tau_s} \right)^{\frac{1}{\bar{D} + 2\alpha}} \right\rceil,$$

we have

$$\rho^{-H(\bar{D}+2\alpha)} \leq \tau_s^{\frac{\bar{D}+\alpha}{\bar{D}+2\alpha}} (\log \tau_s)^{\frac{-(\bar{D}+\alpha)}{\bar{D}+2\alpha}} \quad \text{and} \quad \tau_s \rho^{H\alpha} \leq \rho^\alpha \tau_s^{1-\frac{\alpha}{\bar{D}+2\alpha}} (\log \tau_s)^{\frac{\alpha}{\bar{D}+2\alpha}} .$$

Finally, we use the values found above to upper bound (43), and then use this upper bound in (37), which gives us

$$\bar{w}_{t_s} \leq \sqrt{L} \left( \frac{Q\sigma^2\beta_{\tau_s}}{C_{\mathbf{k}}v_1^\alpha v_2^{\bar{D}}(\rho^{-(\bar{D}+\alpha)} - 1)} \tau_s^{\frac{-\alpha}{\bar{D}+2\alpha}} (\log \tau_s)^{\frac{-(\bar{D}+\alpha)}{\bar{D}+2\alpha}} + (K_2/\sqrt{L}) \tau_s^{\frac{-\alpha}{\bar{D}+2\alpha}} (\log \tau_s)^{\frac{\alpha}{\bar{D}+2\alpha}} \right) .$$

■

Finally, we are ready to state the metric dimension-type bound on the sample complexity.

**Proposition 4.** *Let  $\epsilon = [\epsilon^1, \dots, \epsilon^m]^\top$  be given with  $\epsilon = \min_{j \in [m]} \epsilon^j > 0$ . Let  $\delta \in (0, 1)$  and  $\bar{D} > D_1$ . For each  $h \geq 0$ , let  $V_h$  be defined as in Corollary 1; for each  $\tau \in \mathbb{N}$ , let  $\beta_\tau$  be defined as in Lemma 6. When we run Adaptive  $\epsilon$ -PAL with prior  $GP(0, \mathbf{k})$  and noise  $\mathcal{N}(0, \sigma^2)$ , the following holds with probability at least  $1 - \delta$ .*

*An  $\epsilon$ -accurate Pareto set can be found with at most  $T$  function evaluations, where  $T$  is the smallest natural number satisfying*

$$K_1 T^{\frac{-\alpha}{\bar{D}+2\alpha}} (\log T)^{\frac{-(\bar{D}+\alpha)}{\bar{D}+2\alpha}} + K_2 T^{\frac{-\alpha}{\bar{D}+2\alpha}} (\log T)^{\frac{\alpha}{\bar{D}+2\alpha}} \leq \epsilon ,$$

where  $K_1$  and  $K_2$  are the constants defined in Lemma 15.

*Proof.* According to Lemma 3, we have  $\bar{w}_{t_s} \leq \epsilon$ . In addition, Lemma 15 says that

$$\bar{w}_{t_s} \leq K_1 \tau_s^{\frac{-\alpha}{\bar{D}+2\alpha}} (\log \tau_s)^{\frac{-(\bar{D}+\alpha)}{\bar{D}+2\alpha}} + K_2 \tau_s^{\frac{-\alpha}{\bar{D}+2\alpha}} (\log \tau_s)^{\frac{\alpha}{\bar{D}+2\alpha}} .$$

We use these two facts to find an upper bound on  $\tau_s$  that holds with probability one. Let

$$T = \min \left\{ \tau \in \mathbb{N} : K_1 \tau^{\frac{-\alpha}{\bar{D}+2\alpha}} (\log \tau)^{\frac{-(\bar{D}+\alpha)}{\bar{D}+2\alpha}} + K_2 \tau^{\frac{-\alpha}{\bar{D}+2\alpha}} (\log \tau)^{\frac{\alpha}{\bar{D}+2\alpha}} \leq \epsilon \right\} .$$

Since the event  $\{\tau_s = T\}$  implies that  $\{\bar{w}_{t_s} \leq \epsilon\}$ , we have  $\Pr(\tau_s > T) = 0$ . ■

## A.8 The final step of the proof of Theorem 1

We take the minimum over the two bounds presented in Proposition 3 and Proposition 4 to obtain the result in Theorem 1. ■

## A.9 Proof of Proposition 1

First, let us review some well-known facts about entropies. For an  $m$ -dimensional Gaussian random vector  $\mathbf{g}$  with distribution  $\mathcal{N}(\mathbf{a}, \mathbf{b})$  with  $\mathbf{a} \in \mathbb{R}^m$ ,  $\mathbf{b} \in \mathbb{R}^{m \times m}$ , the entropy of  $\mathbf{g}$  is calculated by

$$H(\mathbf{g}) = H(\mathcal{N}(\mathbf{a}, \mathbf{b})) = \frac{1}{2} \log |2\pi e \mathbf{b}| .$$

More generally, if  $h$  is another random variable (with arbitrary measurable state space  $H$ ) and the regular conditional distribution of  $\mathbf{g}$  given  $h$  is  $\mathcal{N}(\mathbf{a}(h), \mathbf{b}(h))$  for some measurable

functions  $a: H \rightarrow \mathbb{R}^m$  and  $b: H \rightarrow \mathbb{R}^{m \times m}$ , then the conditional entropy of  $\mathbf{g}$  given  $h$  is calculated by

$$H(\mathbf{g}|h) = \frac{1}{2} \mathbb{E} [\log |2\pi e \mathbf{b}(h)|].$$

**Lemma 16.** *We have*

$$I(\mathbf{y}_{[T]}; \mathbf{f}_{[T]}) = \sum_{\tau=1}^T \frac{1}{2} \log |\mathbf{I}_m + \sigma^{-2} \mathbf{k}_{\tau-1}(\tilde{x}_\tau, \tilde{x}_\tau)|,$$

where  $\mathbf{k}_0(\tilde{x}_1, \tilde{x}_1) = \mathbf{k}(\tilde{x}_1, \tilde{x}_1)$ .

**Proof** We have

$$\begin{aligned} I(\mathbf{y}_{[T]}; \mathbf{f}_{[T]}) &= H(\mathbf{y}_{[T]}) - H(\mathbf{y}_{[T]}|\mathbf{f}_{[T]}) \\ &= H(\mathbf{y}_T, \mathbf{y}_{[T-1]}) - H(\mathbf{y}_{[T]}|\mathbf{f}_{[T]}) \\ &= H(\mathbf{y}_T|\mathbf{y}_{[T-1]}) + H(\mathbf{y}_{[T-1]}) - H(\mathbf{y}_{[T]}|\mathbf{f}_{[T]}). \end{aligned}$$

Re-iterating this calculation inductively, we obtain

$$I(\mathbf{y}_{[T]}; \mathbf{f}_{[T]}) = \sum_{\tau=2}^T H(\mathbf{y}_\tau|\mathbf{y}_{[\tau-1]}) + H(\mathbf{y}_1) - H(\mathbf{y}_{[T]}|\mathbf{f}_{[T]})$$

since  $\mathbf{y}_{[1]} = \mathbf{y}_1$ . Note that

$$H(\mathbf{y}_{[T]}|\mathbf{f}_{[T]}) = H(\mathbf{f}(\tilde{x}_1) + \boldsymbol{\epsilon}_1, \dots, \mathbf{f}(\tilde{x}_T) + \boldsymbol{\epsilon}_T|\mathbf{f}_{[T]}) = \sum_{\tau=1}^T H(\boldsymbol{\epsilon}_\tau) = \frac{T}{2} \log |2\pi e \sigma^2 \mathbf{I}_m|.$$

On the other hand, the conditional distribution of  $\mathbf{y}_\tau$  given  $\mathbf{y}_{[\tau-1]}$  is  $\mathcal{N}(\boldsymbol{\mu}_{\tau-1}(\tilde{x}_\tau), \mathbf{k}_{\tau-1}(\tilde{x}_\tau, \tilde{x}_\tau) + \sigma^2 \mathbf{I}_m)$  and the distribution of  $\mathbf{y}_1$  is  $\mathcal{N}(0, \mathbf{k}(\tilde{x}_1, \tilde{x}_1) + \sigma^2 \mathbf{I}_m)$ . Hence,

$$\begin{aligned} &I(\mathbf{y}_{[T]}; \mathbf{f}_{[T]}) \\ &= \sum_{\tau=2}^T H(\mathbf{y}_\tau|\mathbf{y}_{[\tau-1]}) + H(\mathbf{y}_1) - H(\mathbf{y}_{[T]}|\mathbf{f}_{[T]}) \\ &= \sum_{\tau=2}^T \frac{1}{2} [\log |2\pi e(\mathbf{k}_{\tau-1}(\tilde{x}_\tau, \tilde{x}_\tau) + \sigma^2 \mathbf{I}_m)|] + \frac{1}{2} \log |2\pi e(\mathbf{k}(\tilde{x}_1, \tilde{x}_1) + \sigma^2 \mathbf{I}_m)| - \frac{T}{2} \log |2\pi e \sigma^2 \mathbf{I}_m| \\ &= \sum_{\tau=1}^T \frac{1}{2} \log |2\pi e(\mathbf{k}_{\tau-1}(\tilde{x}_\tau, \tilde{x}_\tau) + \sigma^2 \mathbf{I}_m)| - \frac{T}{2} \log |2\pi e \sigma^2 \mathbf{I}_m| \\ &= \sum_{\tau=1}^T \frac{1}{2} \log |2\pi e \sigma^2 \mathbf{I}_m (\sigma^{-2} \mathbf{k}_{\tau-1}(\tilde{x}_\tau, \tilde{x}_\tau) + \mathbf{I}_m)| - \frac{T}{2} \log |2\pi e \sigma^2 \mathbf{I}_m| \\ &= \sum_{\tau=1}^T \frac{1}{2} \log |2\pi e \sigma^2 \mathbf{I}_m| + \sum_{\tau=1}^T \frac{1}{2} \log |\sigma^{-2} \mathbf{k}_{\tau-1}(\tilde{x}_\tau, \tilde{x}_\tau) + \mathbf{I}_m| - \frac{T}{2} \log |2\pi e \sigma^2 \mathbf{I}_m| \\ &= \sum_{\tau=1}^T \frac{1}{2} \log |\sigma^{-2} \mathbf{k}_{\tau-1}(\tilde{x}_\tau, \tilde{x}_\tau) + \mathbf{I}_m|. \end{aligned}$$

■

**Lemma 17.** *Let  $\mathbf{a} = (a_{ij})_{i,j \in [m]}$  be a symmetric positive definite  $m \times m$ -matrix. Then,*

$$|\mathbf{a} + \mathbf{I}_m| \geq \max_{j \in [m]} (1 + a_{jj}).$$

**Proof** Let  $0 < \lambda_{(1)} \leq \dots \leq \lambda_{(m)}$  be the ordered eigenvalues of  $\mathbf{a}$ . It is easy to check that  $\lambda \in \mathbb{R}$  is an eigenvalue of  $\mathbf{a}$  if and only if  $1 + \lambda$  is an eigenvalue of  $\mathbf{a} + \mathbf{I}_m$ . In particular,  $1 + \lambda_{(m)}$  is the largest eigenvalue of  $\mathbf{a} + \mathbf{I}_m$  so that

$$|\mathbf{a} + \mathbf{I}_m| = \prod_{j \in [m]} (1 + \lambda_{(j)}) = \left( \prod_{j \in [m-1]} (1 + \lambda_{(j)}) \right) (1 + \lambda_{(m)}) \geq (1 + \lambda_{(m)}). \quad (44)$$

On the other hand, thanks to the variational characterization of the maximum eigenvalue  $\lambda_{(m)}$ , we have

$$\lambda_{(m)} = \max_{\mathbf{x} \in \mathbb{R}^m: \|\mathbf{x}\|=1} \mathbf{x}^\top \mathbf{a} \mathbf{x} \geq \mathbf{e}_j^\top \mathbf{a} \mathbf{e}_j = a_{jj} \quad (45)$$

for each  $j \in [m]$ , where  $\mathbf{e}_j$  is the  $j^{\text{th}}$  unit vector in  $\mathbb{R}^m$ . The claim of the lemma follows by combining (44) and (45). ■

Next, we will make use of the lemmas derived above to complete the proof. Note that

$$\begin{aligned} I(\mathbf{y}_{[T]}; \mathbf{f}_{[T]}) &= \sum_{\tau=1}^T \frac{1}{2} \log |\mathbf{I}_m + \sigma^{-2} \mathbf{k}_{\tau-1}(\tilde{\mathbf{x}}_\tau, \tilde{\mathbf{x}}_\tau)| \\ &\geq \sum_{\tau=1}^T \frac{1}{2} \max_{j \in [m]} \log(1 + \sigma^{-2} k_{\tau-1}^{jj}(\tilde{\mathbf{x}}_\tau, \tilde{\mathbf{x}}_\tau)) \\ &= \sum_{\tau=1}^T \frac{1}{2} \max_{j \in [m]} \log(1 + \sigma^{-2} (\sigma_{\tau-1}^j(\tilde{\mathbf{x}}_\tau))^2) \\ &\geq \sum_{\tau=1}^T \sum_{j \in [m]} \frac{1}{2m} \log(1 + \sigma^{-2} (\sigma_{\tau-1}^j(\tilde{\mathbf{x}}_\tau))^2), \end{aligned}$$

where the first equality is by Lemma 16 and the first inequality is by Lemma 17. Hence, the claim of the proposition follows.

### A.10 Determination of $\alpha$ and $C_K$ for Squared Exponential type kernels

For Squared Exponential type kernels, the covariance function of objective  $j$  can be written as:

$$k^{jj}(x, y) = k^j(r) = \nu e^{-\frac{r^2}{L^2}}$$

Where  $r = \|x - y\|$  and  $L$  and  $\nu$  are the length-scale and variance hyper-parameters of the  $j^{\text{th}}$  objective. Hence, by Remark 1, the metric  $l_j$  induced by the  $j^{\text{th}}$  objective of the GP on  $\mathcal{X}$  is given by:

$$l_j(x, y) = \sqrt{2k(0) - 2k(0)e^{-\frac{r^2}{L^2}}} = \sqrt{2\nu(1 - e^{-\frac{r^2}{L^2}})} \leq \frac{\sqrt{2\nu}}{L}r .$$

Thus, we can set  $C_{\mathbf{k}} = \frac{\sqrt{2\nu}}{L}$  and  $\alpha = 1$  in Assumption 1.

## References

- Oscar Almer, Nigel Topham, and Björn Franke. A learning-based approach to the automated design of mpso networks. In *International Conference on Architecture of Computing Systems*, pages 243–258. Springer, 2011.
- Peter Auer, Chao-Kai Chiang, Ronald Ortner, and Madalina Drugan. Pareto front identification from stochastic bandit feedback. In *Artificial intelligence and statistics*, pages 939–947. PMLR, 2016.
- Syrine Belakaria and Aryan Deshwal. Max-value entropy search for multi-objective bayesian optimization. In *International Conference on Neural Information Processing Systems (NeurIPS)*, 2019.
- Syrine Belakaria, Aryan Deshwal, Nitthilan Kannappan Jayakodi, and Janardhan Rao Doppa. Uncertainty-aware search framework for multi-objective bayesian optimization. In *Proceedings of the AAAI Conference on Artificial Intelligence*, volume 34, pages 10044–10052, 2020.
- Chai Kian M Williams Chris Bonilla, Edwin V. Multi-task gaussian process prediction. *Advances in neural information processing systems*, pages 153–160, 2007.
- Sébastien Bubeck, Rémi Munos, and Gilles Stoltz. Pure exploration in multi-armed bandits problems. In *International conference on Algorithmic learning theory*, pages 23–37. Springer, 2009.
- Sébastien Bubeck, Rémi Munos, Gilles Stoltz, and Csaba Szepesvári. X-armed bandits. *Journal of Machine Learning Research*, 12(May):1655–1695, 2011.
- Samuel Daulton, Maximilian Balandat, and Eytan Bakshy. Differentiable expected hyper-volume improvement for parallel multi-objective bayesian optimization. *arXiv preprint arXiv:2006.05078*, 2020.
- Michael Emmerich. Single-and multi-objective evolutionary design optimization assisted by gaussian random field metamodells. *University of Dortmund*, 2005.
- Victor Gabillon, Mohammad Ghavamzadeh, and Alessandro Lazaric. Best arm identification: A unified approach to fixed budget and fixed confidence. In *NIPS-Twenty-Sixth Annual Conference on Neural Information Processing Systems*, 2012.

- Alkis Gotovos. Active learning for level set estimation. Master’s thesis, Eidgenössische Technische Hochschule Zürich, Department of Computer Science., 2013.
- Daniel Hernández-Lobato, Jose Hernandez-Lobato, Amar Shah, and Ryan Adams. Predictive entropy search for multi-objective bayesian optimization. In *International Conference on Machine Learning*, pages 1492–1501. PMLR, 2016.
- José Miguel Hernández-Lobato, Matthew W Hoffman, and Zoubin Ghahramani. Predictive entropy search for efficient global optimization of black-box functions. *arXiv preprint arXiv:1406.2541*, 2014.
- C-L Hwang and Abu Syed Md Masud. *Multiple objective decision making—methods and applications: a state-of-the-art survey*, volume 164. Springer Science & Business Media, 2012.
- Donald R Jones, Matthias Schonlau, and William J Welch. Efficient global optimization of expensive black-box functions. *Journal of Global optimization*, 13(4):455–492, 1998.
- Julian Katz-Samuels and Clay Scott. Feasible arm identification. In *International Conference on Machine Learning*, pages 2535–2543. PMLR, 2018.
- Robert Kleinberg, Aleksandrs Slivkins, and Eli Upfal. Multi-armed bandits in metric spaces. In *Proceedings of the fortieth annual ACM symposium on Theory of computing*, pages 681–690, 2008.
- Joshua Knowles. Parego: A hybrid algorithm with on-line landscape approximation for expensive multiobjective optimization problems. *IEEE Transactions on Evolutionary Computation*, 10(1):50–66, 2006a.
- Joshua Knowles. Parego: A hybrid algorithm with on-line landscape approximation for expensive multiobjective optimization problems. *Evolutionary Computation, IEEE Transactions on*, 10:50 – 66, 03 2006b. doi: 10.1109/TEVC.2005.851274.
- H. T. Kung, F. Luccio, and F. P. Preparata. On finding the maxima of a set of vectors. *Journal of the ACM*, 22:469–476, 1975.
- Andrea Locatelli, Maurilio Gutzeit, and Alexandra Carpentier. An optimal algorithm for the thresholding bandit problem. In *International Conference on Machine Learning*, pages 1690–1698. PMLR, 2016.
- Shie Mannor and John N Tsitsiklis. The sample complexity of exploration in the multi-armed bandit problem. *Journal of Machine Learning Research*, 5(Jun):623–648, 2004.
- Biswajit Paria, Kirthevasan Kandasamy, and Barnabás Póczos. A flexible framework for multi-objective bayesian optimization using random scalarizations. In *Uncertainty in Artificial Intelligence*, pages 766–776. PMLR, 2020.
- Wolfgang Ponweiser, Tobias Wagner, Dirk Biermann, and Markus Vincze. Multiobjective optimization on a limited budget of evaluations using model-assisted  $\mathcal{S}$ -metric selection. In *International Conference on Parallel Problem Solving from Nature*, pages 784–794. Springer, 2008.



- Jerome Sacks, William J Welch, Toby J Mitchell, and Henry P Wynn. Design and analysis of computer experiments. *Statistical science*, pages 409–423, 1989.
- R Schmidt. Dose-finding studies in clinical drug development. *European journal of clinical pharmacology*, 34(1):15–19, 1988.
- Amar Shah and Zoubin Ghahramani. Pareto frontier learning with expensive correlated objectives. In *International Conference on Machine Learning*, pages 1919–1927. PMLR, 2016.
- Shubhanshu Shekhar, Tara Javidi, et al. Gaussian process bandits with adaptive discretization. *Electronic Journal of Statistics*, 12(2):3829–3874, 2018.
- Niranjan Srinivas, Andreas Krause, Sham M Kakade, and Matthias W Seeger. Information-theoretic regret bounds for gaussian process optimization in the bandit setting. *IEEE Transactions on Information Theory*, 58(5):3250–3265, 2012.
- E. Zitzler. Evolutionary algorithms for multiobjective optimization: methods and applications. 1999.
- Marcela Zuluaga, Guillaume Sergent, Andreas Krause, and Markus Püschel. Active learning for multi-objective optimization. In *International Conference on Machine Learning*, pages 462–470. PMLR, 2013.
- Marcela Zuluaga, Andreas Krause, and Markus Püschel.  $\varepsilon$ -pal: an active learning approach to the multi-objective optimization problem. *The Journal of Machine Learning Research*, 17(1):3619–3650, 2016.